ESTIMATING NITROGEN STATUS OF CROPS USING NON-DESTRUCTIVE REMOTE SENSING TECHNIQUES

By

Elizabeth Johanna BOTHA

Submitted in fulfillment of the requirements for the degree Master of Science in the Department of Soil Science.

Faculty: Mathematics and Natural Sciences
University of the North
Private Bag X1106
Sovenga
0727
Republic of South Africa

January 2001

Supervisor: Professor P.S.Fouché
Co-supervisor: Professor R.O. Barnard

DECLARATION

I declare that the dissertation for the degree Master of Science at the University of the North hereby submitted has not been previously submitted by me for a degree at this or any other university, that this is my own work in design and execution, and that all the material contained therein has been duly acknowledged.

E.J. Botha

23/01/2001

Date

ACKNOWLEDGEMENTS

I would like to express my thanks and gratitude to the following people:

Prof. Paul Fouché for guidance and assistance throughout the duration of the study.
Ms Tanya Tarassova for soil and plant analysis.
The 1999 second year Soil Science class for their help with the preparation of the pot trials.
The University of the North for financial and technical assistance.
My husband, Hannes, for his patience, support and comments.

SUMMARY:

Nitrogen availability is an important determinant of crop productivity. Spectral reflectance of leaves can be a valuable data source in the evaluation of crop nitrogen status and is of great interest in agricultural communities. A pot trial was conducted, involving burley tobacco (*Nicotiana Tabacum*), tomato (*Lycopersicon Esculentium*) and sunflower (*Helianthus Annuus*). The soil was fertilized optimally for all nutrients except nitrogen, which was added at four different rates ranging from zero to optimal. Crop canopy reflection data was collected at various times during the growth cycle. Optical instruments used for data collection were a spectrometer, a digital infrared camera and a multispectral video camera with four 5nm optical filters. Leaf samples were also collected on the same days for laboratory analysis of leaf nitrogen status. This study established that the most consistent positive correlation between reflectance data and leaf nitrogen status was obtained with an NDVI of the images obtained with the digital infrared camera. The position of the red edge has yielded a consistent correlation with changes in leaf N status over time. The video greenness index and NDVI was only effective in some instances.

LIST OF FIGURES

LIST OF TABLES

CONTENTS

Chapter 4: Data Processing

CHAPTER 1

Background

1.1. Introduction

Remote sensing and digital image analysis are methods of acquisition and interpretation of measurements of an object without physical contact between the measuring device and the object. The object can be analysed many times non-invasively and without damage. The specific properties of vegetation, healthy or diseased, influence the amount of radiation reflected from the leaves. Remote sensing can thus be used as a means of detecting and assessing changes in plants and canopies (Nilson, 1995).

Various types of plant stress have been identified using remote sensing techniques. These include disease detection, water stress (Fouchè *et al.*, 1994), and nutrient stress (Balkeman, 1990; Peñuelas *et al.*, 1994 and Fillela *et al.*, 1995). Physiological changes resulting from nitrogen limitations can be translated into clear spectral differences between treatments, demonstrating the relationship between leaf reflectance and leaf chlorophyll and nitrogen concentrations (Peñuelas *et al.*, 1994).

Nitrogen availability is an important determinant of crop productivity. Detection and rapid accurate quantification of early deficiency symptoms are often difficult (Nilson, 1995). Plant N analysis is time-consuming and the process usually involves destructive sampling, drying, weighing and grinding of samples. Analysis also requires hazardous chemicals and/or expensive equipment (Ladha *et al.*, 1998).

One of the most important functions of nitrogen is the production of chlorophyll A, which is, in general, related to crop yields (Filella *et al.*, 1995). Ordinarily green leaves absorb 75 to 100% of the light in the blue (about 450nm) or red (about 675nm) part of the spectrum. Absorbance is smallest in the wavelength region around 550nm (Thomas and Oerther, 1972). Nitrogen deficiency changes the whole electromagnetic reflectance spectrum of vegetation (Guyot, 1990).

Since nutrient deficiency decreases pigment formation and subsequent leaf colour, it would increase the reflectivity because of decreased radiation absorbance (Thomas an Oerther, 1972). Reflectance measurements can detect changes in leaf colour before visual detection is possible. These measurements suggest the possibility of a non-destructive method involving the least equipment and skill to determine leaf nitrogen (Ladha *et al.*, 1998).

The distribution of chlorophyll within a canopy varies in time and place. As a consequence, the estimation of the levels of chlorophyll content by extrapolating the destructively obtained, individual leaf chlorophyll measurement is labour-intensive and may be inaccurate. In many cases, symptoms caused by physiological stress are not advanced enough to be visual at the time of assessment (Nilson, 1995). Ideally a method is required that is accurate, non-destructive and simple to use at the spatial scale of the canopy rather than the leaf (Curran *et al.*, 1991). A quick method to determine the status of N in plant tissue could be valuable to improve N fertiliser practices (Sembiring *et al.*, 1998). Measuring the reflectance of the leaf pigments, *in situ*, thus, offers the possibility of rapidly estimating crop nitrogen status and therefore crop productivity.

Satellite or aircraft remote sensing can provide detailed, spatially distributed information on crop growth and condition for an individual field or many fields within an agricultural region. Such information can be useful in a variety of applications, including directing precision farming activities and estimating crop production. For most of these applications one must interpret the remotely sensed data (usually in the form of surface reflectance) in terms of some plant canopy physical characteristic (such as LAI or percent ground cover) that is indicative of the state of the crop. One popular approach that has been applied to many different crops has been the development of empirical relationships between remotely sensed and observed plant canopy data. In this approach a mathematical curve is statistically fit to a set of paired measurements of surface reflectance and the plant canopy characteristic of interest. The success of this approach is dependent on the ability to collect one or more field data sets of sufficient quality to support a robust fit between the remotely sensed and plant canopy measurements. However, since the field data sets incorporates the effects of factors (such as soil colour, sun angle, row spacing and row orientation) that may be specific to the region in which the field studies were conducted, the resulting empirical relationships may be less accurate when applied to other regions (Maas, 1998).

1.2 Aim

To develop a methodology to evaluate the nitrogen status of three annual crops using non-destructive, inexpensive remote sensing techniques.

1.3 Objectives

- To correlate the spectral reflectance with nutrient stress from individual pot experiments.
- Using the resulting data to improve spectral classification of canopy reflectance and, thus, early detection of nitrogen deficiency.

1.4. Rationale and value of the research project

Spectral reflectance of leaves provides several options for the derivation of their structure and physiology by quantifying the patterns in the visible, the near infrared, and the red-near-infrared contrast. The remote sensing of chlorophyll content is expected to be a valuable tool in the evaluation of plant nitrogen status and is of great interest in agricultural communities because nitrogen stress is often an important limitation of crop productivity. Thus, accurate spectral characterization at both the leaf and the canopy levels would allow improved optical determination of N deficiency (Peñuelas *et al.*, 1994 and Fillela *et al.*, 1994).

The relationship between leaf reflectance spectra and nitrogen status of crops has been extensively researched (Balkeman, 1990; Peñuelas *et al.*, 1994; Fillela *et al.*, 1994 and Blackmer *et al.*, 1996). However, no simple, easy to use, non-destructive methodology for early detection of nitrogen deficiency in crops has been developed yet. The aim of this study is to develop a methodology to determine nitrogen status under controlled greenhouse conditions. This methodology will, in a later study, be further developed to be utilized under normal field conditions to assess crop nitrogen status.

CHAPTER 2

Literature study

2.1. Optical properties of vegetation canopies

2.1.1 Introduction

Knowledge of how solar radiation interacts with vegetation is necessary to interpret and process remotely sensed data of agricultural crops. These properties are best understood by examining leaf structure at a rather fine level of detail. (Guoliang, 1989; Guyot, 1990 and Campbell, 1996).

A cross section of a typical leaf reveals several layers (fig. 2.1):

- The uppermost layer (epidermis) consists of specialised cells fitting closely together without openings or gaps between the cells. The cuticle, a waxy translucent layer, covers this.
- The lower epidermis, similar to the upper epidermis protects the underside of the leaf except that it includes openings (stomata) that permit the movement of air into the interior of the leaf.
- On the upper side of the leaf just below the epidermis is the palisade tissue consisting of vertically elongated cells arranged in parallel, at right angles to the epidermis. Palisade cells include chloroplasts (cells composed of chlorophyll and other pigments active in photosynthesis).
- Below the palisade tissue is the spongy mesophyll tissue, which consists of irregularly shaped cells separated by interconnected openings. The mesophyll has a very large surface area; it is the site for the oxygen exchange necessary for photosynthesis and respiration

Although leaf structure is not identical for all plants, this description provides a general outline of the major elements common to most plants (Campbell, 1996).

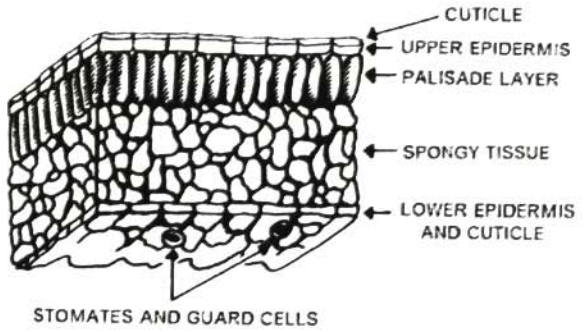

Fig 2.1: Diagram of cross section of a typical leaf (Campbell, 1996).

2.1.2 Reflectance spectra

All of the reflectance spectra of plant leaves have the same shape. Different spectral domains can be considered according to the different leaf optical properties of vegetation, a combination of different energy-matter interactions in the visible and near infrared spectra being responsible for the characteristic spectral reflectance of vegetation (see figure 2.2) (Collins, 1978; Guyot, 1990 and Guoliang, 1989). The amount of reflected light as a percentage of incoming light is usually called the reflectance factor (Nilson, 1995).

In the visible domain leaf reflectance is low (less than 15%). Leaf pigments such as chlorophyll, xanthophyl, carotenoids and anthocyanins absorb the main part of the incident radiation. Chlorophyll does not absorb all the incident sunlight equally. The chlorophyll molecules preferentially absorb blue and red light for use in photosynthesis (as much as 70% to 90% of incident light). Much less of the green light is absorbed (Guyot, 1990 and Campbell, 1996). The interaction of electromagnetic radiation with plant leaves depends on the chemical and physical characteristics of these leaves. The absorption is essentially a function of changes in the spin and angular momentum of electrons, transitions between orbital states of electrons in particular atoms and vibrational rotational modes within polyatomic molecules (Jacquemoud and Baret, 1990).

In the near infrared spectrum, reflection of the leaf is controlled by the structure of the spongy mesophyll tissue (see fig. 2.3). The cuticle and epidermis are almost completely transparent to infrared radiation, so very little infrared radiation is reflected from the outer portion of the leaf.

Radiation passing through the upper epidermis is strongly scattered by optical density boundaries within the mesophyll tissue and cavities within the leaf. Very little of this infrared energy is absorbed internally - most (up to 60%) is scattered upwards (reflected energy) or downwards (transmitted energy). Thus the internal structure of the leaf is responsible for the bright infrared reflectance of living vegetation (Collins 1978 and Campbell, 1996).

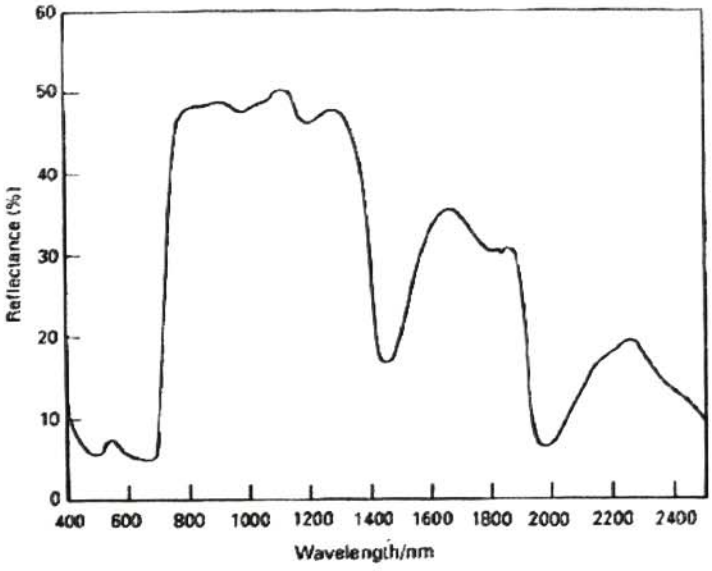

Fig. 2.2: Spectral reflectance function of a typical leaf. After Steven *et al.* (1990).

Although the enhanced reflectivity in the infrared and the absorption in the visible spectrum are due to different processes of energy-matter interaction, they are related insofar as chlorophyll production and mesophyll development are interdependent functions of plant growth and vigour (Collins; 1978).

2.1.3 Factors influencing spectral reflectance of vegetation

Factors influencing leaf optical properties include anatomical structure of the leaf, leaf age, leaf water content and mineral deficiencies. Near-infrared reflectance is strongly influenced by anatomical structure. It depends on the number of cell layers and the relative thickness of the spongy mesophyll. Thus, the leaves of dicotyledons have a higher reflectance than those of monocotyledons having the same thickness because their spongy mesophyll is more developed.

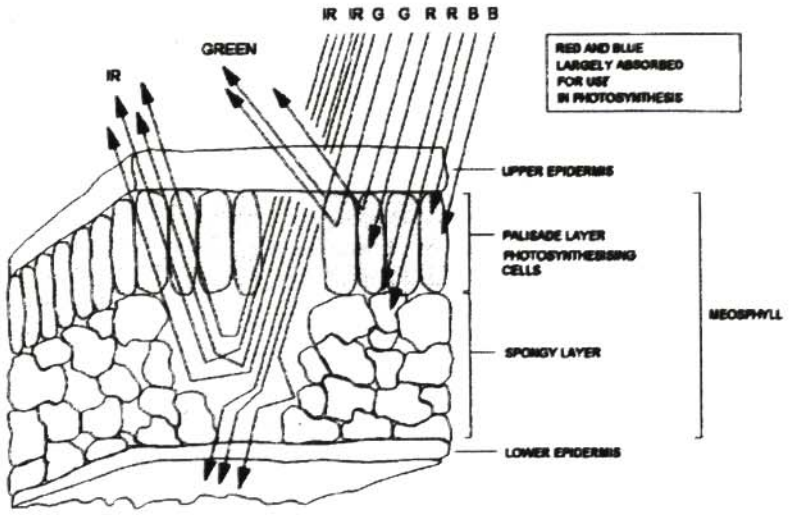

Fig. 2.3: Generalised cross-section through a leaf, illustrating various parts responsible for reflection/ absorption of different components of light. (Scurlock *et al.* 1995; Campbell, 1996).

During the major part of their life the leaves of plants have practically constant optical properties. Laboratory studies of reflectance from single leaves showed that pubescence, growth-regulating chemicals, nutrient supply in the soil, position of the leaf on the plant, thickness and water content, salinity and physiological age of the leaf affect absorption, transmission and reflection of light by plant leaves, as do several other physiological factors (Leamer *et al.*, 1978). Leaf water content has an indirect effect on the visible and near-infrared reflectance because it affects leaf turgor. Thus, a decrease in leaf water content induces an increasing reflectance in the whole spectrum (Guyot, 1990).

As a plant is subjected to stress by disease, insect attack or moisture or nutrient shortage, the spectral characteristics of the leaf may change (Campbell, 1996). Mineral deficiencies mainly affect leaf chlorophyll content. Chlorosis, caused by iron and nitrogen deficiency is the most common phenomenon. Nitrogen deficiency changes the whole reflectance spectrum. The visible reflectance is increased (due to decreasing chlorophyll content) and the near-infrared reflectance is decreased (due to decreasing number of cell layers) (Thomas *et al.*, 1972 and Guyot, 1990).

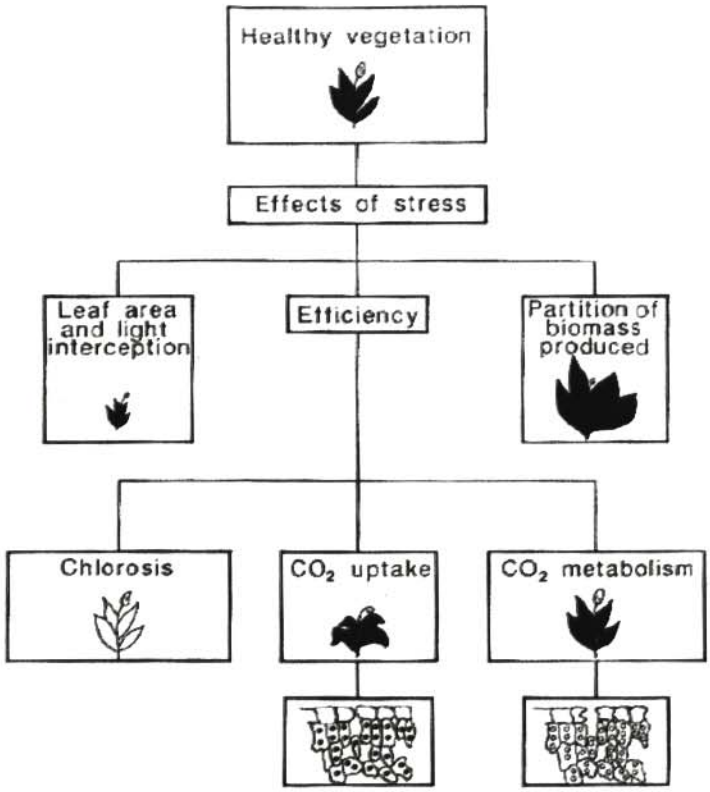

Fig. 2.4. Schematic model of vegetation response to stress. After Steven *et al. (1990)*.

2.2 Assessment of different techniques of detecting Nitrogen status in crops.

The term remote sensing is usually restricted to instruments that measure electromagnetic radiation reflected or emitted from an object. Techniques for recording information in non contact sensing include: cameras with films and filters in differing combinations; specialised electronic instruments like radiometers, video systems etc. and various platforms at different heights above the vegetation canopy (Nilson, 1995).

2.2.1 Introduction

According to Tucker (1979) the use of photographic infrared and red linear combinations for monitoring vegetation biomass and physiological status have become common in the remote sensing community. The use of a near infrared/ red ratio method for estimating biomass or leaf area index (LAI) was first reported by Jordan (1969).

A number of spectral indicators have been proposed for the purpose of estimating crop growth and yield. They include individual band reflectance factors, linear combinations of bands by multiple regression, and ratios of infrared and red bands (Dusek *et al.*, 1985).

Reflectance measurements on canopies are generally achieved with broadband radiometers (bandwidths wider than 60nm). These spectral bands are similar to those of earth observation satellites. These measurements have aided the interpretation of satellite data by establishing relationships between biological parameters and spectral measurements.

It is impractical to measure the chlorophyll concentration of the canopy as a whole and so the majority of studies have related the concentration of chlorophyll in sample leaves to the red edge of the canopy. Such studies are undertaken on the assumption, implicit in laboratory studies of an optically thick and/or spatially invariant biomass. Where this assumption is violated and biomass varies spatially the red edge of the canopy will be more sensitive to the chlorophyll content of the canopy than the chlorophyll concentration of its leaves (Pinar *et al.*, 1996).

Leaf chlorophyll concentrations are strongly correlated with plant N concentration, which is a good predictor of yield potential because of the association between photosynthetic activity and leaf N. The commercial availability of hand-held metres that measure light transmission through a leaf has recently been used with reasonable success to predict leaf traits and crop N sufficiency on crops (MacKown and Sutton, 1998).

The measurement of N content involves destructive sampling, drying, weighing and grinding of samples by either wet Kjeldal oxidation or dry oxidation automated analysis. The whole procedure is labour-intensive and time consuming, and requires the use of large amounts of potentially hazardous chemicals. There have also been attempts to predict plant N by non-destructive methods such as remote sensing techniques involving multi-spectral reflectance data recording and laser-induced chlorophyll fluorescence coupled with various prediction models. However, these methods involve sophisticated and expensive equipment and also demand expertise (Ladha *et al.*, 1998).

The use of broad bands is justified if the spectral characteristics of objects have no high frequency variations in terms of wavelength. This is usually the case for vegetation in the visible and near infrared domains. However, a number of features on the spectral signature of vegetation are too fine to discriminate using broadband sensors (Steven *et al.*, 1990). For instance, reflectance increases very rapidly at the boundary between the visible and near infrared spectral domains (670-760nm, the red edge) and therefore the above assumption may not be valid.

The use of fine spectral features reduces ambiguity of the spectral signal by helping to eliminate or reduce the effects of background variables. Much of the value of high spectral resolution lies in its ability to represent the slopes of absorption bands. These slopes correspond to regions of competing effects and are sensitive to small changes. Reflectance measurements of leaves using high-resolution laboratory spectrophotometers have related the maximum slope of the red edge to the chlorophyll content. With a decrease in chlorophyll content, the maximum slope shifts to shorter wavelengths by 10-30nm, depending on the particular species and on the relative variation of chlorophyll content (Baret *et al.*, 1987 and Steven *et al.*, 1990).

Richardson *et al.* (1992) compared aerial video and hand-held ground reflectance measurements of nitrogen treatments on sorghum. It was found that the ground reflectance measurements were better related to plant growth measurements than aerial video reflectance measurements. The results indicated that the video reflectance data did not have the necessary radiometric precision to respond to subtle reflectance differences for plant growth developmental stages as compared with that of the ground reflectance measurements.

Wiegand *et al.* (1992) concluded that vegetation indices from videographic systems correspond to those made with a hand-held spectroradiometer calibrated to yield reflectance factors. It was found that the automatic gain control in the video cameras make the processing of data and the comparison of vegetation indices among different dates more difficult than hand-held radiometer measurements. Possible solutions to this problem include obtaining calibrated hand-held observations simultaneously with the aerial video observations and to use fixed gains on the video cameras.

Everitt *et al.* (1992) concluded that aerial video data and ground reflectance measurements were equally related to herbaceous cover measurements on rangeland study sites. Red reflectance and video values were inversely related to ground cover and NDVI reflectance and video values were directly related to ground cover.

2.2.2 The Red Shift (red edge)

Collins (1978) reports the results of studies that show changes in the spectral response of crops as they approach maturity. His research used high-resolution multi-spectral scanner data of numerous crops at various stages of the growth cycle. The research focussed on the far-red region of the spectrum, where chlorophyll absorption decreases and infrared reflection increases. In this region (between 690-750nm), the spectral response of living vegetation increases sharply as wavelength increases.

Several studies (Collins, 1978; Curran *et al.*, 1991; Railyan *et al.*, 1993 and Fillela *et al.*, 1994) observed that, as crops approach maturity, the position of the chlorophyll absorption edge shifts towards longer wavelengths, a change referred to as the "red edge". The red edge is a unique feature of green vegetation because it results from two special optical properties of plant tissue, high interval leaf scattering causing large near infrared reflectance and chlorophyll absorption resulting in low red reflectance (Nilson, 1995).

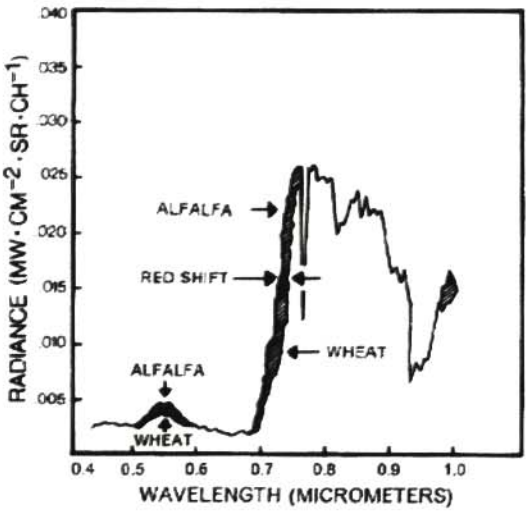

Fig. 2.5: Red shift. The absorption edge of chlorophyll shifts towards longer wavelengths as plants mature. The shaded area

represents the magnitude of the shift as the differences between the spectral response of headed wheat and mature alfalfa. Similar shifts have been observed in other plants (After Collins, 1978).

Collins (1978) suggests that one of the causes for the red shift lies in the type of chlorophyll present in the plant. Chlorophyll A appears to increase in abundance as the plant matures. Increased concentrations change the molecular form in a manner that adds absorption bands to the edge of the chlorophyll A absorption region, thereby producing the red shift.

Studies estimating the chlorophyll content of green leaves utilising reflectance spectra rely strongly on the correlation between chlorophyll concentration and the point of maximum slope (red edge) (Pinar and Curran, 1996). An increase in chlorophyll concentration causes a broadening of the chlorophyll absorption feature and this, in turn will move the long wavelength boundary of the absorption feature and thereby the red edge to longer wavelengths (Munden *et al.*, 1994; Fillela *et al.*, 1994 and Pinar *et al.*, 1996).

Curran *et al.* (1990) found a linear relationship between the red edge position and chlorophyll content of slash-pine leaves. The red edge was used to estimate the chlorophyll content of branches with a rms error of 7.44 mg, which was slightly more than half the error associated with the colorimetric determination of chlorophyll content.

Plant leaves experiencing nutrient stress (deficiency) produce less chlorophyll A. This results in an inhibition of the normal chlorophyll absorption spectrum and, thus, an apparent shift of the red edge to shorter wavelengths (Collins, 1978 and Milton *et al.* 1991).

The red edge is highlighted in the reflectance derivative curve (Fillela *et al.*, 1994). The classical method of reducing background noise is to take the ratio or the difference at two wavelengths. With this technique the analytical signal at a wavelength in an absorption band is normalised by the signal at another wavelength where there is no specific absorption, close to the analytical wavelength. Any level background signal will be similar at both wavelengths and will be eliminated when the ratio or the difference is taken. Thus, band-ratios (for example near infrared/ red ratio) and related spectral indices are more useful than individual bands (Demetriades-Shah *et al.*, 1990).

Ratios and differences at different wavelengths will, however, only correct background signals completely if these signals are spectrally level or have a constant slope from one sample to another. Soil reflectance, for instance, is not spectrally level but increases gradually from the visible to the near infrared. Also, this rate of increase differs for different soils. A more elegant technique to deal with the problem of background signal is the derivative spectrum. The derivative spectrum is the rate of change with respect to wavelength. In remote sensing mostly the first derivative has been used so far to facilitate the location of the critical wavelengths such as the red edge (Demetriades-Shah *et al.*, 1990).

The calculation of derivative spectra eliminates additive constants (for example illumination changes) and reduces linear functions such as an increase in background reflectance with wavelength to constants. This has led researchers to conclude that the red edge is essentially invariant with illumination or the amount of background within the field of view of a spectroradiometer (Curran *et al.*, 1990 and Demetriades-Shah *et al.*, 1990).

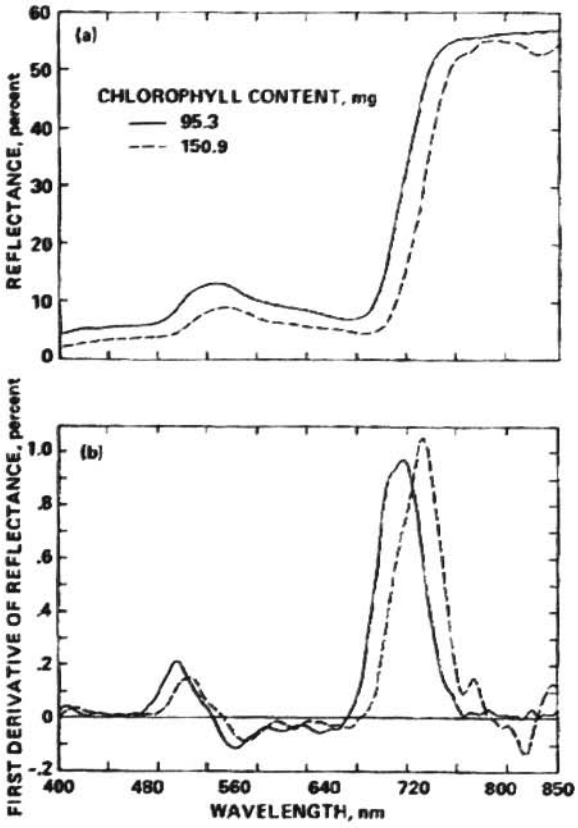

Fig. 2.6. The reflectance spectrum (a) and derivative spectrum (b) of two slash pine branches. Note that the higher chlorophyll content associated with a red/near-infrared boundary that is displaced toward longer wavelengths in

(a) and a derivative maximum that is displaced toward longer wavelengths in (b). After Curran *et al.* (1990).

Railyan (1993) found that the red edge slope and position vary continuously throughout the growing season. Its near and far boundaries are shifted towards the long wavelength region of the spectrum during the vegetative stage, and towards shorter wavelengths during the reproductive stage.

Demetriades-Shah *et al.* (1990) suggested that derivatives of vegetation canopy spectral reflectance might be useful in remote sensing for eliminating the effects of soil background reflectance and canopy architecture, thereby improving the estimation of certain variables such as leaf chlorosis, which can be an indication of nitrogen shortage.

It has been shown that chlorophyll is not the only factor that determines the shape of the red edge peak in the reflectance derivative curve. Boochs *et al.* (1990) identified two components to be responsible for the position and shape of the red edge peak: chlorophyll content, that causes changes around 700nm and scattering properties, that affect the spectrum at longer wavelengths. Water stress is another factor that could also affect the shape of the red edge peak in the first derivative curve because water stress affects near infrared reflectance through structural and, therefore, scattering changes (Fouchè *et al.*, 1994 and Fillela *et al.*, 1994).

Fillela *et al.* (1994) found that pepper plants experiencing nitrogen stress exhibited a red edge shift towards shorter wavelengths and a slight decrease in the amplitude of the first derivative red edge peak. Demetriades-Shah *et al.* (1990) have found that the use of derivative spectra for monitoring chlorosis induced by nitrogen deficiency in sugar-beet is superior to conventional broadband spectral indices such as the NIR/R ratio. Milton *et al.* (1991) observed that phosphorus deficient soybean plants show higher reflectance in the 500-650nm portion of the spectrum than those of the control plants, and the red edge is observed at shorter wavelengths.

Keegan, quoted by Collins (1978), reported in laboratory observations a rounding effect on the shoulder of the absorption edge in the near infrared spectra of plants experiencing disease (wheat rust) stress.

Collins (1978) observed a spectral shift of 7-10nm toward longer wavelengths, in the spectra of wheat and sorghum crops in the green-headed stage. Munden *et al.* (1994) found a linear relationship between chlorophyll concentration and yield, and an asymptotic relationship between red edge and yield in wheat. They were able to use the red edge to estimate chlorophyll concentrations up to 0.5 mg/g and yield up to 6 t/ha. Pinar *et al.* (1996) found the red edge of a grass canopy to be strongly correlated with chlorophyll content.

The red edge region is considered a transition region that, when using wide spectral bands of the order of 50nm or more, does not contain information useful in remote sensing of vegetation canopies. This is because broad bands are insensitive to the small chances in wavelength intensity that are present in this region (Collins, 1978).

Differentiation can be used to estimate the different plant pigments of intact vegetation canopies. Such measurements may be important for the detection of different types of stresses. For example, a variation in the chlorophyll a/b ratio has been shown to be related to soil N availability (Collins, 1978).

2.2.3 Vegetation Indices

Red and photographic infrared spectral data have been demonstrated by various workers (Tucker, 1979; Tucker *et al.*, 1980; Dusek *et al.*, 1985; Yuzhu, 1990 and Peñuelas *et al.*, 1994) to be highly correlated with the photsynthetically active biomass of vegetation. The red spectral data are highly correlated with the chlorophyll concentration whereas the photographic infrared data are highly correlated with the green leaf area index (LAI). Thus various linear combinations of these two adjacent spectral regions are highly related to the photsynthetically active biomass (Tucker *et al.*, 1980). Tucker (1979) concluded that the IR/red ratio and related IR and red linear combinations were superior to the green/red ratio. The IR/red ratio, square root of the IR/red ratio, IR-red difference vegetation index and the transverse vegetation index are sensitive to the amount of photosynthetically active vegetation present in the plant canopy.

Vegetation indices are quantitative measures, based on digital values, which attempt to measure

biomass or vegetative vigour. Usually a vegetation index is formed from a combination of several spectral values that are added, divided, or multiplied in a manner designed to yield a single value that indicates the amount of vigour of vegetation within the pixel. High values of the vegetation index identify pixels covered by substantial proportions of healthy vegetation. The simplest form of vegetation index is simply a ratio between two digital values from separate spectral bands. Some band ratios have been defined by applying knowledge of the spectral behaviour of living vegetation (Campbell, 1996).

Band ratios are quotients between measurements of reflectance in separate portions of the spectrum. Ratios are effective in enhancing or revealing latent information when there is an inverse relationship between two spectral responses to the same biophysical phenomenon. If two features have the same spectral behaviour, ratios provide little additional information, but if they have quite different spectral responses, the ratio between the two values provides a single value that concisely expresses the contrast between the two reflectances.

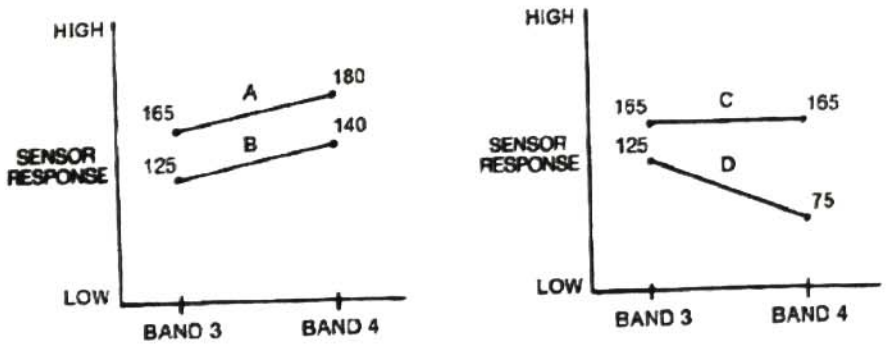

Fig. 2.7: Example of band ratios. Four hypothetical materials are observed in two spectral bands. Materials A and B have similar patterns of response in bands 3 and 4. Ratios therefore reveal little about the differences between them. For A the ratio of band 3 to band 4 is 0.916 (165/180); for B, it is 0.89 (125/140). The relationship between C and D is quite different, and the ratio clearly reveals the contrast between the two materials. For C it is 1.00 (165/165); For D it is 1.67 (125/175). From Campbell (1996) p. 461.

For living vegetation, the strategy of deriving ratios has been found to be especially effective because of the inverse relationship between the vegetation brightness in the red and infrared spectral region (Tucker, 1979 and Tucker *et al.*, 1980). That is, absorption of red light (R) by chlorophyll (and therefore chlorophyll concentration), and strong reflection of infrared (IR)

radiation by mesophyll tissue (which is highly correlated with LAI) ensures that the red and near infrared values will be quite different and that the ratio (R/IR) will be high (Tucker *et al.*, 1980 and Campbell, 1996). Non vegetated surfaces, including bare soil and dead or stressed vegetation, will not display this specific spectral response, and the ratios will decrease in magnitude. Thus, the IR/R ratio can provide a measure of the importance of vegetative reflectance within a given pixel.

The use of an IR/R ratio method for establishing biomass or LAI was first reported by Jordan in 1969 who used a radiance ratio of 800/675nm to derive the LAI of forest canopies in a tropical rain forest (Tucker, 1979).

Kanemasu (1974) found that IR/R ratio is not influenced by solar elevation. This enabled him to compare the reflectance ratios of wheat, soybeans and sorghum over a large portion of the growing season without serious error due to changes in sun angle. The Normalized difference Vegetation Index (NDVI) appears to be almost insensitive to variations in canopy geometry (Tucker, 1978 and Kanemasu *et al.*, 1990). It was found that the reflectance ratio of a crop over a growing season followed the LAI curve. The ratio increased above unity (ratio equalling 1.0) at a LAI of about 1.0 and remained above unity during maximum growth, then decreased to below unity at maturity (LAI < 1.0) (Tucker, 1979 and Kanemasu *et al.*, 1990). Kanemasu *et al.* (1990) found that the relationship between the NDVI and the fraction of solar energy intercepted by the crop is near-linear and appears to be less sensitive to variations in canopy structure and soil background reflectance.

Kanemasu (1974) concluded that the 545/655nm wave bands provided useful information regardless of crop type. For all crops studied, the green/red ratio closely followed crop growth and development and appeared to be more desirable than the near infrared reflectance as an index of growth.

The IR/R ratio is only one of many related measures of vegetation vigour and abundance. The green/red (G/R) ratio is based on the same concepts as used for the IR/R ratio, although it is considered to be less effective. These ratios can be applied to any remote sensing system although

most of the research on this topic has been conducted using Landsat MSS data. Dusek *et al.* (1985) reported better correlations between different plant parameters and several ratio indices than for the individual band reflectance factors. One of the most widely used vegetation indices is known as the Normalised Difference Vegetation Index (NDVI):

$$NDVI = \frac{IR + R}{IR - R}$$

This index in principle conveys the same kind of information as the IR/R and G/R ratios but is defined to produce desirable statistical properties in the resulting values. The simple IR/R ratio could be used as a measurement of relative greenness, but location and cycle deviations could introduce a large error component (Tucker 1978). These indices have physical significance in that the IR reflectance increases and the red reflectance decrease with increasing vegetation (Dusek *et al.*, 1985 and Campbell, 1996).

Tucker (1978) concluded that combinations of the red and near infrared bands are more sensitive to photsynthetically active biomass or green leaf area percent than combinations of green and red bands. Combinations investigated include: IR/R ratio, the square root of the IR/R ratio, the NDVI and the TVI.

$$TVI = \sqrt{\frac{IR - R}{IR + R} + 0.5}$$

Guoliang (1989) concluded that R and IR radiance measurements were significantly correlated with corn and soybean total wet biomass, percentage crop cover, plant height, percentage chlorosis, and percentage leaf area, all of which are likely to be correlated with one another.

Jackson, quoted by Guoliang (1989), commented that an ideal vegetation index would be highly sensitive to vegetation, insensitive to soil background changes, and only slightly influenced by atmospheric path radiance. None of the indices examined fully met these criteria. It appears that no one index can optimally assess vegetation over an entire growing season, and that two or more indices may be required.

2.2.4 Image Classification

Digital image classification is the process of assigning pixels to classes. The overall objective of image classification procedures is to automatically categorise all pixels in an image into themes. Normally, multi-spectral data is used to perform the classification and each pixel is treated as an individual unit composed of values in several spectral bands. The spectral pattern present within the data is used as the numerical basis for categorisation. That is, different feature types manifest different combinations of digital numbers based on their inherent spectral reflectance and emmittance properties (Lillesand *et al.*, 1987 and Campbell, 1996).

The term classifier refers loosely to a computer program that implements a specific procedure for image classification.

The simplest form of image classification is to consider each pixel individually by assigning it to a class based on its several values measured in separate spectral bands. Sometimes such classifiers are referred to as spectral or point classifiers because they consider each pixel a "point" observation. Although point classifiers offer the benefit of simplicity and economy, they are not capable of exploiting information contained in relationships between each pixel and those that neighbour it (Campbell, 1996).

2.2.4.1 Supervised Classification

Supervised classification can be defined informally as the process of using samples of known identity to classify pixels of unknown identity (Campbell, 1996). In this type of classification, the image analyst "supervises" the pixel categorisation process by specifying, to the computer algorithm, numerical descriptors of the various themes present in the scene. To do this, representative sample sites of known themes, called training areas, are used to compile a numerical "interpretation key" that describes the spectral attributes for each feature type of interest. Each pixel in the data set is then compared numerically to each category in the

interpretation key and labelled with the name of the category it "looks most like" (Lillesand *et al.*, 1987).

To obtain meaningful and accurate image classifications, careful choice of the relevant wavebands, the location of small but representative training areas, the determination of the relationship between object type and digital number (DN) in the chosen wavebands, the extrapolation of these relationships to the whole image data set and the display and accuracy assessment of the resultant images must be observed (Curran, 1985).

2.2.4.2 Unsupervised Classification

Like supervised classifiers, the unsupervised procedures are applied in two separate steps. The fundamental difference is that supervised classification involves a training step followed by a classification step. In the unsupervised approach, the image data are first classified by aggregating them into natural spectral groupings or clusters present in the scene. Then, the image analyst determines the theme identity of these spectral groups by comparing the classified image data to ground reference data (Lillesand *et al.*, 1987).

Spectral groupings can be achieved using several readily available statistical packages of which 'cluster analysis' has proved to be the most popular. This works by locating the desired number of cluster centres in the waveband to waveband measurement space and continues to move the cluster centres until the clusters have maximum statistical separability. The results of this classification are dependent upon the number of classes that are initially chosen (Curran, 1985).

A typical sequence of classification might begin with the analyst specifying minimum and maximum numbers of categories to be generated by the classification algorithm. The classification starts with a set of arbitrarily selected pixels as cluster centers (centroids). The classification algorithm then finds distances between pixels and forms initial estimates of cluster centers as permitted by the constraints specified by the analyst. In the next step, all the remaining pixels in the scene are assigned to the nearest class centroid. To begin the next step, the algorithm finds new centroids for each class, then the entire scene is classified again, with each pixel assigned to

the nearest centroid. Again new centroids are calculated; if the new centroids differ from those found in the preceding step, the process repeats until there is no significant change detected in locations of class centroids and all the classes meet all constraints required by the operator (Campbell, 1996).

The advantages of an unsupervised classification method are that no extensive prior knowledge of the region is required, the opportunity for human error is minimalised and unique classes are recognised as distinct units. The disadvantages are that the classes generated by the classification do not necessarily match the classes intended by the operator and there is little control over the classes and their specific identities (Campbell, 1996).

CHAPTER 3

Research methodology and research instruments

3.1 Soil and soil preparation

Two soil samples of the Hutton form (MacVicar, 1991) were utilised in this experiment. Both samples were collected at the Syferkuil experimental farm of the University of the North. Soil collected were not recently exposed to any fertilizer treatment.

The soil was dried and passed through a 2mm sieve after which it was analysed for inherently present nutrients (N, P and K) as well as pH. Nitrogen was determined using the Kjeldal method, phosphorous, using Bray-1 extraction and spectrography, potassium using ammonium acetate extraction and atomic absorption spectrophotometry and pH using water extraction (refer to addendum A for methodology).

Table 3.1: Nutrient status of soil samples used in pot trials.

Sample	N (mg kg^{-1} soil)	P (mg kg^{-1} soil)	K (mg kg^{-1} soil)	Ca (mg kg^{-1} soil)	Mg(mg kg^{-1} soil)	Na (mg kg^{-1} soil)	pH_{H2O}	pH_{KCl}
1	68	23.5	456				5.86	4.78
2	27.2	17.1	382.4	360	406.6	16	6.13	

Table 3.2: Optimum fertiliser requirements of experimental crops at selected projected yields.

Crop type	Projected yield(t ha^{-1})	Optimum N (kg ha^{-1})	Optimum P (kg ha^{-1})	Optimum K (kg ha^{-1})
Tomato (*Lycopersicon esculentium*)	35	120	80	30
Sunflower (*Helianthus annuus*)	3	87	26	0
Burley tobacco (*Nicotiana tabacum*)	2.5	220	110 (irrigated, >20 mg kg^{-1} P already available)	120 (irrigated, >175 mg kg^{-1} K already available)

(Buys et al. 1991)

3.2 Pot Trials

The weight of 1ha of soil at 30cm plough depth was calculated at a soil bulk density of 1.33g cm^{-3} (Buys et al. 1991):

$$100m \times 100m \times 0.3m \text{ (plough depth)} \times 1333kg\ m^{-3} \text{ (bulk density)} = 3.999 \times 10^{6}\ kg\ ha^{-1}$$

The weight of the soil in one 20cm diameter plastic planting pot used in the trial was 4kg. The ratio of one pot to one hectare was thus calculated to be:

1: 999 750

Utilising this ratio, plastic pots (20cm diameter) with drainage holes at the bottom and drip trays were filled with the selected soil samples. The soil was fertilised optimally for all nutrients except nitrogen. Nitrogen was added at four different rates ranging from zero to optimum (Thomas and Oerther, 1972). Four replicates of each treatment were introduced under controlled greenhouse conditions.

Fertiliser used in the pot trials were Urea [NH_2COCH_2] (46% N), superphosphate [$Ca(H_2PO_4)$] (10.5% P) and KCl (50% K).

Table 3.3: Fertiliser for Sunflower pot trial (soil sample 2)

Pot no.	Urea (kg ha^{-1})	N (g)/pot	Superphosphate (kg ha^{-1})	P (g)/pot	KCl (kg ha^{-1})	K (g)/pot
S1	0	0	70.98	0.2477	0	0
S2	63.1	0.0631 (equivalent to 29 kg ha^{-1})	70.98	0.2477	0	0
S3	126.1	0.1261 (equivalent to 59 kg ha^{-1})	70.98	0.2477	0	0
S4	189.2	0.1892 (equivalent to 87 kg ha^{-1})	70.98	0.2477	0	0

Table 3.4: Fertiliser for Tomato pot trial (soil sample 2)

Pot no.	Urea (kg ha^{-1})	N (g)	Superphosphate (kg ha^{-1})	P (g)	KCl(kg ha^{-1})	K (g)
T1	0	0	761.91	0.7621	60	0.0600
T2	86.98	0.0870 (equivalent to 40 kg ha^{-1})	791.91	0.7621	60	0.0600
T3	173.91	0.1740 (equivalent to 80 kg ha^{-1})	761.91	0.7621	60	0.0600
T4	260.87	0.2609 (equivalent to 120 kg ha^{-1})	761.91	0.7621	60	0.0600

Table 3.5: Fertiliser for Tobacco pot trial (soil sample 1)

Pot no	Urea (kg ha^{-1})	N (g)	Superphosphate (kg ha^{-1})	P (g)	KCl (kg ha^{-1})	K (g)
TOB1	0	0	1047.6	0.5372	240	0.1231
TOB2	159	0.0818 (equivalent to 73.3 kg ha^{-1})	1047.6	0.5372	240	0.1231
TOB3	318	0.1635 (equivalent to 146.6 kg ha^{-1})	1047.6	0.5372	240	0.1231
TOB4	478	0.2453 (equivalent to 220 kg ha^{-1})	1047.6	0.5372	240	0.1231

The fertiliser was weighed into glass beakers using a Mettler AC100 balance that is accurate up to 0.0001g. Distilled water was added and the fertiliser salts were allowed to dissolve. The soil was weighed with a Mettler PE6000 balance accurate up to 0.01g.

The soil was spread out in a black refuse bag and the fertiliser solution (drawn up in a 100ml pipette) was evenly sprinkled onto the soil surface. The bag was closed and the soil and fertiliser solution thoroughly mixed. This process was repeated three to four times until all the fertiliser was mixed with the soil and the soil was evenly moistened.

Coarse sand was put at the bottom of each pot to ensure good drainage. The prepared soil was then added to the pot and lightly firmed. Tomato and sunflower seeds were sown in the respective pots and tobacco seedlings were planted. The soil was watered regularly to ensure it being moist

at all times.

After germination, reflectance data were collected at different growth stages of the crop. Data collection was made with various optical instruments in full sunlight, between 10h00 and solar noon on days when there was no visible cloud cover (Collins, 1978; Dusek *et al.*, 1985 and Munden *et al.*, 1994). Measurements were made on cloudless days resulting in similar irradiances during each instance of data collection (Filella *et al.*; 1994). Leaf samples were collected from the same relative position on the plants at the same time that optical sampling took place. The leaf samples were analysed for total N content making use of the micro Kjeldal method (see addendum A).

Plants were allowed to mature up to the stage of formation of flower heads. After the onset of flower formation, the entire plant was harvested and dried to a constant weight at 60°C and analysed for total N content using the micro-Kjeldal method (see addendum A).

3.3 Instruments used in reflectance data collection:

3.3.1 Kodak Professional DCS420 digital camera

The Kodak DCS420 digital camera was used to obtain colour infrared imagery of the pot experiments. The resultant images have three bands (green, red and near infrared). Because the imagery is already in digital format, results are available instantaneously and there is no delay before interpretation is possible.

The camera uses a charged-coupled device (CCD) as a sensor. A CCD is a shift register formed by a string of closely spaced metal oxide semiconductor (MOS) capacitors. It can store and transfer analogue charge signals introduced optically. When light is incident on a CCD array, photons cause a release of electrons from each MOS capacitor and a signal proportional to the radiation is collected in its potential well (Warner *et al.*, 1996).

The digital camera allows an image to be imported directly into the host computer. Unlike still video systems, the DCS420 digital camera does not require a frame grabber or other special

equipment.

The system uses an unmodified Nikon 801S camera body that retains all the usual features. The full range of Nikkor lenses can be used, but since the CCD image sensor is only 9.3 x 14 mm it effectively multiplies the focal length by a factor of 2.6 (Warner *et al.*, 1996).

3.3.1.1 Data acquisition

The Kodak DCS 420 camera was used with 20mm infrared lens to acquire three-band infrared images of each plant in the pot trial. The lens has a built-in filter to filter out blue and ultra violet light. The camera was set with an ISO speed of 400 and an f-stop opening of 8. Photographs were taken of the crown of each plant.

3.3.2 Ocean Optics S2000 Spectrometer

The spectrometer (fig.3.1a) was used to obtain a continuous reflectance spectrum of the vegetation canopy. This spectrum covers wavelengths in both the visual and near infrared domain of the spectrum (200-1100nm).

The S2000 has a compact optical bench coupled to a 2048-element linear CCD-array detector (fig.3.1b), making it especially useful for applications that demand high detector sensitivity. The S2000 accepts light energy transmitted through single-strand optical fibre and disperses it via a fixed grating across the CCD array, which is responsive from 200-1100nm (Ocean Optics, 1998).

The instrument is connected to a NoteIT pentium laptop computer using a DAQ700 PCI card. Reflectance spectra can be accessed and analysed using the Ocean Optics IOOBASE software. Data can also be exported to regular database and spreadsheet programmes for further statistical analysis.

3.3.2.1 Data acquisition

The reflectance spectrum was calibrated with a Labsphere certified reflectance standard to determine 100% reflectance. After calibrating the spectrometer, leaf reflectance of mature leaves at the same relative position on each plant was measured using the IOOBASE software supporting the spectrometer.

The data sets representing the reflectance spectra of the plants were first exported from the IOOBASE programme as an ASCII file with data being separated by commas. This data was imported into the Microsoft Excel software for further data processing.

Fig. 3.1: The Ocean Optics S2000 spectrometer. (a)A and (b)B: Optical cable. (a)B: Optical probe. (b)C: Box containing optical bench and linear CCD-array detector. (b)A: Laptop computer with DAQ700 card.

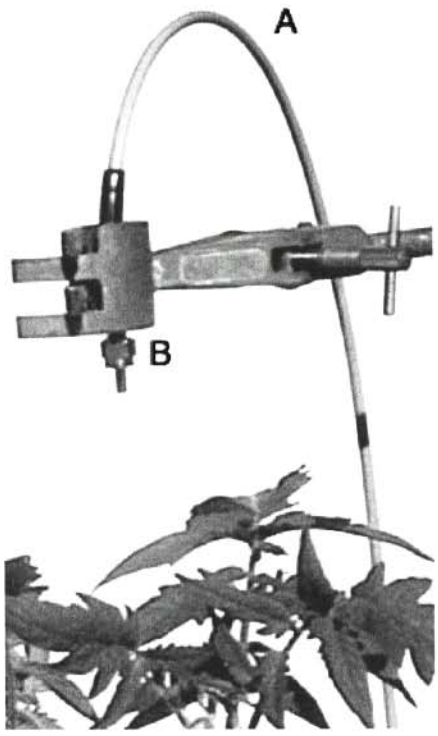

(a)

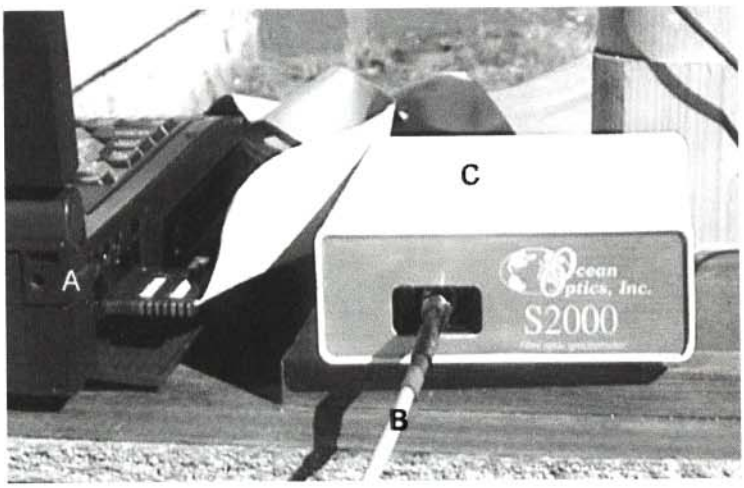

(b)

3.3.3 Multi spectral video camera

The multi spectral video camera obtains imagery at various wavelengths of the spectrum. These wavelengths range from green (450nm) through to near-infrared (770nm).

The MultiSpec Agro-Imager (fig. 3.2(a)) is a common aperture imaging spectrometer system that separates four spectral images spatially on a single image plane. All spectral information is acquired simultaneously and no moving parts are used in image acquisition. Any object of interest can be separated into its component colours represented by the filters placed in the system (450, 550, 650 and 770nm). An objective lens forms an intermediate image of the object of interest. Proprietary optics separates the optical energy into four paths through the system. A separate filter is placed in each of the paths eliminating all the optical energy that is not in the transmission band of the filter. The energy that is allowed to pass through each of the filters is then imaged onto a single detector. After the detector data is acquired, it can be read out and processed in a computer (Optical Insights, 1998).

3.3.3.1 Data acquisition

The MultiSpec AgroImager video camera was connected to a NoteIT Pentium laptop computer via a Snappy frame grabber (fig.3.2(b)) connected to the parallel port of the laptop. The Snappy frame grabbing software was used to save the required images on the hard disk.

Imagery of the foliage of each pot in the trial was obtained and the images were saved as BMP files. The resulting files were opened in the Adobe Photoshop software and an image of each of the four spectral bands that were acquired were cut out and saved individually as a BMP file. These files were imported into the TNTMips image processing software for analysis.

Fig.3.2: (a) Optical Insights AgroImager video camera fastened to a horizontal aluminum boom. (b) Snappy frame grabber hardware connected to the parallel port of the NoteIT pentium computer. The two instruments are connected via a standard video cable.

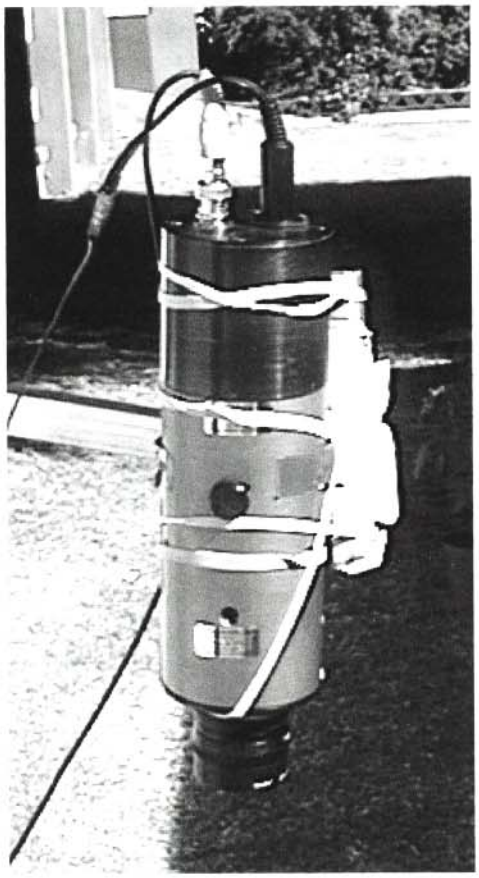

(a)

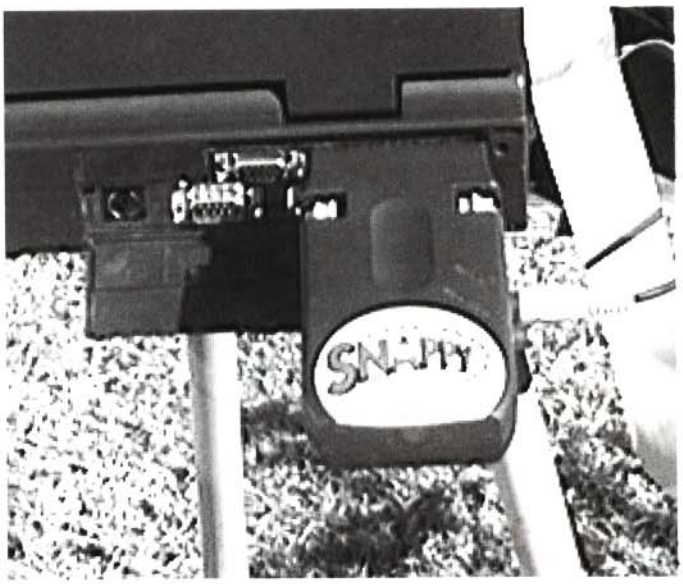

(b)

CHAPTER 4

Data Processing

4.1 Introduction

A Pentium 266 Mhz Personal computer, with 6 Gb HDD, 64 Mb RAM and 12" monitor were used as hardware during processing. TNTlite ver. 6.x and Adobe Photoshop ver. 3.0 were used for image processing and MS Excell was used for statistical analysis.

4.1.2 TNTlite

The TNTlite version of TNTmips is intended for use by students learning about spatial data analysis and its applications.

Principal Limitation:

The TNTlite version of TNTmips is a reduced capacity version of the professional version produced by MicroImages. The principal limitation of TNTlite is that it restricts the size of each spatial object to be studied.

Object Size Limitations:

All TNT software store spatial data as objects in a Project File. The free TNTlite software controls the maximum size of each separate object in a Project File as follows:

- each raster object (pixels of 1 to 128 bits each) is limited to 614x512 = 314,368 cells (pixels) with maximum dimensions of 1024 lines or 1024 columns
- each vector object (topological line structures) is limited to 1500 points, 1500 lines, 500 polygons, and 1500 labels

- each CAD object (overlapping point, line, polygon, and geometric elements) is limited to 500 elements and 5 blocks
- each TIN object (Triangular Irregular Network with topology) is limited to 5000 triangles, 5000 edges, and 1500 nodes
- each relational database is limited to 1500 records per table

The TNT professional software places no limits on the size of the spatial objects or the Project File.

Additional Limitations of the free TNTlite software:

- The spatial objects created and used in Project Files within TNTlite are identical to those used in the TNT professional software except for their size limitations.
- Project Files can be exchanged without conversion and used freely with any other TNTlite software on any kind of computer platform. However, Project Files created with TNTlite software cannot be used in the TNT professional software.
- The TNTlite software also has the facility to import, access and use the data of many other commercial systems. However, all the data conversion and export capabilities to other commercial software have been disabled in the TNTlite software (MicroImages, 1999).

4.2 Kodak professional DCS420 digital imagery

4.2.1 Pre-processing

The digital images obtained by the Kodak DCS420 camera, were imported into a computer utilising Adobe Photoshop software in conjunction with a specialised Kodak Twain software driver. Images were cut and reduced in size and saved as TIFF files. These TIFF files were imported into the TNTlite software for processing and interpretation.

4.2.1.1 Colour conversion

The images were first split into its three components (green, red and near IR) utilising the Convert Colour process from the Process / Raster / Combine menu of TNTlite. When the Convert Colour process is selected, the *Raster Colour Conversions* window opens.

After opening the desired project file and selecting the composite raster to be converted, the RGB option is selected from the output selection. The three components of the output raster object type are listed as fields and a name and description is given for each new raster object (MicroImages, 1999).

4.2.1.2 Raster extraction

Images of individual plants were cut out for further processing utilising the Process/Raster/Extract module and specifying manual resampling. The extraction of these images of individual plants and leaves eliminates the need to classify the background as a separate class.

The *Raster Extract* process was accessed from the Extract option on the Process / Raster menu. The Raster Extract process can be used to manually resample data. The Extraction Area Definition Tools window opens when the Manual extraction method is selected. The manual extraction method allows the user to manually draw an extraction window around the desired areas in the image with CAD sketching tools. The Raster Extract process can be applied to extract all or part of one raster object or identical areas from multiple raster objects (in this instance the green, red and near IR channels). The extraction area is applied to all identical objects when the process is run (MicroImages, 1999).

4.2.2 Data Processing

4.2.2.1 NDVI

The NDVI of each image was calculated utilising the Predefined option on the Process/Raster/Combine cascade (this offers a selection of predefined, standard raster operations).

The Normalised Difference operation creates an output raster object known as the ND or green biomass raster which shows a measure of the difference between the values of two input raster objects A (near IR) and B (red) chosen for comparison. The resulting output raster indicates the vegetation biomass (MicroImages, 1999).

4.2.2.2 Image classification

NDVI images have a digital number (DN) range of -1.0 to +1.0. Three classes were selected for classification. Values lower than +0.1 (high stress) indicate vegetation that is not photosynthetically active (senescent leaves or leaves suffering from severe chlorosis). This is manifested in low absorption of red light and lower near IR reflection. A value between +0.1 and +0.2 (moderate stress) indicates vegetation that has moderate photosynthetic activity. Values higher than +0.2 (low stress) are considered to represent healthy very active plant material and are manifested as very high absorption of red light and very high near IR reflectance (Collins, 1978).

Supervised classification was conducted with the Feature Mapping process initiated by selecting the *Feature Map* option from the Process/Raster/Interpret menu cascade. TNTmips provides Feature Mapping as a hybrid combination of direct photointerpretation and automated image interpretation. The goal of Feature Mapping is to identify, mark, and measure features in a set of processing rasters by combining knowledge of the study site and the processing power of the software (MicroImages, 1999). Refer to Addendum B for the classified images (featuremaps) of the individual plant samples. After classifying the images, an automatic statistical report was

generated with the classification results.

Because of the limitations of TNTlite, some feature rasters could not generate a statistical report because only the first 100 polygons are considered. When this was the case an alternative method was used to determine the number of pixels representing each class.

The feature class raster was displayed in the raster display module. The Raster Histograms option on the Tool dropdown menu in the layer icon row was used to open the Raster Histogram Display window. A graphic display of the histogram in the window as well as analytical information on the cell value distribution for the raster object is displayed. Raster histograms can be viewed for any single-value data type. The cell value information was saved as an ASCII text file and handled in the same way as the statistical report.

4.2.2.3 Interpretation

The statistical report generated by the TNTlite software is saved as an ASCII text file. The text was opened in MS Word and copied to MS Excell for further analysis. In Excell the percentage leaf area of each class was determined. The arithmetic mean value of each replicate was then determined using the AVERAGE function. The resulting values were analysed for correlations with leaf N status utilising the CORRELATE function.

The correlate analysis tool of MS Excell measures the relationship between two data sets that are scaled to be independent of the unit of measurement. The population correlation calculation returns the covariance of two data sets divided by the product of their standard deviations. The Correlation tool can be used to determine whether two ranges of data have a positive or negative correlation with one another (MS Excell, 1996).

To test if the correlation coefficient values are significantly different from 0 (no correlation) a specialized Student's t-test (see chapter 5 for more detail) was applied to all the correlation coefficient values within Excell.

$$t = \frac{\rho\sqrt{2}}{\sqrt{1-\rho^2}}$$

Where ρ = the correlation coefficient.

The resulting values were compared with a student's t-distribution table in Steyn *et al* (1987) to determine if the values are significantly different from zero.

4.3 Ocean Optics S2000 Spectroradiometer data

4.3.1 Pre-Processing

The data sets representing the reflectance spectra of the plants was first exported from the IOOBASE program as an ASCII file with data being separated by commas. This data was imported into the Microsoft Excel software as two columns. Column one represented the wavelength and column two represented the percentage reflectance.

The data for each of the replicates of the four treatments were copied to the same Excel workbook and the mean of the values was calculated. This gave rise to one single spectrum for each treatment.

4.3.1.1 Smoothing

Because the spectral data generated by the spectrometer contained some noise, an exponential smoothing operation was done on the reflectance values before any other operation could be considered.

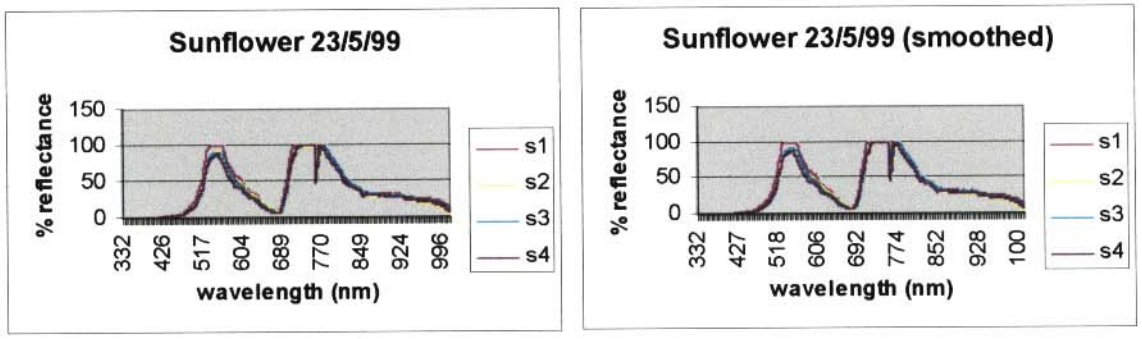

(a) (b)

Fig 4.1: Examples of raw unsmoothed spectra (a) and smoothed spectra (b).

The Exponential Smoothing analysis tool and its formula

$$F_{t+1} = F_t + a(A_t - F_t) = F_t + (1 - dampFact)(A_t - F_t)$$

in MS Excell predict a value based on the forecast for the prior period, adjusted for the error in that prior forecast. The tool uses the smoothing constant a, the magnitude of which determines how strongly forecasts respond to errors in the prior forecast. Values of 0.2 to 0.3 are reasonable smoothing constants. These values indicate that the current forecast should be adjusted 20 to 30 percent for error in the prior forecast. Larger constants yield a faster response but can produce erratic projections. Smaller constants can result in long lags for forecast values (MSExcell, 1996).

4.3.2 Data processing and interpretation

4.3.2.1 First derivative values

The first derivative of a data set is used to determine the values that exhibit the greatest change from one value to the next. The first derivative values of each spectrum were calculated using the formula:

(Value 2-Value 1) x *scale factor*.

A scale factor of 10 was used to enhance the changes.

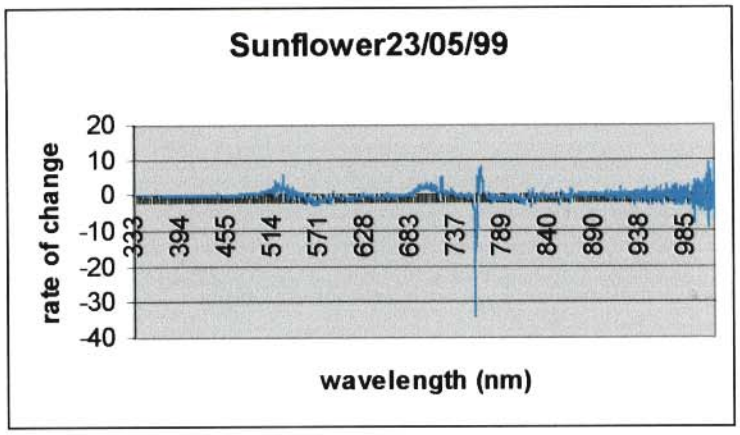

Fig 4.2 Example of first derivative spectrum

4.3.2.2 Maximum change

The wavelength where the maximum positive change took place in the visible and near-infrared part of the first derivative spectrum was determined with the MAX function in MS Excell. This value usually shows the position of the red edge. These values were copied to a new table and a bar graph was generated for interpretation purposes.

4.3.2.3 NDVI and individual reflectance values

Individual reflectance values of the reflectance spectrum were also chosen and correlated with leaf N status. The values chosen were: 550nm, because maximum reflectance occurs here in the visual spectrum, 675nm, because maximum absorptance occurs here in the visual spectrum and 770nm as a reference in the near IR spectrum (Thomas *et al.*, 1972). These values were correlated with the leaf N status using the Correlate function on the Tools / Data Analysis menu of MS Excell.

The correlation analysis tool measures the relationship between two data sets that are scaled to be independent of the unit of measurement. The population correlation calculation returns the covariance of two data sets divided by the product of their standard deviations. The Correlation tool is used to determine whether two ranges of data correlate positively or negatively with each other (MS Excell, 1996).

The 675nm and 770nm reflectance values were also used to generate an NDVI value using the formula $\frac{770-675}{770+675}$. These values were also correlated with the leaf N status.

4.4 Multi-spectral video camera

4.4.1 Pre-processing

Imagery of the foliage of each pot in the trial was obtained with optical videography and the images saved as BMP files. The resulting files were opened in the Adobe Photoshop software and an image of each of the four spectral bands that was acquired was cut out and saved individually as a BMP file. These files were imported into the TNTlite software for analysis.

4.4.1.1 Colour Conversion

The TNT software can only do band-ratio operations on 8-bit greyscale imagery. Because the images were imported as RGB packed images, they had to be converted to 8-bit images before any raster operations could be done. The process used was the Convert Colour option on the Process/Raster/Combine menu. The single option from the Input Type option menu was selected to convert a single composite colour raster object to an 8-bit greysacale object. Run was selected to open the File/Object Selection window and the input raster object type was given a name and a description (MicroImages, 1999).

4.4.1.2 Georeferencing

The four images representing each spectral band had to be co-referenced before they could be used simultaneously.

The *Georeference* window opens when the Georeference option from the Edit menu is selected. An object for georeferencing is opened using the Open option on the File menu. The Object

selected is displayed in an Object Georeferencing (Input Object View) window. Additionally, a Reference Layer Controls window opens and a reference object is selected. The reference object is displayed in a separate Object Georeferencing (Reference Object View) window in which initial points to tie the objects together can be selected (MicroImages, 1999).

One of the four spectral bands was used as a reference object after being given an arbitrary set of reference points. This method for georeferencing lets you select the desired projection, the reference point, the orientation, and enter co-ordinates and cell sizes to create a georeference sub-object for the entire raster.

Control point location in the reference object was selected by positioning the mouse over the corresponding control point location in the input object. Apply is selected on the Georeference window to accept the control point. When enough control points have been added (at least three), the georeference subobject can be saved with the Save As option on the File menu.

4.4.1.3 Resampling

Each of the four images had to be resampled to have corresponding rows and columns. The process used is Automatic Resampling on the Process/Raster/Resample menu.

The File menu allows selection of input raster objects to resample. The output projection and cell size of the output rasters was set to match a reference raster chosen from the set. The *Nearest Neighbor Sampling* method, that was used, resamples a source raster to yield a new output raster by computing the distance between the centre of each cell in the output raster and the four nearest corresponding cells in the input raster. The value of the closest input cell is assigned as the value of the output cell (MicroImages, 1999). The Run option on the file menu was used to open an output object and to finish the process.

4.4.1.4 Raster extraction

Individual images of plants were cut out for further processing utilising the Process/Raster/Extract module and specifying manual resampling. The extraction of these images eliminates the need to classify the background as a separate class.

The *Raster Extract* process was accessed from the Extract option on the Process / Raster menu. The Raster Extract process can be used to manually resample data. The Extraction Area Definition Tools window opens when the Manual extraction method is selected. The manual extraction method allows the user to manually draw an extraction window around the desired areas in the image with CAD sketching tools. The Raster Extract process can be applied to extract all or part of one raster object or identical areas from multiple raster objects (in this instance the four spectral bands of the video image). The extraction area is applied to all identical objects when processed (MicroImages, 1999).

4.4.2 Data Processing and interpretation

The data processing and interpretation that was done from the video images is the same as for the Kodak DCS420 digital data described in section 4.2.2. The bands used for the NDVI were 550nm and 770nm. An additional vegetation index, the video greenness index, using the green (450nm) and red (550nm) band was also calculated and classified in the same way.

Because of the low resolution of the video capturing device (71 dpi for the multispectral camera), it was difficult to accurately georeference the four spectral bands. Consequently, some of the images that were used in the band-ratioing operations were slightly skewed around the edges of the leaves. This might have had a negative influence on the interpretation of the results.

CHAPTER 5

Results

5.1 Introduction

As already mentioned in previous chapters, the aim of this study is to determine if Nitrogen deficiency in crops can be detected with non-destructive remote sensing techniques. Three remote sensing instruments were used to collect data in the data collection phase (Kodak DCS420 digital infrared images, MultiSpec AgroImager video imagery and Ocean Optics S2000 reflection spectra).

To assess the functionality of the data and the collection techniques, total % N content of leaves sampled at the dates of data collection was correlated with the results obtained from the data processing phase of this study. For each data set the correlation coefficient (ρ) between the image processing results and the N content of the leaves was calculated to give an index of association between two sets of variables. The correlation coefficient is a measure of the intensity of association. As such, it must be symmetric in the two variables. The correlation coefficient is independent of the units of measurement; it is an absolute or dimensionless quantity (Steel and Torrie, 1986). It can vary only within certain restricted limits, -1 and +1 with no correlation when $\rho = 0$. When $\rho = +1$ the correlation is complete or perfect. This can show that some fixed positive relationship exists between each element of the two data sets. On the other hand when $\rho = -1$ there exists a negative correlation between the variables. For the other values of ρ, the situation is intermediate between a fixed relation and complete independence (Bailey, 1969).

To test if the values of ρ are significantly different from 0 (no correlation) a specialised Student's t-test was applied to all the correlation coefficient values.

$$t = \frac{\rho\sqrt{n-2}}{\sqrt{1-\rho^2}}$$

Where n = the amount of observations made for each sample (Nemenyi *et al.*, 1977).

The value of t has a different distribution for each value of the degrees of freedom. In this instance the degrees of freedom are three (four observations per sample minus one). A standard table (Steyn *et al.*, 1987) with student's t-distribution that gives the percentage points most frequently required for significance tests and confidence limits was used to determine if the correlation values significantly differed from zero.

5.2 Soil N content

To determine if the amount of nitrogen in the leaves of the crops used for the pot trials corresponds to the soil N status, the soil was analysed for total soil N at the end of the trial.

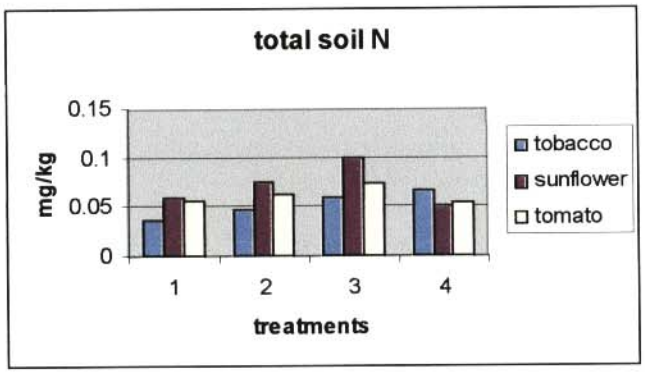

Fig 5.1 Bar graph showing the N status of the soil for the three pot trials and four different N application rates (none to optimal)

From the graph it is apparent that there is an increase in soil N content with an increase in N application except for the highest N rate that exhibits a decrease in N content. The high amount of urea fertilizer applied in the optimal (highest) application rate resulted in high N losses due to ammonia volatilization. It has been shown in a number of studies (Chao *et al.*, 1964, Hargrove *et al.* 1979, Haynes, 1996) that there exists a linear relationship between the rate of fertilizer application and the total NH_3 loss. The higher the NH_4^+ application, the more NH_3 will be lost due to volatilization. This explains the fact that the soil N content of the highest N application is consistently slightly less than the second highest application. The soil N content is also reflected in the leaf N status of the different pot trials where there is a slight decrease in leaf N content in the highest application (see section 5.3).

5.3 Leaf N content

Comparing leaf N status of the different sample dates of the tobacco trial, it is apparent from the graph in fig. 5.2 that the young plants have a much higher % leaf N than the older plants. It is also apparent that there is an increase in leaf N content as the amount of N in each treatment increases except for the 220 kg ha^{-1} treatment that shows a slight decrease in leaf N content in relation to the 146.6 kg ha^{-1} treatment. This observation is confirmed by the soil N status that shows a decrease in soil N in the highest N treatment.

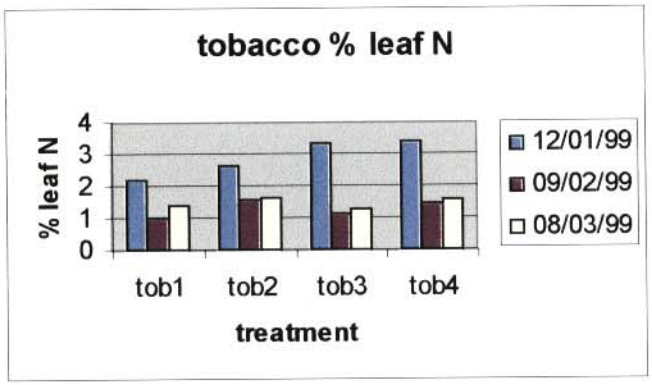

Fig. 5.2 Bar graph of the leaf N status for tobacco showing three sample dates for the four different N treatments (0, 73.3, 146.6 and 220 kg.ha^{-1}).

Comparing leaf N status of the different sample dates of the tomato trial, it is apparent from the graph in fig 5.3 that the % leaf N of the leaves decreases as the plants reach maturity. It is also apparent, as for the tobacco trial, that there is an increase in leaf N content as the amount of N in each treatment increases except for the 120 kg.ha^{-1} that shows a slight decrease in leaf N content in relation to the 80 kg.ha^{-1} treatment. This observation is also confirmed by the soil N analysis.

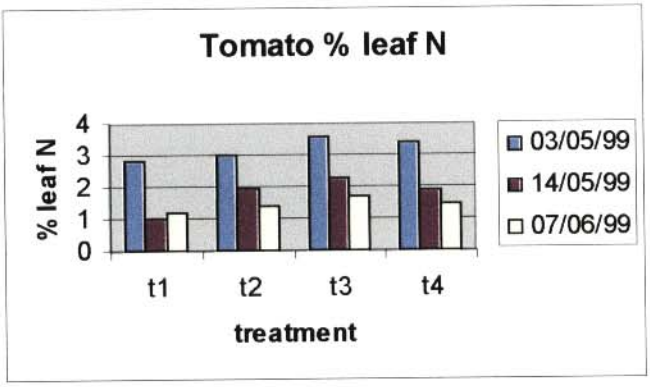

Fig. 5.3 Bar graph of the leaf N status for tomato showing three sample dates for the four different N treatments (0, 40, 80 and 120 kg.ha^{-1}).

Comparing leaf N status of the different sample dates of the sunflower trial, it is apparent from the graph in fig 5.4 that the young plants have a higher % leaf N than the older plants. There is an increase in leaf N content as the amount of N in each treatment increases.

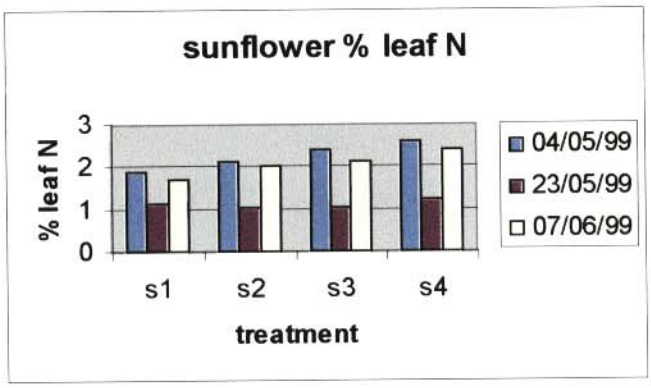

Fig. 5.4: Bar graph of the leaf N status for sunflower showing three sample dates for the four different N treatments (0, 27, 59 and 87 kg.ha^{-1}).

5.4 Kodak professional DCS420 digital imagery

Due to a hardware problem developed by the hard disk of the camera that resulted in corrupted images, only the tobacco samples were used in this part of the study.

Fouché *et al.* (1997 and 1999) found that supervised classification of CIR images gave good results for the assessment of N-stress on winter wheat, tobacco and cotton. It was decided,

however, that for this particular study, it would not be possible to use supervised classification. The supervised classification technique depends on the assumption that there is a baseline to classify from (i.e. a low application of N fertilizer resulting in severely stressed vegetation). In this study, individual images of plants in the pot trials were acquired. It was thus impossible to classify from a baseline. Because images of each plant were not acquired at once, small changes in light quality would also have influenced the accuracy of the data. Kanemasu (1974) found that IR/R ratio, such as the NDVI, is not influenced by solar radiation or variations in canopy geometry and for this reason it was decided to apply an NDVI to the digital infrared images.

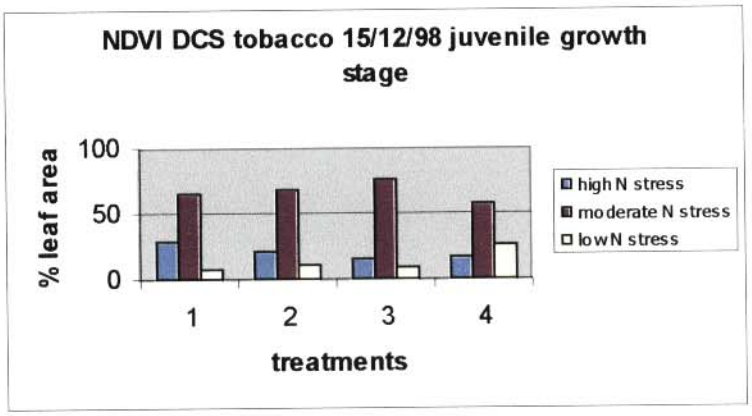

(a)

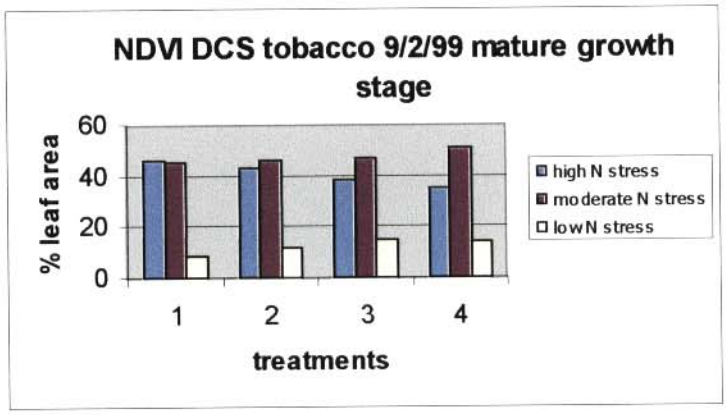

(b)

Fig. 5.5 Bar graphs of the two sample dates, (a) 15/12/98 and (b) 9/2/99, showing the three different NDVI stress classes as % leaf area for the four different N treatments (0, 73.3, 146.6 and 220 $kg.ha^{-1}$).

The first sample date (15/12/98, fig.5.5a) represents the juvenile growth stage of tobacco. Leaf area that represents very active (low N stress) and senescent/ chlorotic (high N stress) vegetation are both quite low and most of the leaf area is represented by the moderate stress class. This confirms laboratory

observations by Collins (1978) that near IR reflectivity of the vegetation canopy is dependent on the development of the mesophyll structure of leaves and thus increases as the plant matures. However, it is already apparent that photosynthetic activity increases as the N status of the soil increases.

The second sample date (09/02/99, fig. 5.5b) represents the mature growth stage of tobacco. A definite decreasing trend from low to high soil N status can be observed in the class representing the low photosynthetic activity (high N stress). The opposite is also observed for the healthier leaf area.

Table 5.1 Statistical analysis of DCS NDVI results and leaf N content of tobacco trial.

TOBACCO NDVI						
DCS	**15/12/98**			**09/02/99**		
photosynthetic activity	Correlation Coefficient	t-test	Significant	Correlation Coefficient	t-test	significant
low (high N stress)	-0.97189	-5.83795	y	-0.35234	-0.53243	y
moderate (moderate stress)	0.037586	0.053192	n	0.347277	0.523719	n
high (low N stress)	0.617915	1.11144	y	0.297095	0.440024	y

Comparing high stress values that indicates senescent leaves and leaves suffering from chlorosis, the results show that there is a statistically significant negative correlation between leaf N content and % leaf area covered by that class. This suggests that plants with high leaf N content will have a lower amount of leaf area showing up as senescent in a NDVI of the digital infrared images. On the other hand, there is a statistically significant positive correlation between high NDVI values (low stress) that indicates healthy leaves. This confirms that an NDVI of the digital infrared images can be used to determine if plants are suffering from N deficiency or not.

It must be noted that there is a much stronger positive and negative correlation between leaf N content and NDVI values of samples from young plants (15/12/98), than there is of samples of mature plants (09/02/99). This suggest that the growth stage of the plant plays an important role in canopy reflectance as well as leaf N status, confirming laboratory observations by Collins (1978). It would thus be much easier to determine leaf N status with digital infrared imagery in tobacco when the plants are still young.

5.5 Multi spectral video camera

Of the four spectral bands sampled by the multi-spectral video camera, only three bands (450, 550 and 770nm) could be utilised. The 650nm band was situated at the near IR reflectance peak and all the samples rendered over-saturated images for this band and were discarded. The 770nm spectral band was used for all the band-ratios that utilises a near IR band as part of the equation.

Leaf reflectance in the visible spectrum is primarily influenced by chlorophyll pigments (Peñuelas *et al.*, 1994 and Fillela *et al.*, 1995). Since severe N limitations should result in loss of chlorophyll, information contained in the reflectance spectra has been used to determine plant N status (Thomas *et al.*, 1972).

Two band ratios have been used with the multi-spectral video imagery: a greenness index involving the green (450nm) and red (550nm) spectral bands and the normal NDVI involving the red (550nm) and near IR (770nm) spectral bands. The greenness index, $\frac{R_{550} - R_{450}}{R_{550} + R_{450}}$, represents the difference between the green reflection and the red absorption of a vegetation canopy. Leaves with a high chlorophyll content will have higher reflection in the green spectral band and higher absorption in the red spectral band. The NDVI, $\frac{R_{770} - R_{550}}{R_{770} + R_{550}}$, represents the difference between the red absorption and the near IR reflection of a vegetation canopy. Healthy, mature and photsynthetically active leaves will have high absorption in the red spectral band and high reflection in the near IR spectral band.

5.5.1 Tobacco

The trial was sampled twice during the growing season of the tobacco. The first data set (15/12/98) was sampled during the juvenile growth stage of the tobacco 21 days after planting. The second data set (09/02/99) was sampled during the adult growth stage of the tobacco 77 days after planting.

5.5.1.1 Greenness index

In the first sample date (15/12/98, fig. 5.6a), representing the juvenile growth stage of tobacco, the leaf area that represents healthy green vegetation (low stress, high photosynthetic activity) decreases in the first three treatments but increases again for the highest N treatment (220 kg.ha^{-1}). The plant material with low amounts of chlorophyll (high stress) increases in the first three treatments but decreases again for the highest N treatment. The leaf area represented by the moderate stress class is uniformly low.

The second sample date (09/02/99, fig. 5.6b) represents the mature growth stage of tobacco. A definite decreasing trend from low to high soil N status can be observed in the class representing the plant material with low amounts of chlorophyll (high stress) except for the third treatment (146.6 kg.ha^{-1}) which increases slightly. The opposite is also observed for the healthier green vegetation. The leaf area represented by the moderate class is uniformly low.

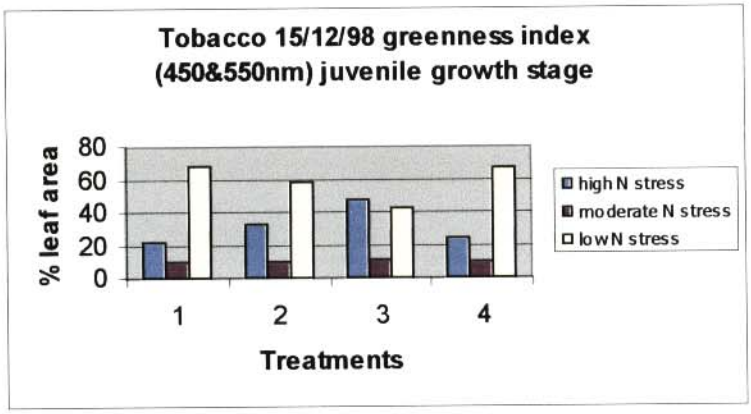

(a)

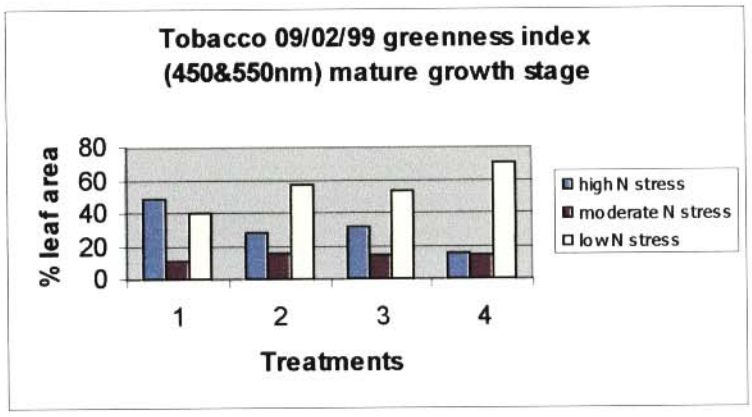

(b)

Fig. 5.6 Bar graphs of the two sample dates, (a) 15/12/98 and (b) 9/2/99, representing the three different greenness index stress classes as % leaf area for the four different N treatments (0, 73.3, 146.6 and 220 kg.ha^{-1})

Table 5.2 Statistical analysis of video greenness index results and leaf N content of tobacco trial.

TOBACCO greenness index						
VIDEO	**15/12/98**			**09/02/99**		
photosynthetic activity	Correlation Coefficient	t-test	Significant	Correlation Coefficient	t-test	Significant
low (high stress)	0.515361	0.850471	y	-0.7579	-1.64298	y
moderate	0.119404	0.17008	n	0.689377	1.345835	n
high (low stress)	-0.49406	-0.80364	y	0.736617	1.54032	y

There is a statistically significant positive correlation between leaf N content and % leaf area covered by low greenness index values (high stress) for the juvenile growth stage (15/12/98) and a statistically significant negative correlation for the adult growth stage (09/02/99). The percentage leaf area covered by high greenness index values (low stress), that indicates healthy, green vegetation, for the juvenile stage has a statistically significant negative correlation with the leaf N content whilst the adult growth stage exhibits a statistically significant positive correlation between the two values. The percentage leaf area covered by the intermediate greenness index values (moderate stress) in the juvenile stage has a very weak positive correlation with leaf N status and the values for the adult growth stage exhibit a strong positive correlation. These values are, however, not statistically significant.

5.5.1.2 NDVI

The first sample date (15/12/98, fig. 5.7a), representing the juvenile growth stage of tobacco shows an increase in the leaf area that represents healthy green vegetation (low stress) except for the 120 $kg.ha^{-1}$ treatment that shows a decrease in relation to the 146.6 $kg.ha^{-1}$ treatment. The opposite is observed for the low NDVI values (high stress) that indicates senescent leaves and leaves suffering from chlorosis.

The second sample date (09/02/99, fig. 5.7b) represents the mature growth stage of tobacco. A definite decreasing trend from low to high soil N status can be observed in the class representing the low NDVI values (high stress) except for the highest treatment (220 $kg.ha^{-1}$) which decreases slightly in relation to the 146.6 $kg.ha^{-1}$ treatment. There is no observable pattern in the other two classes.

The high NDVI values (low stress) patterns observed in the video imagery correlate with the patterns

observed in the DCS infrared imagery. The same conclusions can thus be drawn from the visual interpretation of the graphs as for the digital infrared images.

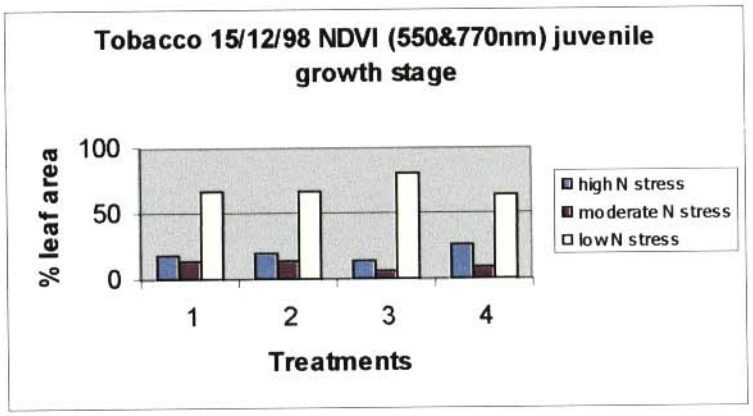

(a)

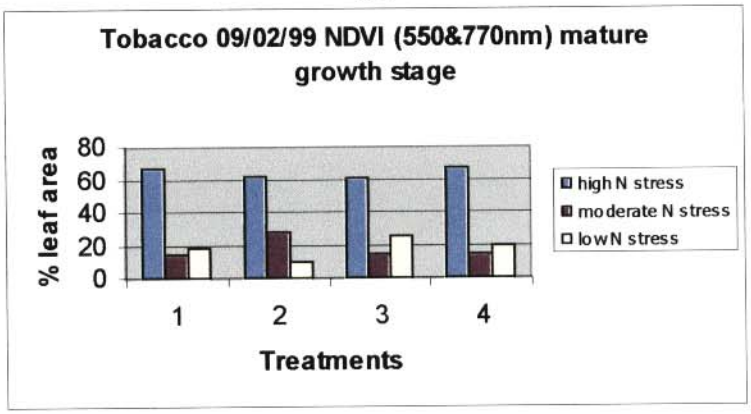

(b)

Fig. 5.7 Bar graphs of the two sample dates, (a) 15/12/98 and (b) 9/2/99, representing the three different video NDVI stress classes as % leaf area for the four different N treatments (0, 73.3, 146.6 and 220 $kg.ha^{-1}$).

Table 5.3 Statistical analysis of video NDVI results and leaf N content of tobacco trial.

TOBACCO NDVI						
VIDEO	**15/12/98**			**09/02/99**		
photosynthetic activity	Correlation Coefficient	t-test	significant	Correlation Coefficient	t-test	Significant
low (high stress)	0.140413	0.200561	n	-0.24504	-0.35744	y
moderate	-0.89359	-2.81526	y	0.746939	1.588725	y
high (low stress)	0.343289	0.516896	y	-0.70348	-1.39982	y

There is a weak positive correlation between leaf N content and % leaf area covered by the low NDVI values (high stress) for the juvenile growth stage (15/12/98) and a weak negative correlation for the adult growth stage (09/02/99). Although the correlation for the adult growth stage is statistically

significant, the correlation for the juvenile growth stage is not. The percentage leaf area covered by high NDVI values (low stress), that indicates healthy actively photosynthesising vegetation, for the juvenile stage has a statistically significant positive correlation with the leaf N content whilst the adult growth stage exhibits a statistically significant negative correlation between the two values. The percentage leaf area covered by the intermediate NDVI values (moderate stress) in the juvenile stage has a statistically significant negative correlation with leaf N status, however, the values for the adult growth stage exhibit a statistically significant positive correlation.

5.5.2 Sunflower

The trial was sampled twice during the growing season of the sunflower. The two data sets were sampled 19 days apart, but because the sunflower has a fairly short growth season of 90-100 days (Myers *et al.*, 1993) the two sets are considered to represent two different growth stages. The first data set (04/05/99) was sampled during the juvenile growth stage of the sunflower 49 days after planting. The second data set (23/05/99) was sampled during the adult growth stage of the sunflower 78 days after planting.

5.5.2.1 Greenness index

In the first sample date (04/05/99, fig. 5.8a), representing the juvenile growth stage of the sunflower, the leaf area that represents plant material with low amounts of chlorophyll (high stress) decreases in the first three treatments but increases again for the highest N treatment (87 $kg.ha^{-1}$). The healthy, green plant material (low stress) increases in the first three treatments but decreases again for the highest N treatment. The leaf area represented by the moderate class, although representing a high percentage of the leaf area in some of the treatments, does not exhibit any discernible pattern.

The second sample date (23/05/99, fig. 5.8b) represents the mature growth stage of sunflower. A definite decreasing trend from low to high soil N status can be observed in the class representing the plant material with low amounts of chlorophyll (high stress) except for the highest treatment (80 $kgha^{-1}$) which increases in relation to the 59 $kg.ha^{-1}$ treatment. The opposite is also observed for the healthier green vegetation. The leaf area represented by the moderate stress class exhibits a steady decrease from low to high N treatments. This confirms laboratory observations made by Thomas *et al.* (1972) that

N deficiency decreases the absorption of red (550nm) and the reflection of green (450nm).

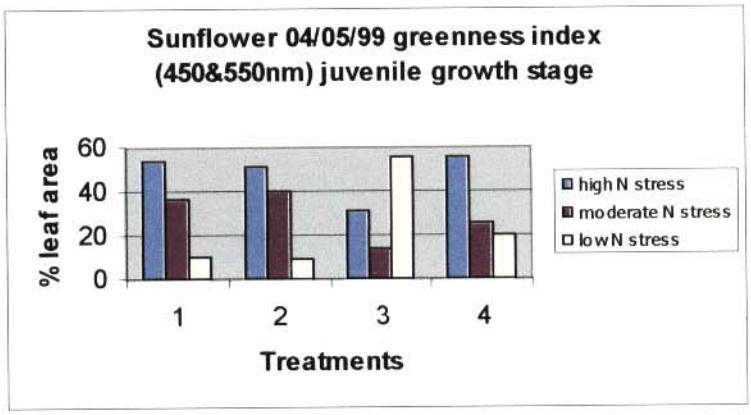

(a)

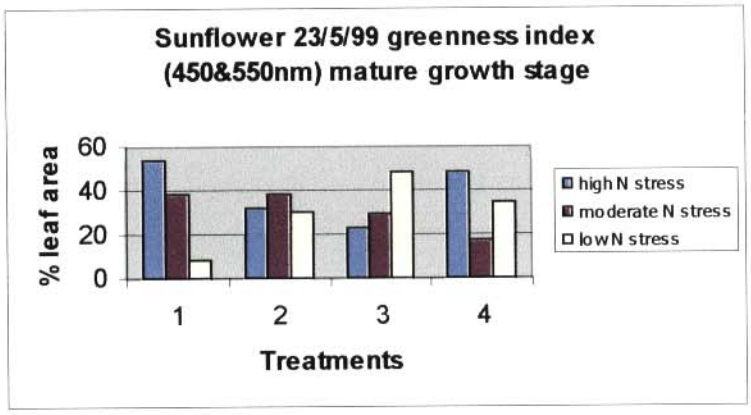

(b)

Fig. 5.8: Bar graphs of the two sample dates, (a) 04/05/99 and (b) 23/05/99 representing the three different video greenness index stress classes as % leaf area for the four different N treatments (0, 27, 59 and 87 kg.ha^{-1}).

Table 5.4 Statistical analysis of video greenness index results and leaf N content of sunflower trial.

SUNFLOWER greenness index						
VIDEO	**04/05/99**			**23/05/99**		
photosynthetic activity	Correlation Coefficient	t-test	significant	Correlation Coefficient	t-test	significant
low (high stress)	-0.22907	-0.3328	y	0.816929	2.003183	y
moderate	-0.68555	-1.3317	y	-0.65524	-1.22667	y
high (low stress)	0.492252	0.799756	y	-0.3049	-0.45275	y

There is a statistically significant negative correlation between leaf N content and % leaf area covered by the low greenness index values (high stress) for the first sample date (04/05/99) and a strong positive correlation for the second sample date (23/05/99). The percentage leaf area covered by high greenness index values (low stress), that indicates healthy, green vegetation, for the first sample date has a statistically significant positive correlation with the leaf N content whilst the second data set exhibits a significant negative correlation between the two values. The percentage leaf areas covered by the intermediate greenness index values (moderate stress) in the juvenile stage for both sample dates exhibit a significant negative correlation with leaf N status.

These observations do not suggest any pattern in the correlation between the leaf area covered by the various classes and the leaf N status of the plants.

5.5.2.2 NDVI

In the first sample date (04/05/99, fig. 5.9a), representing the juvenile growth stage of the sunflower, the only pattern that can be observed is the decreasing leaf area in the class representing moderate greenness (class2) from low to high N treatments. This is true for all the treatments with the exception of the highest treatment (87 $kg.ha^{-1}$) that shows a decrease in relation to the 59 $kg.ha^{-1}$ treatment.

The second sample date (23/05/99, fig. 5.9b) represents the mature growth stage of sunflower. A definite decreasing trend from low to high soil N status can be observed in the class representing the healthy green plant material (low stress) except for the highest treatment (87 $kg.ha^{-1}$) which increases in relation to the 59 $kg.ha^{-1}$ treatment. The class representing moderate greenness decreases from low to high N treatments except for the lowest treatment (0 $kg.ha^{-1}$) where it is also low. This contradicts laboratory observations made by Thomas *et al.* (1972) that low leaf N status leads to a decrease in red (550nm) absorption and near IR (770nm) reflection.

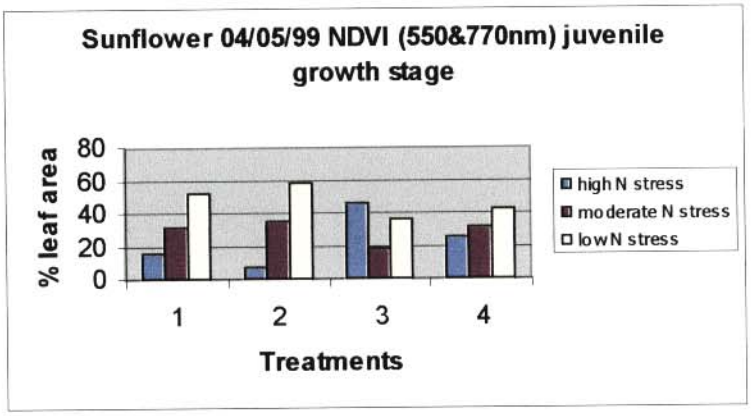

(a)

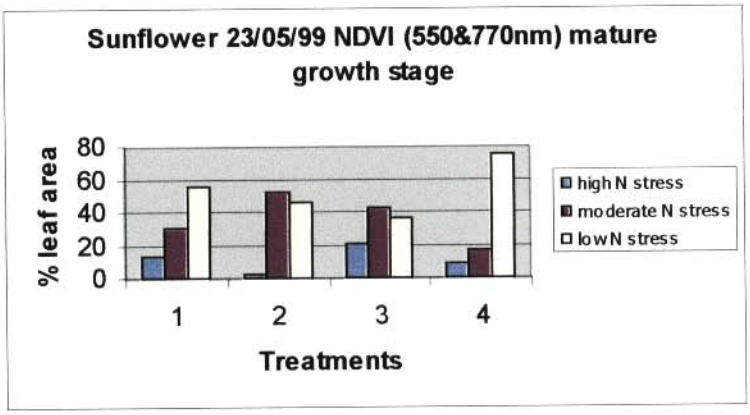

(b)

Fig. 5.9 Bar graphs of the two sample dates, (a) 04/05/99 and (b) 23/05/99, representing the three different video NDVI stress classes as % leaf area for the four different N treatments (0, 27, 59 and 87 $kg.ha^{-1}$).

Table 5.5 Statistical analysis of video NDVI results and leaf N content of sunflower trial.

SUNFLOWER NDVI						
VIDEO	**04/05/99**			**23/05/99**		
photosynthetic activity	Correlation Coefficient	t-test	significant	Correlation Coefficient	t-test	significant
low (high stress)	0.572591	0.987711	y	-0.16718	-0.2398	n
moderate	-0.37089	-0.5648	y	-0.95708	-4.67013	y
high (low stress)	-0.69818	-1.37917	y	0.977584	6.56634	y

There is a significant positive correlation between leaf N content and % leaf area covered by the low NDVI values (high stress) for the first data set (04/05/99) and a weak negative (non-significant) correlation for the second data set (23/05/99). The percentage leaf area covered by high NDVI values (low stress), that indicates healthy actively photosynthesising vegetation, for the first data set has a significant negative correlation with the leaf N content whilst the second data set exhibits a significant

positive correlation between the two values. The percentage leaf area covered by the intermediate NDVI values (moderate stress) in the first data set has a significant, although weak, negative correlation with leaf N status, however, the values for the second data set exhibit a strong significant negative correlation.

5.5.3 Tomato

The trial was sampled three times during the growing season of the tomato. The three data sets were sampled two weeks apart. The first data set (15/04/99) was sampled 30 days after planting. The second data set (03/05/99) was sampled 48 days after planting. The last data set (14/05/99) was sampled as the first blooms started to appear 59 days after planting.

5.5.3.1 Greenness index

The first (15/04/99, fig. 5.10a) and second (03/05/99, fig. 5.10b) sample dates show no observable pattern in the distribution of the leaf area covered by the three different classes except for the fact that the class representing healthy green vegetation (low stress) dominates the leaf area.

The third sample date (14/05/99, fig. 5.10c) representing the adult growth stage of tomato exhibits an increase in the leaf area in the healthy green vegetation class (low stress) from low to high N treatment. This is true except for the highest N treatment (120 $kg.ha^{-1}$) which exhibits a slight decrease in leaf area in relation to the 80 $kg.ha^{-1}$ treatment. The opposite can be observed for the class representing the leaf area with low amounts of chlorophyll (high stress). This confirms observations made by Thomas *et al.* (1972) that N deficiency decreases the absorption of red (550nm) and the reflection of green (450nm).

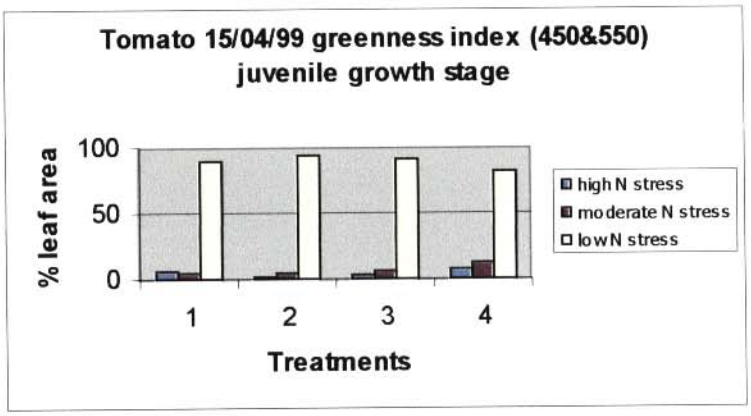

(a)

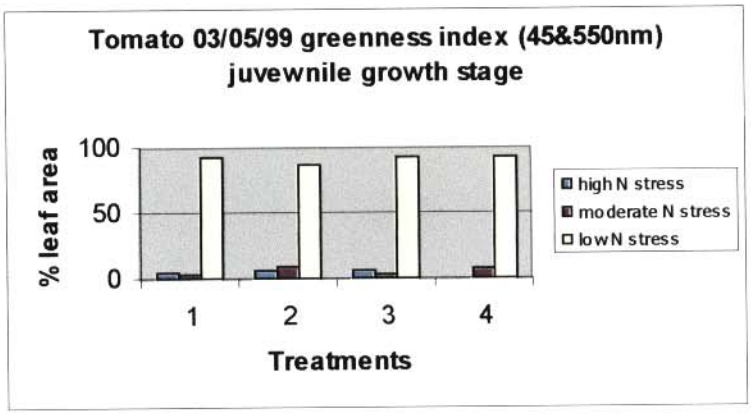

(b)

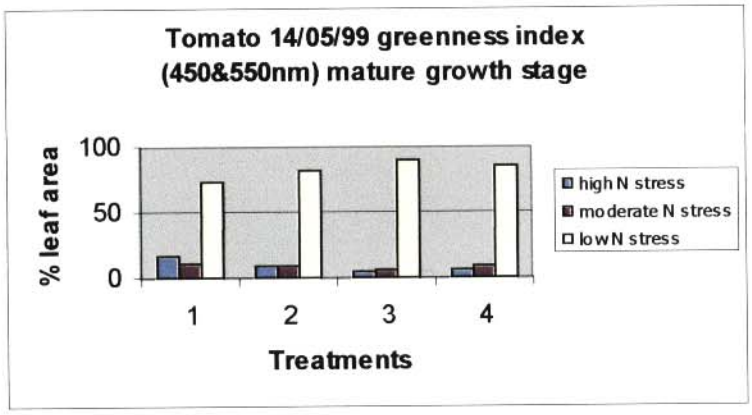

(c)

Fig. 5.10: Bar graphs of the three sample dates, (a) 15/04/99, (b) 03/05/99 and (c) 14/05/99 representing the three different video greenness index stress classes as % leaf area for the four different N treatments (0, 40, 80 and 120 $kg.ha^{-1}$).

Table 5.6 Statistical analysis of greenness index values and leaf N content of tomato trial.

TOMATO greenness index									
VIDEO	**15/04/99**			**03/05/99**			**14/05/99**		
photosynthetic activity	Correlation Coefficient	t-test	significance	Correlation coefficient	t-test	significance	Correlation Coefficient	t-test	significance
low (high stress)	-0.08444	-0.11984	n	-0.29322	-0.43374	y	-0.95017	-4.31057	y
moderate	0.52149	0.86434	y	-0.1759	-0.2527	n	-0.92138	-3.35259	y
high (low stress)	-0.29209	-0.43191	y	0.39486	0.6078	y	0.96405	5.13092	y

There is a weak negative (non-significant) correlation between leaf N status and % leaf area covered by the low greenness index values (high stress) for the first data set (15/04/99). This increases to a strongly significant negative correlation for the last data set representing the adult growth stage (14/05/99). The percentage leaf area covered by high greenness index values (low stress), that indicates healthy, green vegetation, for the first data set has a weakly significant negative correlation with the leaf N status. The adult growth stages (03/05/99 and 14/05/99) exhibit a significant positive correlation between the two values with the last data set exhibiting a strong positive correlation between the two values. The percentage leaf area covered by the intermediate greenness index values (moderate stress) exhibits at first a weak negative correlation between % leaf area covered by that class and leaf N status and for the final data set a weak positive correlation.

The last data set (14/05/99) suggests that plants with high leaf N content will have a lower amount of leaf area showing up as senescent in a greenness index. On the other hand, there is a positive correlation between high greenness index values (low stress) that indicates healthy leaves. This confirms observations made by Collins (1978). The observations are only true for the sample date representing adult tomato plants just as the first blooms start appearing. This might suggest that N deficiency in tomatoes could be detected easier by means of multi-spectral video remote sensing utilising the greenness index during early maturity. As nitrogen, applied when the first cluster of fruit is set, stimulates fruit growth and increases yield (Knott, 1955), deficiency detected at this stage can still be rectified.

5.5.3.2 NDVI

The first sample date (15/04/99, fig. 5.11a) shows no discernible pattern in the leaf area distribution

of the different classes.

The second sample date (03/05/99, fig. 5.11b) shows a decrease in leaf area from low to high N treatments of the class representing low NDVI values (high stress). The opposite can be observed for the moderate NDVI values with no discernible pattern in the highest NDVI values (low stress).

The third sample date (14/05/99, fig. 5.11c) representing the adult growth stage of tomato shows an increase in the low NDVI values (high stress) from low to high N treatment except for the highest N treatment (120 $kg.ha^{-1}$) that shows a decrease in relation to the 80 $kg.ha^{-1}$ treatment. The moderate NDVI values show an increase from the second N treatment (40 $kg.ha^{-1}$) to the highest N treatment. There is no observable pattern in the highest NDVI class (low stress).

The observations of the lowest NDVI values (high stress) confirms laboratory observations made by Thomas *et al.* (1972) that leaf N deficiency is manifested as a lowering in red (550nm) absorption and near IR (770nm) reflection.

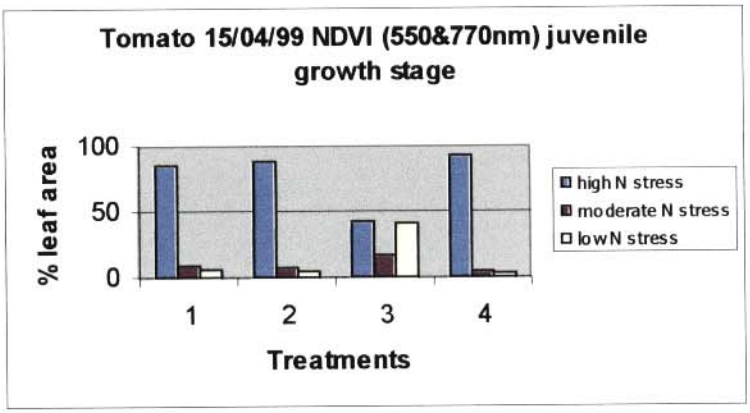

(a)

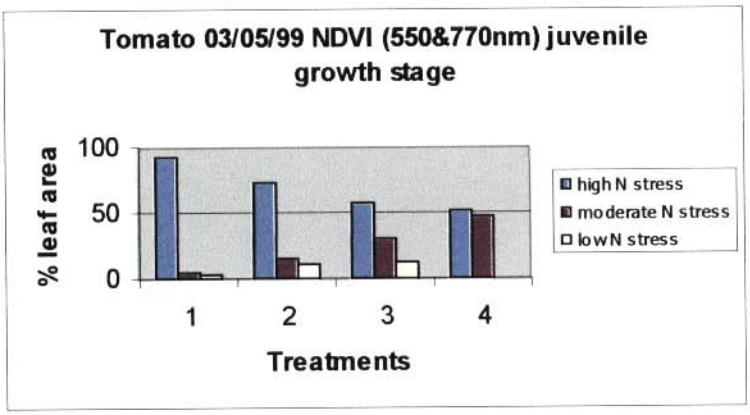

(b)

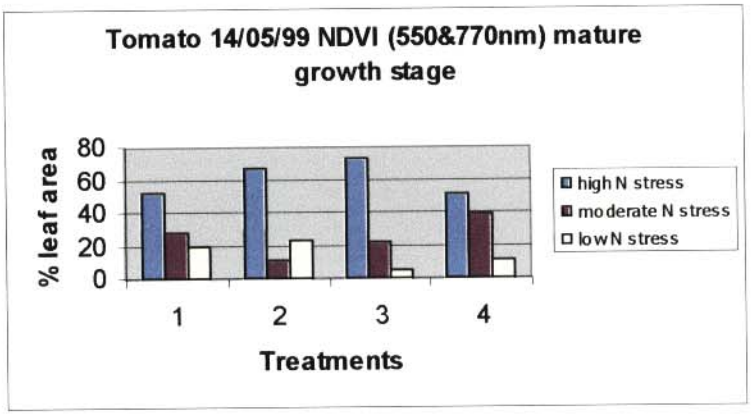

(c)

Fig. 5.11: Bar graphs of the three sample dates, (a) 14/04/99, (b) 03/05/99 and (c) 14/05/99, representing the three different NDVI stress classes as % leaf area for the four different N treatments (0, 40, 80 and 120 kg.ha^{-1}).

Table 5.7 Statistical analysis of video NDVI results and leaf N content of tomato trial.

TOMATO NDVI									
VIDEO	**15/04/99**			**03/05/99**			**14/05/99**		
photosynthetic activity	Correlation Coefficient	t-test	Significant	Correlation Coefficient	t-test	Significant	Correlation Coefficient	t-test	significant
Low (high stress)	-0.61001	-1.08871	y	-0.91205	-3.14533	y	0.70723	1.414711	y
Moderate	0.38762	0.59468	y	0.82539	2.06755	y	-0.29867	-0.44258	y
High (low stress)	0.66202	1.24917	y	0.19130	0.27562	n	-0.55409	-0.94131	y

There is a significant negative correlation between leaf N content and % leaf area covered by the low NDVI values (high stress) for the first and second data sets (14/04/99 and 03/05/99) and a significant positive correlation for the last data set (14/05/99). The percentage leaf area covered by high NDVI values (low stress), that indicates healthy actively photosynthesising vegetation, for the first data set has a significantly strong positive correlation with the leaf N status. The second data set exhibits a weak positive correlation between the two values and the final data set exhibits a moderate negative correlation. The percentage leaf area covered by the intermediate NDVI values (moderate stress) in the first data set has a weakly significant positive correlation with leaf N status, that of the second data set exhibits a significantly strong positive correlation and that of the last data set exhibits a weak negative correlation.

5.6 Ocean Optics S2000 Spectroradiometer

5.6.1 Individual spectral values

The 550nm wavelength was chosen because it represents the area of the reflectance spectrum where green light is reflected by the chlorophyll in healthy vegetation (see fig. 5.12). The 675nm wavelength was chosen because it represents the part of the reflectance spectrum where red light is very strongly absorbed by healthy vegetation containing sufficient chlorophyll (see fig. 5.12). The 770nm wavelength represents the near IR spectrum where there is high reflection from healthy green vegetation (see fig 5.12). The NDVI is a value representing the difference between the 650nm absorption dip and the 770nm-reflection peak. Healthy green vegetation will strongly absorb red light and strongly reflect near IR light resulting in higher NDVI values.

The wavelength of the maximum green reflectance peak and minimum red reflectance of the different crops was also determined individually to determine if crop-specific reflectance values will increase the effectiveness of the probe.

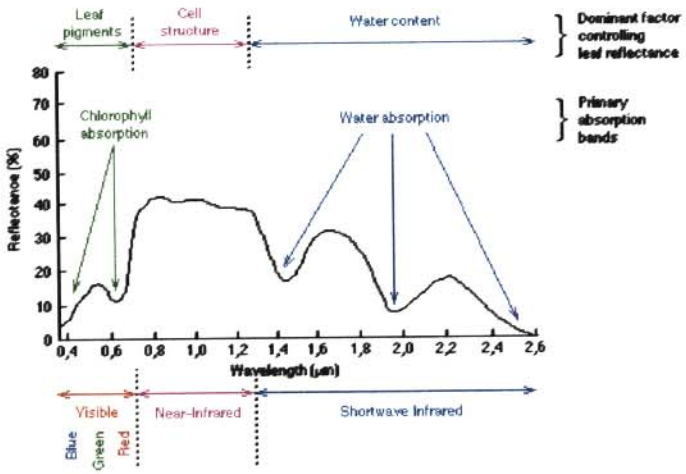

Fig 5.12. Typical reflectance spectrum of green vegetation indicating the main reflectance and absorption features (after Leblon, 1997)

5.6.1.1 Sunflower

Table 5.8 Statistical analysis of individual reflection values and NDVI of those values with leaf N content of sunflower trial.

SUNFLOWER						
	04/05/99			23/05/99		
	Correlation Coefficient	t-test	significant	Correlation Coefficient	t-test	significant
550nm	-0.75789	-1.64293	y	-0.30205	-0.44809	y
675nm	-0.78583	-1.79698	y	-0.35765	-0.54162	y
770nm	0.020712	0.029297	n	0.752388	1.61531	y
Ndvi	0.585619	1.021717	y	0.536624	0.899362	y

The percentage reflection and the leaf N status of the 550nm wavelength exhibits a statistically significant strong negative correlation for the first sample date and a weak negative correlation for the second sample date. This suggests that green light is not reflected very strongly in the juvenile growth stage of the sunflower. The 675nm wavelength has a statistically significant strong negative correlation with leaf N status in the juvenile growth stage and a weaker negative correlation in the adult growth stage. This suggests that higher leaf N content is manifested in stronger red absorption by the leaves. The 770nm wavelength has a non-significant weak positive correlation with leaf N status in the juvenile growth stage and a significant strong positive correlation in the adult growth stage suggesting that higher leaf N content is manifested in stronger near IR reflection. These observations confirm laboratory observations made by Collins (1978) that near IR reflectivity of the vegetation canopy is dependent on the development of the mesophyll structure of leaves and thus increases as the plant matures.

The NDVI values of both the juvenile and the adult growth stage exhibit a statistically significant positive correlation with leaf N status. This suggests that as the leaf N content increases, so do the NDVI values and thus the differences between the red absorption and the near IR reflection.

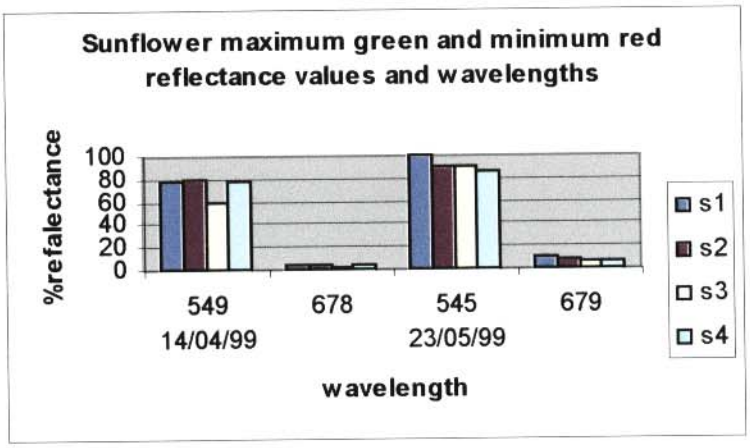

Fig. 5.13: Bar graph of the two sample dates, 14/04/99 and 23/05/99, of the sunflower trial representing the maximum green reflectance peak and maximum red absorption peak as % reflectance for the four different N treatments (0, 27, 59 and 87kg.ha^{-1}).

Comparing the maximim and minimum reflectance values in the visual part of the reflectance spectrum of the sunflower trial, it is apparent from the graph in fig. 5.13 that the reflectance peaks change slightly during the growing season. The maximum green reflectance peak changes with 4nm toward a shorter wavelength while the maximum red absorption peak (minimum reflectance) changes with 1nm towards a longer wavelength. In the juvenile growth stage (14/04/99), there is no apparent pattern in the reflectance values. The adult growth stage (23/05/99) exhibits a decrease in green reflectance and an increase in red absorption as the amount of N in each treatment increases, confirming field observations made by Rock *et al.* (1988).

Table 5.9 Statistical analysis of crop-specific individual green and red reflection values with leaf N content of sunflower trial.

SUNFLOWER						
	14/04/99			23/05/99		
	Correlation Coefficient	t-test	significant	Correlation Coefficient	t-test	Significant
549/545nm	-0.32925	-0.49313	y	-0.09825	-0.13962	n
678/679nm	-0.34901	-0.52669	y	-0.12993	-0.18532	n

The percentage reflection and the leaf N status of both the 549 and 678nm wavelength of the juvenile growth stage (14/04/99) exhibit a statistically significant negative correlation, suggesting that an increase in leaf N content results in a decrease in reflection. This observation confirms

findings by Peñuelas *et al.* (1994) that visible reflectance was negatively related to leaf N status. The percentage reflectance of the adult growth stage (23/05/99) exhibited a weak statistically non-significant negative correlation with leaf N status. It is apparent that the juvenile growth stage exhibits a much better correlation between visible reflectance values and leaf N status than the adult growth stage in sunflower.

5.6.1.2 Tobacco

Table 5.10 Statistical analysis of individual reflection values and the NDVI of those values with leaf N content of tobacco trial.

TOBACCO						
	15/12/98			09/02/99		
	Correlation Coefficient	t-test	significant	Correlation Coefficient	t-test	significant
550nm	-0.12712	-0.18125	n	-0.40655	-0.6293	y
675nm	0.390445	0.599779	y	-0.34987	-0.52817	y
770nm	0.609583	1.087494	y	0.534541	0.894471	y
NDVI	-0.24263	1.071509	y	0.603906	1.071509	y

The percentage reflection and the leaf N status of the 550nm wavelength exhibits a non-significant negative correlation for the first sample date and a statistically significant negative correlation for the second sample date. The 675nm wavelength has a statistically significant weak positive correlation with leaf N status in the juvenile growth stage and a weak negative correlation in the adult growth stage. This suggests that higher leaf N content is manifested in stronger red absorption by the leaves. The 770nm wavelength has a statistically significant moderate positive correlation with leaf N status in both the juvenile and the adult growth stage, suggesting that higher leaf N content is manifested in stronger near IR reflection. These observations confirm laboratory observations made by Thomas *et al.* (1972) that higher leaf N content is manifested as an increase in red absorption and near IR reflection.

The NDVI values of the juvenile growth stage exhibit a statistically significant weak negative correlation with leaf N status. The adult growth stage exhibits a statistically significant moderate positive correlation with leaf N status. The adult growth stage suggests that as the leaf N content increases, so do the NDVI values and thus the differences between the red absorption and the near IR reflection.

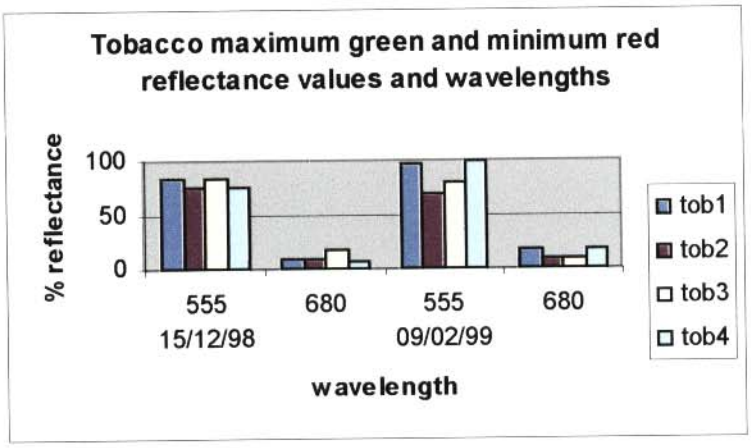

Fig. 5.14: Bar graph of the two sample dates, 15/12/98 and 09/02/99, of the tobacco trial representing the maximum green reflectance peak and maximum red absorption peak as % reflectance for the four different N treatments (0, 73.3, 146.6 and 220kg.ha^{-1}).

Comparing the maximum and minimum reflectance values in the visual part of the reflectance spectrum of the tobacco trial, it is apparent from the graph in fig. 5.14 that the reflectance peaks do not change during the growing season. In the juvenile growth stage (15/12/98), there is no apparent pattern in the reflectance values. The adult growth stage (23/05/99) exhibits an increase in green reflectance as the amount of N in each treatment increases except for the lowest N treatment which is higher than the other reflectance values. This observation contradicts field observations made by Rock *et al.* (1988).

Table 5.11 Statistical analysis of crop-specific individual green and red reflection values with leaf N content of tobacco trial.

TOBACCO						
	15/12/98			09/02/99		
	Correlation Coefficient	t-test	significant	Correlation Coefficient	t-test	Significant
555nm	-0.11545	-0.16437	n	-0.44138	-0.69563	y
680nm	0.420645	0.823058	y	-0.2961	-0.4384	y

The percentage reflection and the leaf N status of the 550nm wavelength exhibit a statistically non-significant negative correlation for the juvenile growth stage (15/12/98) and a significant negative correlation for the adult growth stage (09/02/99), suggesting that an increase in leaf N content results in a decrease in reflection. This observation confirms findings by Peñuelas *et al.*

(1994) that visible reflectance was negatively related to leaf N status. The 680nm wavelength has a statistically significant positive correlation with leaf N content for the juvenile growth stage and a significant negative corellation for the adult growth stage. The adult growth stage confirms field observation made by Peñuelas *et al.* (1994) that there is a negative relationship between visible reflectance and leaf N status.

5.6.1.3 Tomato

Table 5.12 Statistical analysis of individual reflection values and the NDVI of those values with leaf N content of tomato trial.

TOMATO						
	03/05/99			14/05/99		
	Correlation Coefficient	t-test	significant	Correlation Coefficient	t-test	Significant
550nm	0.066442	0.094171	n	-0.17964	-0.25825	y
675nm	0.055135	0.078091	n	0.7898	1.821015	y
770nm	0.317894	0.474167	y	0.423528	0.661188	y
NDVI	0.041127	0.058212	n	-0.73106	-1.51525	y

The percentage reflection and the leaf N status of the 550nm wavelength exhibits a statistically non-significant positive correlation for the first sample date and statistically significant negative correlation for the second sample date. The 675nm wavelength has a non-significant positive correlation with leaf N status in the juvenile growth stage and a statistically significant positive correlation for the adult growth stage. This suggests that higher leaf N content be manifested in stronger red absorption by the leaves as they mature. The 770nm wavelength has a statistically significant positive correlation with leaf N status in both the juvenile and the adult growth stage, suggesting that higher leaf N content is manifested in stronger near IR reflection. The 675nm and 770nm observations confirm laboratory observations made by Thomas *et al.* (1972) that higher leaf N content is manifested as an increase in red absorption and near IR reflection.

The NDVI values of the juvenile growth stage exhibit a non-significant positive correlation with leaf N status. The adult growth stage exhibits a statistically significant negative correlation with leaf N status.

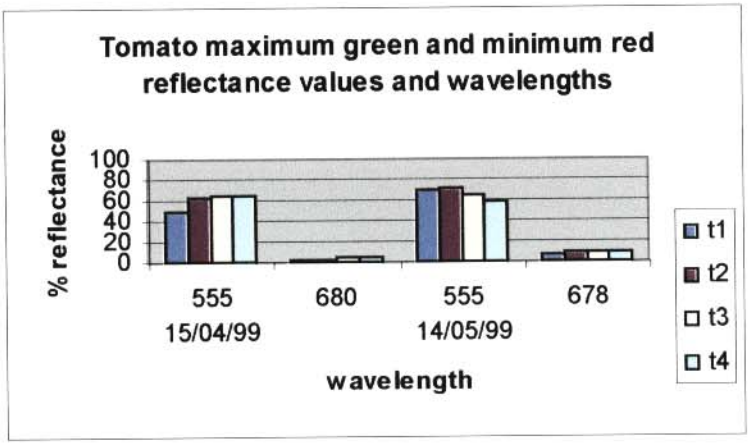

Fig. 5.15: Bar graph of the two sample dates, 15/04/99 and 14/05/99, of the tomato trial representing the maximum green reflectance peak and maximum red absorption peak as % reflectance for the four different N treatments (0, 40, 80 and 120kg.ha^{-1}).

Comparing the maximum and minimum reflectance values in the visual part of the reflectance spectrum of the tomato trial, it is apparent from the graph in fig. 5.15 that the reflectance peaks of the maximum red absorption peak change with 2nm towards shorter wavelengths during the growing season. In the juvenile growth stage (15/04/99), there is an increase in reflectance as the amount of N in each treatment increases for both the green (550nm) and the red (680nm) wavelength, contradicting field observations made by Rock *et al.* (1988). The adult growth stage (14/05/99) exhibits a decrease in green reflectance as the amount of N in each treatment increases except for the lowest N treatment which is lower than the 40 kg.ha^{-1} treatment, confirming field observations made by Rock *et al.* (1988).

Table 5.13 Statistical analysis of crop-specific individual green and red reflection values with leaf N content of tomato trial.

TOMATO						
	15/04/99			14/05/99		
	Correlation Coefficient	t-test	significant	Correlation Coefficient	t-test	significant
550nm	0.798097	1.873239	y	-0.20177	-0.29133	n
680/678nm	0.928539	5.097775	y	0.840136	2.190608	y

The percentage reflection and the leaf N status of both the green (550nm) and the red (680nm) wavelengths of the juvenile growth stage (15/04/99) exhibits a statistically significant positive

correlation contradicting findings by Peñuelas *et al.* (1994) that visible reflectance was negatively related to leaf N status. The 550nm wavelength in the adult growth stage (14/05/99) has a statistically non-significant negative correlation with leaf N content and the 678nm wavelength has a significantly positive correlation.

Both tobacco and tomato have similar wavelengths of maximum and minimum reflectance (550nm and 680nm) except for the red value of the adult growth stage of tomato (678nm). This suggests similar internal leaf structure. Tomato and tobacco both belong to the *solanaceae* plant family and this might be the reason for the similar reflection peaks.

5.6.2 First derivative maxima

The maximum inflection of the first derivative of the reflectance spectrum is the point where there is maximum change in the reflectance from one wavelength to that of the next. This point is situated in that area of the reflectance spectrum where red absorption changes to near IR reflection. This absorption edge or red edge shifts progressively to longer wavelengths during plant growth and maturation.

5.6.2.1 Tobacco

The first two sample dates (15/12/98 and 29/12/98, fig5.16) represent the juvenile growth stage of tobacco. It is apparent from the graph that the position of the red edge has uniformly moved to slightly longer wavelengths. This confirms laboratory observations made by Collins (1978) that the red edge shifts progressively towards longer wavelengths during crop growth and maturity. The position of the red edge of the second sample date (29/12/98) exhibits a decrease in wavelength as the amount of N in each treatment increases except for the 220 $kg.ha^{-1}$ treatment that shows a slight increase in wavelength. This contradicts observations made by Peñuelas *et al.* (1994) that N-limited leaves showed a red shift towards shorter wavelengths.

The last sample (09/02/99, fig 5.16) was collected in the mature stage when the plants had already started blooming. This may be the reason why there is such a dramatic shift of the red edge towards

shorter wavelengths as chlorophyll pigments in the leaves had already started breaking down.

In general there is no discernible pattern in the distribution of the position of the red edge that correlates with any finding in the literature.

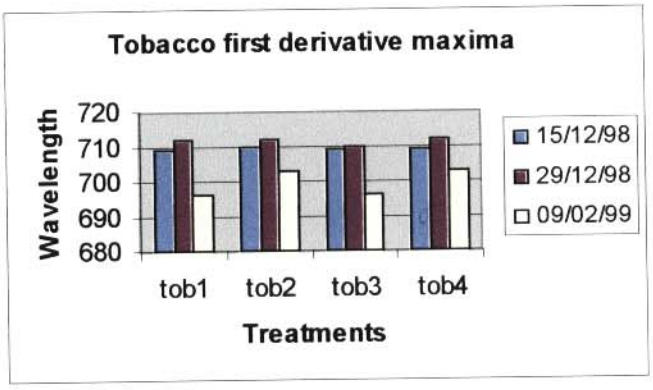

Fig. 5.16 Bar graph showing the position of the maximum inflection of the first derivative (red edge) for the four different treatments at three different sample dates of the tobacco trial.

5.6.2.2 Sunflower

The first sample date (14/4/99, fig.5.17), representing sunflower seedlings, has a uniform distribution of the red edge position with no discernible pattern. The second sample date (04/05/99, fig.5.17) represents the juvenile growth stage of the plants and exhibits an increase in the red edge position towards longer wavelengths as the amount of N in each treatment increases except for the 87kg.ha^{-1} which exhibits a slight decrease in wavelength. The third sample date (23/05/99, fig.5.17) represents the mature growth stage of sunflower and exhibits an increase in the red edge position towards longer wavelengths as the amount of N in each treatment increases except for the 87kg.ha^{-1} which exhibits a slight decrease in wavelength towards shorter wavelengths. This confirms observations made by Peñuelas *et al.* (1994) that N-limited leaves showed a red shift towards shorter wavelengths.

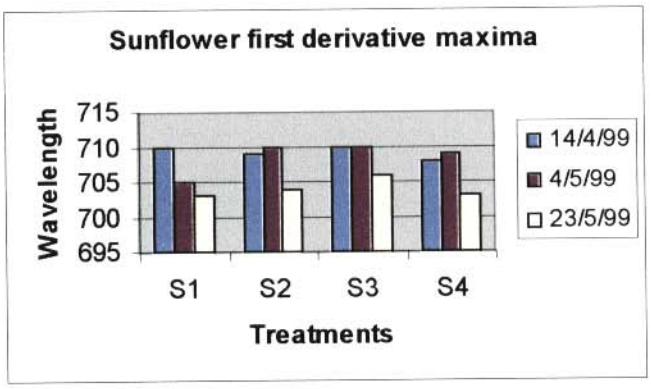

Fig. 5.17 Bar graph showing the position of the maximum inflection of the first derivative (red edge) for the four different treatments at three different sample dates of the sunflower trial.

5.6.2.3 Tomato

The first sample date (15/04/99, fig. 5.18) represents the juvenile growth stage of tomato. No discernible pattern to the distribution of the red edge wavelength can be detected for this growth stage except for a slight decrease in wavelength towards higher N applications. The second sample date (03/05/99, fig. 5.18) represents maturing plants and exhibits an increase in the red edge position towards longer wavelengths as the amount of N in each treatment increases except for the 120kg.ha^{-1} which exhibits a slight decrease in wavelength. The third sample date (14/05/99, fig. 5.18) represents mature plants as blooming starts to take place. There is an increase in the red edge position towards longer wavelengths as the amount of N in each treatment increases. Both dates confirm observations made by Peñuelas *et al.* (1994) that N-limited leaves showed a red shift towards shorter wavelengths.

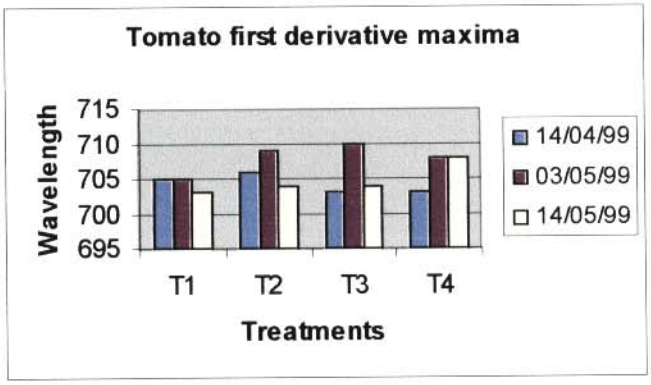

Fig. 5.18 Bar graph showing the position of the maximum inflection of the first derivative (red edge) for the four different treatments

at three different sample dates of the tomato trial.

All three trials (tobacco, sunflower and tomato) exhibit a marked decrease of the red edge position towards shorter wavelengths for the final sample date. This corresponds to changes in leaf N status over time (see section 5.3).

The change in the wavelength of the red edge toward longer wavelengths in the mature growth stages of sunflower and tomato corresponds with the low stress values of the video NDVI for the same dates (see section 5.5).

CHAPTER 6

Discussion

6.1 Introduction

Nitrogen availability is an important determinant of crop productivity. Various types of plant stress have been identified using remote sensing techniques (Balkeman, 1990; Fouchè *et al.*, 1994; Peñuelas *et al.*, 1994 and Fillela *et al.*, 1995). Physiological changes resulting from nitrogen limitations can be translated into clear spectral differences between treatments, demonstrating the relationship between leaf reflectance and leaf chlorophyll and nitrogen concentrations (Peñuelas *et al.*, 1994).

6.2 Evaluation of research

6.2.1 Summarizing of study aims and objectives

To ascertain whether the aims and objectives of this study were met; the original aim will again be presented:

"To develop a methodology to evaluate the N status of three annual crops using non-destructive, inexpensive remote sensing techniques."

The objectives of the study were as follows:

- To correlate the spectral reflectance with N deficiency stress from individual pot experiments.
- Using the resultant data to improve spectral classification of canopy reflectance and, thus, early detection of N-deficiency.

6.2.2 Discussion of results in terms of instruments and techniques

6.2.2.1 Kodak DCS420 digital imagery

A hardware problem with the memory disk of the digital camera rendered the sunflower and tomato images corrupted and unfit for processing. Consequently, the only image data available in this study was those of the tobacco trial which was conducted before the camera developed this problem.

The results obtained after image processing and classification indicate that there is a strong relationship between leaf N status and NDVI values obtained from the images. NDVI values representing leaf area with high photosynthetic activity increase as the N content of the leaf increases. The opposite is true for NDVI values representing leaf area with low photosynthetic activity, which decrease as the leaf N status increases.

It was also noted that this relationship is much stronger in the juvenile growth stage than in the mature growth stage, confirming observations made by Collins (1978). This observation suggests that it would be easier to determine crop N status in the juvenile growth stage of tobacco with a Kodak DCS420 digital camera than in mature crops.

It would be possible to obtain the same results from any infrared digital camera with similar spectral bandwidths. The use of digital imagery has seen rapid development in the past number of years (King, 1995). It is, however still in its infancy. The digital camera used in this study, although top-of-the-range, still has a number of drawbacks. Most digital cameras require small focal length lenses in order to produce a view angle adequate for area-based coverage (King, 1995). The digital camera used in this study produced an image about $^{1}/_{3}$ the size of a corresponding 35mm film camera. If this technique of N-stress detection is to be utilized commercially on a large scale, instruments with the same spectral array but with a larger 'footprint' must be used. The Kodak DCS460 digital camera, for instance, has a six million pixel resolution and its imager magnifies the focal length of the lens only 1.3 times (Kodak, 2000).

6.2.2.2 Ocean Optics S2000 spectroradiometer

Three individual wavelengths (550, 675 and 770nm) were identified in areas that represent critical points in the reflectance spectrum of vegetation canopies. The 550nm wavelength represents the area where maximum reflection of green light takes place (positive correlation with leaf N status), 675nm represents the area where maximum red light is absorbed (negative correlation with leaf N status) and 770nm represents near IR reflectance (positive correlation with leaf N status). These values were chosen to correspond with the filter array of the multi-spectral video camera used in the study (see section 6.2.2.3).

The 550nm wavelength correlated negatively with the leaf N content of all the trials. The 675nm wavelength correlated negatively with both the juvenile and adult growth stages of the sunflower trial and the adult growth stage of the tobacco trial but not with the tomato trial. The 770nm wavelength correlated positively with the leaf N status of all the trials except for the juvenile growth stage of the sunflower trial.

The results of the individual wavelengths suggest that all three crops have the same response to N status in the near IR portion of the reflectance spectrum. However, differences in leaf structure generate variable responses in the visible spectrum. There is not one specific wavelength in the visible spectrum that will respond to N status in the same way for all the crops. Crop-specific wavelengths for the green reflectance and red absorbance peak were determined from reflection values of the individual crops.

The maximum green reflectance for the sunflower trial was found to change from 549nm to 545nm as the growth season progressed. The minimum red reflectance (maximum absorption) changed from 678nm to 679nm during the growing season. The reflectance of both the juvenile and adult growth stages correlated negatively with leaf N status with the juvenile stage exhibiting the strongest negative correlation, confirming observations by Peñuelas *et al.* (1994) that visible reflectance was negatively related to leaf N status. The reflectance values at the green and red peaks will give more reliable indications of N stress during the juvenile growth stage of a sunflower crop.

The tobacco and tomato values for the green reflextion and red absorption maxima were found to be similar, possibly due to the fact that they both belong to the *solanaceae* plant family. The maximum green reflection peak was found to be 555nm throughout the growing season. The minimum red reflection (maximum absorption) was found to be a constant 680nm during the growing season for tobacco but changed from 680nm to 678nm during the growing season for tomato.

The reflectance of the adult growth stage of tobacco correlated negatively with leaf N status, confirming observations by Peñuelas *et al.* (1994) that visible reflectance was negatively related to leaf N status. The juvenile growth stage of tobacco exhibited a non-significant negative correlation with leaf N status for the green reflection peak and a positive correlation for the red absorption peak, contradiciting observations made by Peñuelas *et al.* (1994). The reflectance values at the green and red peaks will give more reliable indications of N stress during the adult growth stage of a tobacco crop.

The red reflectance of tomato correlated positively with leaf N status for both the juvenile (680nm) and the adult (678nm) growth stage. The green reflectance peak (550nm) correlated positively with leaf N status in the juvenile growth stage and negatively in the adult growth stage. Both the juvenile and adult growth stage contradicts findings in the literature (Rock *et al.*, 1988; Peñuelas *et al.*, 1994 and Fillela *et al.*, 1995) that there is a negative correlation between visible reflectance values and leaf N content.

The NDVI (an IR/red ratio) of the individual wavelengths correlated positively with leaf N status for all the trials except for the juvenile growth stage of tobacco and the adult growth stage of tomato.

The position of the red edge (maximum change in the first derivative of the reflectance spectrum) changed towards longer wavelengths with higher leaf N content in both the juvenile and adult growth stages of the tomato and sunflower trial. The position of the red edge in the tobacco trial did not change significantly for the juvenile growth stages but exhibited a variable response in the adult growth stage.

For all three of the trials there is a noticeable shift in the red edge position towards shorter wavelengths for the adult growth stage. This corresponds with the N content of the leaf samples collected at the same dates, confirming that leaf N status has an influence on the position of the red edge.

The red edge position can be seen as a much more reliable indicator of leaf N status and subsequent N deficiency than the individual reflectance values. There is no need to determine the position of the red edge for each individual crop because a change in the position of the red edge from one sample date to the next can give an indication of a change in nutrient status.

6.2.2.3 AgroImager multi-spectral video camera

Of the four spectral bands sampled by the multi-spectral video camera, only three bands (450, 550 and 770nm) could be utilized. The 650nm band was situated at the near IR reflectance peak and all the samples rendered over-saturated images for this band and were discarded. The 770nm spectral band was used for all the band-ratios that utilize a near IR band as part of the equation.

It is apparent out of the multi-spectral video results that no one index was consistent over time in being correlated with leaf N status for all the pot trials. The greenness index correlates well with leaf N status in the adult growth stages of tobacco and tomato plants and with the juvenile growth stage of the sunflower plants. The video NDVI correlates with leaf N status in both the juvenile and adult growth stages of tobacco and tomato but only with the adult growth stage of the sunflower trial.

For tobacco and tomato the video NDVI can be used throughout the growth cycle to determine the N status of the crops. However, the greenness index can only be utilized during the adult growth stage. The reason that the video greenness index does not yield reliable results during the juvenile growth stage is due to the fact the chlorophyll of the leaves is still developing (Collins, 1978) and does not absorb and reflect the visible red and green light optimally.

The leaf N status of the sunflower trial correlated with the greenness index in the juvenile growth stage and the video NDVI in the adult growth stage. It is not clear if these results would be repeatable and it would be advisable to repeat this particular pot experiment to determine that.

The filters used for the video camera have a very narrow bandwidth (5nm). In the light of the findings outlined in section 6.2.2.2, the filters used in this study might not be the most optimal. It would be advisable to determine crop-specific reflection values and use filters of those wavelengths for the video indices. This would, however, defeat the aim of this study in that it would not be an inexpensive remote sensing technique anymore as these narrow-band filters tend to be expensive.

6.3 Conclusions

All the instruments used to obtain the data yielded some positive correlation with leaf N status in one way or another:

1. The most consistent positive correlation was obtained with an NDVI of the images obtained with the digital infrared camera. It is, however, impossible to say if the same positive results would have been obtained in the other two pot trials, as this particular technique could only be applied to the tobacco trial.

2. The position of the red edge, calculated from spectral data obtained with the radiometer, has also yielded a consistent correlation with changes in leaf N status over time. This technique cannot yield instantaneous results as it indicates a shift over time in contrast with the other techniques that render single images of a specific instant. The change in the position of the red edge can give an early warning of N deficiency if the crop is sampled at short intervals during the growing season.

3. The video greenness index and NDVI were only effective in the tobacco and tomato trials, consistently correlating with leaf N status. The greenness index is not reliable in the juvenile growth stages of these crops, due to the development stage of the chlorophyll in the young

leaves. The sunflower trial did not yield corresponding results.

6.4 Recommendations

1. It is evident from the study that the use of a digital infrared camera, like the Kodak DCS420, to obtain broadband infrared imagery yields an NDVI image that indicates N deficiency in crops. The results were obtained under carefully controlled conditions without interference of the soil background. Further trials under field conditions must be conducted to determine if the index is robust enough to yield the same positive results under less controlled circumstances.

2. Trials could be conducted into the possibility of crop-specific filters for the multi-spectral video system to determine if the narrow band detection of crop stress through band-ratio indices could yield improved results. This would, however, limit the cost-effectiveness of the operation as individual filters might prove to be expensive.

3. The possibility of hyperspectral remote sensing can be investigated. True hyperspectral sensors are still in a developmental stage and would require a high capital outlay and a large amount of computer memory and RAM to do the image processing. If crop-specific wavelengths and indices are developed with the radiometer and video devices, it could be applied to the hyperspectral data when it becomes commercially viable sometime in the future.

BIBLIOGRAPHY

Bailey, N.T.J. (1969). Statistical methods in biology. The English University Press. London.

Balkeman, R.H. (1990). The identification of crop disease and stress by aerial photography. *In: Steven, M.D. and Clark, J.A. Applications of Remote Sensing in Agriculture.* Butterworths. London.

Baret, F., Champion, I., Guyot, G. and Podaire, A. (1987). Monitoring wheat canopies with a high resolution radiometer. *Remote sens. of environ.* 22: 367-378.

Barnard, R.O., Buys, A.J., Coetzee, J.G.K., Du Preez, C.C., Meyer, J.H., Van der Merwe, A.J., Van Vuuren, J.A.J., and Volchenk, J.E. (1990). Handbook of standard soil testing methods for advisory purposes. Soil Science Society of South Africa. Pretoria.

Black, C.A., Evans, D.D., White, J.L., Ensminger, L.E., Clark, F.E and Dinauer, R.C. (1965). Methods of soil analysis. Amaerican Society of Agronomy. Madison, WI.

Blackmer, T.M., Schepers, J.S.,Varvel, G.E. and Meyer, G.E. (1996). Analysis of aerial photography for Nitrogen stress within corn fields. *Agron. J.* 88:729-733.

Boochs, F., Kupfer, G., Duckter, K. and Kühbauch, W. (1990). Shape of the red edge as a vitality indicator for plants. *Int. J. Remote Sens.* 11:1741-1753.

Brako, L., Rossman, A.Y. and Farr, D.F. (1995). Scientific and common names of 7 000 vascular plants in the United States. APS Press. St. Paul. Minn.

Buys, A.J. (editor). (1991). Bemestingshandleiding, 5th ed. FSSA. Hennopsmeer.

Campbell, J.B. (1996). Introduction to Remote Sensing. Taylor and Francis. London.

Chao, T.T. and Kroontjie, W. (1964). Relationship between ammonia volatilisation, ammonia concentration and water evaporation. *Soil Sci. Soc. Am. Proc.* 28: 393-395.

Collins, W. (1978). Remote sensing of crop type and maturity. *Photogrammetric Engineering and Remote Sensing.* 44(1): 43-55.

Curran, C.T. (1985). Principles of remote sensing. Longman Scientific and Technical. New York.

Curran, P.J., Dungan, J.L and Gholz, H.L. (1990). Exploring the relationship between reflectance red edge and chlorophyll content in slash pine. *Tree Physiology.* 7: 33-48.

Curran, P.J., Dungan, J.L., Macler, B.A. and Plummer, S.E. (1991). The effect of a red leaf pigment on the relationship between red edge and chlorophyll concentration. *Remote Sens. Environ.* 33: 69-76.

Demitriades-Shah, T.H., Steven, M.D. and Clark, J.A. (1990). High resolution derivative spectra in remote sensing. *Remote Sens. Environ.* 33: 55-64.

Dusek, D.A., Jackson, R.D. and Musick, J.T. (1985). Winter wheat vegetation indices calculated from combinations of seven spectral bands. *Remote Sens. Environ.* 18: 255-267.

Everitt, J.H., Escobar, D.E. and Richardson, A.J. (1992). Estimating grassland phytomass production with near infrared and mid infrared spectral variables. *Remote Sens. Environ.* 30:257-261.

Filella, I. and Peñuelas, J.(1994). The red edge position and shape as an indication of plant chlorophyll content, biomass and hydric status. *Int. J. Remote Sensing.* 15(7): 1459-1470.

Filella, I., Serrano, L., Serra, J. and Peñuelas, J. (1995). Evaluating wheat Nitrogen status with canopy reflectance indices and discriminant analysis. *Crop Sci.* 35: 1400-1405.

Fouchè, P.S. and Booysen, N.W. (1994). Assessment of crop stress conditions using low altitude aerial colour-infrared photography and computer image processing. *Geocarto International*. 9(2): 25-31.

Fouché, P.S., Botha, E.J. and Ayisi, K. (1997). Detecting nitrogen deficiency using near infrared aerial photography and reflected radiation on irrigated cotton, tobacco and wheat. In: *Proceedings of 3rd Int. Airborne Remote Sensing Conference and exhibition, Denmark (July 1997).* II 381-388.

Fouché, P.S., Botha E.J. and Ounnaike, O.A. (1999). Monitoring nitrogen response on wheat using airborne multispectral imaging. In: *Proceedings of 4th Int. Remote Sensing Conference and Exhibition, Canada (June 1999).*

Guoliang, T. (1989). Spectral signatures and vegetation indices of crops. Divisional Report 89/4. CSIRO, Australia.

Guyot, G. (1990). Optical properties of vegetation canopies. *In: Steven, M.D. and Clark. J.A. Applications of Remote Sensing in Agriculture*. Butterworths. London.

Hargrove, W.L. and Kissel, D.E. (1979). Ammonia volatilisation from surface applications of urea in the field and laboratory. *Soil Sci. Soc. Am. J.* 43: 359-363

Haynes, R.J. (1986). Mineral Nitrogen in the plant-soil system. Academic press, Inc. Orlando.

Hesse, P.R. (1971). Textbook of soil chemical analysis. John Murray Publishers. London.

Jacquemoud, S. and Baret, F. (1990). PROSPECT: A model of leaf optical properties spectra. *Remote Sense. Environ.* 34: 75-91.

Jordan, C.F. (1969). Derivation of leaf area index from quality of light on the forest floor.

Ecology. 50: 663-666.

Kanemasu,E.T. (1974). Seasonal canopy reflectance patterns of wheat, sorghum and soybean. *Remote Sens. Environ.* 3: 43-47.

Kanemasu,E.T., Demetriades-Shah, T.H., Su, H. and Lang, A.R.G. (1990). Estimating Grassland biomass using remotely sensed data. *In: Steven, M.D. and Clark, J.A. Applications of remote sensing in agriculture.* Butterworths. London.

King, D. (1995). Airborne multispectral digital cameras and video sensors: a critical review of system designs and applications. *Canadian J. Remote Sens.* 21(3):245-273.

Knott, J.E. (1955). Vegetable growing. Henry Kimpton. London.

Kodak. (2000). Kodak Professional DCS460 Camera specifications. Electronically published at: http://www.kodak.com/global/en/professional/products/cameras/dcs460/specs.shtml.

Ladha, J.K., Tirol-Padre, A., Punzalan, G.C., Castillo, E., Singh, U. and Reddy, C.K. (1998). Nondestructive estimation of shoot Nitrogen in different rice genotypes. *Agron. J.* 90: 33-40.

Leamer, R.W., Noriega, J.R. and Wiegand, C.L. (1978). Seasonal changes in reflectance of two wheat cultivars. *Agron. J.* 20:113-118.

Leblon, B. (1997). Soil and vegetation optical proterties. *In: The Remote Sensing Core Curriculum.* Electronically published: http://umbc7.umbc.edu/~tbenja1/leblon/frame9.html.

Lillesand, T.M. and Kiefer, R.W. (1987). Remote sensing and image interpretation, 2nd ed. John Wiley & Sons. New York.

Maas,S.J. (1998). Estimating cotton canopy ground cover from remotely sensed scene reflectance. *Agron. J.* 90: 384-388.

MacKown, C.T. and Sutton, T.G. (1998). Using early-season leaf traits to predict Nitrogen sufficiency of burley tobacco. *Agron. J.* 90: 21-27.

MacVicar, C.N. (conv.). (1991). Soil Classification: a taxonomic system for South Africa. Department of Agricultural Development. Pretoria.

MicroImages. (1999). TNTmips online manual. MicroImages. Lincoln.

Milton, N.M., Eiswerth, B.A. and Ager, C.M. (1991). Effect of Phosphorous deficiency and spectral reflectance and morphology of soybean plants. *Remote Sens. Environ.* 36: 121-127.

MS Excell. (1996). Microsoft Excell 97 Step by Step. Microsoft Press. Redmond.

Munden, R., Curran, P.J. and Catt, J.A. (1994). The relationship between red edge and chlorophyll concentration in the Broadbalk winter wheat experiment at Rothamsted. *Int. J. Remote Sensing*. 15(4): 705-709.

Myers, R.L. and Minor, H.C. (1993). Sunflower: An American native. Agricultural Publication G4290. University Extension. University of Missouri-Columbia.

Nemenyi, P., Dixon, S.K., White, N.B. and Hedström, M.L. (1977). Statistics from scratch. Holden-Day Inc. San Francisco.

Nilson, H-E. (1995). Remote sensing and image analysis in plant pathology. *Annu. Rev. Phytopathol.* 15: 489-527.

Ocean Optics. (1998). S2000 Fiber Optic Spectrometer - Features and Benefits. Electronically published at: http://www.oceanoptics.com/ProductSheets/S2000.asp.

Optical Insights. (1998). The MultiSpec Agro-Imager hardware operation manual. Optical

Insights, LLC. Tucson.

Peñuelas, J., Gamon, J.A., Fredeen, A.L., Merino, J. and Field, C.B. (1994). Reflectance indices associated with physiological changes in Nitrogen- and water-limited sunflower leaves. *Remote Sens. Environ.* 48: 135-146.

Pinar, A. and Curran, P.J. (1996). Grass chlorophyll and the reflectance red edge. *Int. J. Remote Sensing.* 17(2): 351-357.

Purvis, M.J., Collier, D.C. and Wallis, D. (1964). Laboratory techniques in botany. Butterworths. London.

Railyan, V.Y. and Korobov, R.M. (1993). Red edge structure of canopy reflectance spectra of Triticale. *Remote Sens. Environ.* 46:173-182.

Richardson, A.J., Wiegand, C.L., Wanjura, D.F., Dusek, D. and Steiner, J.L. (1992). Multisite analysis of spectral-biophysical data for sorghum. *Remote Sens. Environ.* 41:71-82.

Rock, B.N., Hoshizaki, T. and Miller, J.R. (1988). Comparison of *in situ* and airborne spectral measurements of the blue shift associated with forest decline. *Remote Sens. Environ.* 24: 109-127.

Scurlock, J.M.O., Wooster, M.J. and D'Souza, G. (1995). Natural vegetation as a resource: A remote sensing workbook for East and Southern Africa. Commonwealth Science Council. Commonwealth Secretariat. London.

Sembiring, H., Raun, W.R., Johnson, G.V., Stone, M.L., Stolie, J.B. and Philips, S.B. (1998). Detection of Nitrogen and Phosphorous nutrient status in winter wheat using spectral radiance. *J. of Plant Nutrition.* 21(6): 1207-1233.

Steel, R.G.D and Torrie, J.H. (1986). Principles and procedures of statistics, a biometrical approach. McGraw-Hill. Singapore.

Steven, M.D., Malthus, T.M., Demetriades-Shah, T.H., Danson, F.M. and Clark, J.A. (1990). High-spectral resolution indices for crop stress. *In: Steven, M.D. and Clark, J.A. Applications of Remote Sensing in Agriculture.* Butterworths. London.

Steyn, A.G.W., Smit, C.F. and Du Toit, S.H.C. (1987). Moderne statistiek vir die praktyk. JL Van Schaik. Pretoria.

Thomas, J.R. and Oerther, G.F. (1972). Estimating Nitrogen content of sweet pepper leaves by reflectance measurements. *Agronomy Journal.* 64: 11-13.

Tucker, C.J. (1979). Red and Photographic infrared linear combinations for monitoring vegetation. *Remote Sensing of Environment.* 8: 127-150.

Tucker, C.J., Holben, B.N., Elgin, J.H. and McMurtrey, J.E. (1980). Relationship of spectral data to grain yield variation. *Photogrammetric Engineering and Remote Sensing.* 46(5): 657-666.

Warner, W.S., Graham, R.W. and Read, R.E. (1996). Small format aerial photography. American Soc. for Photogrammetry and Remote Sensing. Interprint Ltd. Malta.

Wiegand, C.L., Escobar, D.E. and Everitt, J.H. (1992). Comparison of vegetation indices from aerial video and hand-held radiometer observations for wheat and corn. *Proceedings, 13th biennial workshop on color photography in the plant sciences and related fields,* Orlando, Florida, May 6-9, American Society of Photogrammetry and Remote Sensing. 98-109.

Yuzhu, L. (1990). Estimating production of winter wheat by remote sensing and unified ground network. *In: Steven, M.D. and Clark, J.A. Applications of Remote Sensing in Agriculture.* Butterworths. London.

ADDENDUM A

Analysis methodology

1. Soil Analysis

1.1. pH(H_2O) (Barnard *et al.*, 1990)

This procedure determines the pH of a soil in a 1:2.5 soil/water ratio suspension.

Apparatus

balance
50cm^3 beakers
stirring rod
pH meter with glass-calomel electrode

Reagents

Commercial buffer solutions for pH 4 and 7

Procedure

- pH meter is calibrated with the commercial buffer solutions at a given temperature
- place 10g died soil in a beaker
- add 25cm^3 de-ionized water
- stir contents with glass rod, allow to stand for 50 minutes and stir again
- allow to stand for 10 minutes
- determine pH with the electrode positioned in the supernatant solution.

1.2 **Extractable cations (ammonium acetate)** (Barnard *et al.*, 1990)

This method is used to determine the extractable cations Ca^{2+}, Mg^{2+}, and K^{+}, extracted with a neutral ammonium acetate solution.

Apparatus

balance
100cm^3 extraction bottles
reciprocating shaker
funnels and funnel rack
Whatman no 40 filter paper
Volumetric flasks and pipettes
Atomic adsorption spectrophotometer

Reagents

NH_4OAc solution, 1 mol dm^{-3} (at pH 7)
K, Ca and Mg standard solutions (1000 mg dm^{-3})

Procedure

- place 5g air-dried soil in extraction bottle
- add 50cm^3 NH_4OAc solution to the soil and shake horizontally on a reciprocating shaker at 180 oscillations per minute for 30 minutes
- filter extract trough Whatman no 40 filter paper
- collect filtrate but discard the first few drops

Analysis

The elements K, Ca and Mg in the filtrate can be determined by atomic adsorption

spectrophotometry.

1.3 **Extractable Phosphorus (Bray-1)** (Black, 1965 and Barnard *et al.*, 1990)

This procedure is used as an index of available phosphorus in soils by extracting the easily acid-soluble forms of P.

Apparatus

balance
extracting bottles
Whatman no2 filter paper
spectrophotometer
spectrophotometer curvet

Reagents

Bray-1 extracting solution (NH_4F and HCl)
Flocculant
1-amino-2-naphtol-4-sulphonic acid (ANSA)
Ammonium molybdate
phosphorous standard solution

Procedure

Extraction

- place 6.67g of soil in an extraction bottle
- add 50cm^3 Bray-1 solution
- stopper bottle and shake contents manually for 60 seconds
- add 2 drops of flocculant

- filter immediately through Whatman no 2 filter paper

Analysis

- add 2ml ammonium molybdate and a few drops of the ANSA solution
- allow color to develop for 10 minutes
- transfer the solution to a curvet and measure the percentage transmittance with a spectrophotometer.

1.4. **Total Nitrogen (Kjeldal)** (Hesse, 1971)

In this method organic nitrogen is converted into ammonia by boiling with sulfuric acid. The ammonia is subsequently liberated from the sulfate by distillation with alkali and estimated.

Apparatus

balance
digestion tubes
digestion block
Kjeldal nitrogen still
100cm^3 conical flasks
burette

Reagents

concentrated H_2SO_4
catalyst mixture (potassium sulfate, copper sulfate and selenium)
NaOH solution
H_3BO_3 (pH 7) solution with methyl red and methylene blue indicator
0.1 N HCl

Procedure

Extraction

- place 10g soil in an extraction cylinder
- add 20cm^3 H_2SO_4 and 10g of the catalyst mixture
- digest in digestion block for three hours

Distillation

- dilute acid solution with de-ionized water
- add excess NaOH to create an alkaline medium
- distill solution in a Kjeldal nitrogen still and catch the distillate in 20cm^3 boric acid solution

Analysis

- Titrate with HCl until end-point is reached

2. Plant analysis

2.1. Total Nitrogen (Kjeldal) (Purvis *et al.*, 1964)

In this method plant material is oxidized by sulfuric acid and nitrogen is converted to ammonia. The ammonia is liberated by distillation in the presence of an alkaline solution and collected in boric acid.

Apparatus

balance
digestion tubes
digestion block
Kjeldal nitrogen still
$50cm^3$ conical flasks
burette

Reagents

concentrated H_2SO_4
catalyst mixture (potassium sulfate, copper sulfate and selenium)
NaOH solution
H_3BO_3 (pH 7) solution with methyl red and bromocresol green indicator
0.1 N HCl

Procedure

Extraction

- place 50-100mg dried plant material in an extraction cylinder
- add $1cm^3$ H_2SO_4 and a spatula-tip of the catalyst mixture
- digest in digestion block until the digest is apple green and then for half an hour longer

Distillation

- dilute acid solution with de-ionized water
- add excess NaOH to create an alkaline medium
- distill solution in a Kjeldal nitrogen still and collect the distillate in $10cm^3$ boric acid solution

Analysis

- Titrate with HCl until end-point is reached

ADDENDUM B

Featuremapping results

Classified images of the individual plant samples.

Plate #	Description
Tobacco TOB1/2/3/4 refers to the replicate and A, B, C and D indicates the N treatment (0, 73.3, 146.6 and 220 $kg.ha^{-1}$). High stress (orange) indicates low photosynthetic activity and high N stress, moderate stress (purple/yellow) indicates moderate photosynthetic activity and moderate N stress, and low stress (green) indicates high photosynthetic activity and low N stress.	
1, 2 and 3	Featuremaps of NDVI of the red and near infrared channels of the DCS images of individual tobacco plants (15/12/98).
4, 5 and 6	Featuremaps of NDVI of the red and near infrared channels of the DCS images of individual tobacco plants (09/02/99).
7, 8 and 9	Featuremaps of the video greenness index of the green (450nm) and red (550nm) channels of the multispectral video images of individual tobacco plants (15/12/98).
9, 10 and 11	Featuremaps of the video NDVI of the red (550nm) and near infrared (770nm) channels of the multispectral video images of individual tobacco plants (15/12/98)
12 and 13	Featuremaps of the video greenness index of the green (450nm) and red (550nm) channels of the multispectral video images of individual tobacco plants (09/02/99).
14 and 15	Featuremaps of the video NDVI of the red (550nm) and near infrared (770nm) channels of the multispectral video images of individual tobacco plants (09/02/99)

Sunflower S1/2/3/4 refers to the replicate and A, B, C and D indicates the N treatment (0, 27, 59 and 87 $kg.ha^{-1}$). High stress (orange) indicates low photosynthetic activity and high N stress, moderate stress (yellow) indicates moderate photosynthetic activity and moderate N stress, and low stress (green) indicates high photosynthetic activity and low N stress.	
16, 17 and 18	Featuremaps of the video NDVI of the red (550nm) and near infrared (770nm) channels of the multispectral video images of individual sunflower plants (04/05/99)
18, 19 and 20	Featuremaps of the video greenness index of the green (450nm) and red (550nm) channels of the multispectral video images of individual sunflower plants (04/05/99)
21 and 22	Featuremaps of the video NDVI of the red (550nm) and near infrared (770nm) channels of the multispectral video images of individual sunflower plants (23/05/99)
23 and 24	Featuremaps of the video greenness index of the green (450nm) and red (550nm) channels of the multispectral video images of individual sunflower plants (23/05/99)
Tomato T1/2/3/4 refers to the replicate and A, B, C and D indicates the N treatment (0, 40, 80 and 120 $kg.ha^{-1}$). High stress (orange) indicates low photosynthetic activity and high N stress, moderate stress (yellow) indicates moderate photosynthetic activity and moderate N stress, and low stress (green) indicates high photosynthetic activity and low N stress.	
25 and 26	Featuremaps of the video NDVI of the red (550nm) and near infrared (770nm) channels of the multispectral video images of individual tomato plants (15/04/99)
27 and 28	Featuremaps of the video greenness index of the green (450nm) and red (550nm) channels of the multispectral video images of individual tomato plants (15/04/99)
29 and 30	Featuremaps of the video NDVI of the red (550nm) and near infrared (770nm) channels of the multispectral video images of individual tomato plants (03/05/99)
30 and 31	Featuremaps of the video greenness index of the green (450nm) and red (550nm)

	channels of the multispectral video images of individual tomato plants (03/05/99)
32 and 33	Featuremaps of the video NDVI of the red (550nm) and near infrared (770nm) channels of the multispectral video images of individual tomato plants (14/05/99)
34 and 35	Featuremaps of the video greenness index of the green (450nm) and red (550nm) channels of the multispectral video images of individual tomato plants (14/05/99)

Tobacco (15/12/98)
Plate 1

DCS NDVI featuremaps

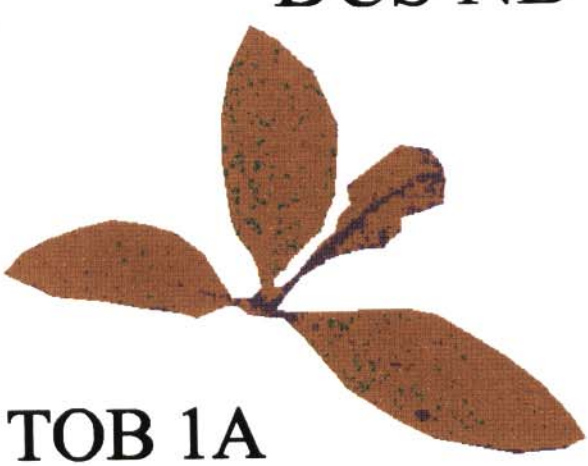

TOB 1A

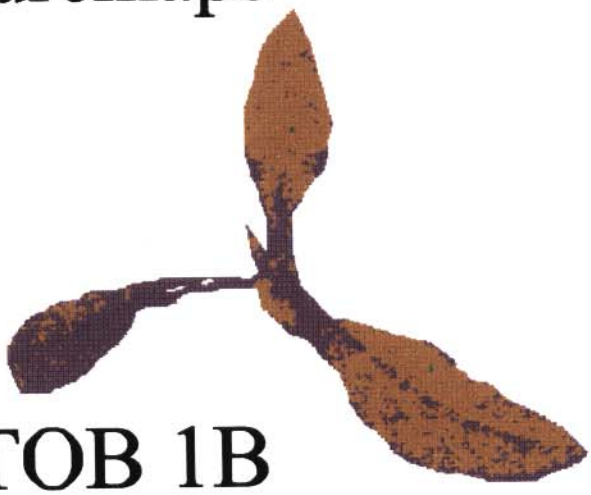

TOB 1B

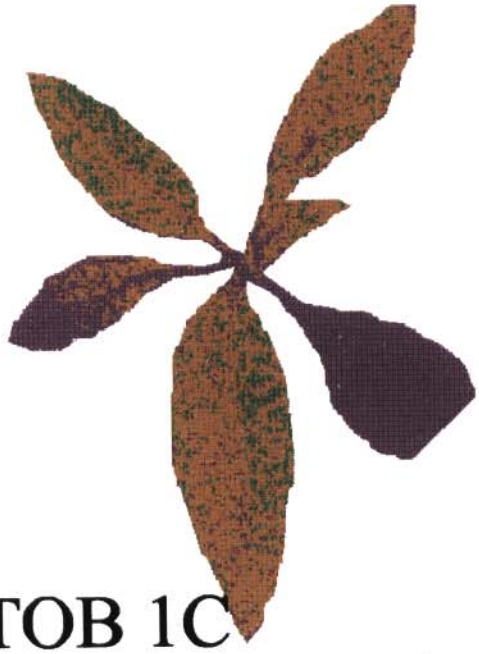

TOB 1C

TOB 1D

TOB 2A

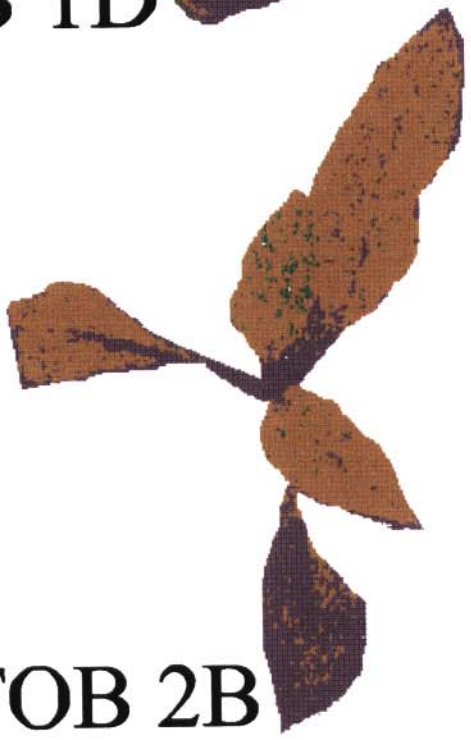

TOB 2B

high stress
moderate stress
low stress

Plate 2

Tobacco (15/12/98)
DCS NDVI featuremaps

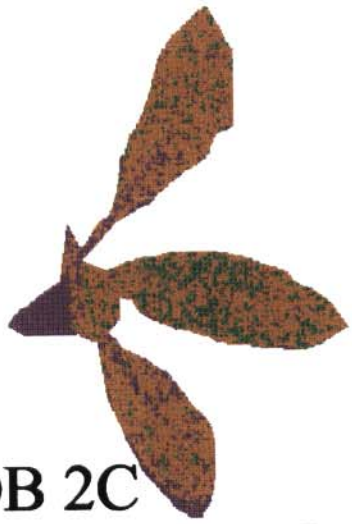

TOB 2C

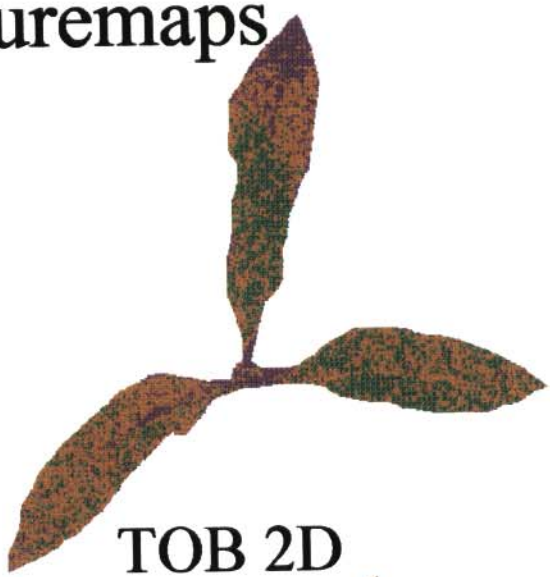

TOB 2D

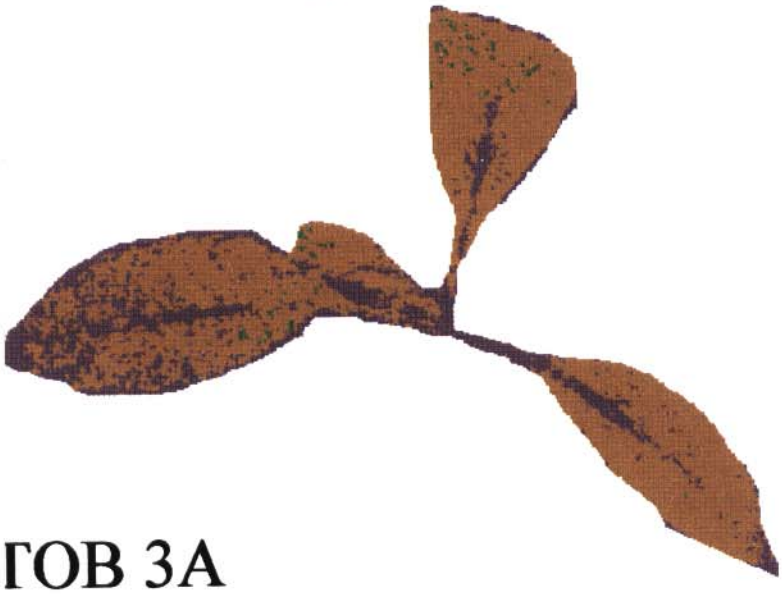

ГОВ 3A

TOB 3B

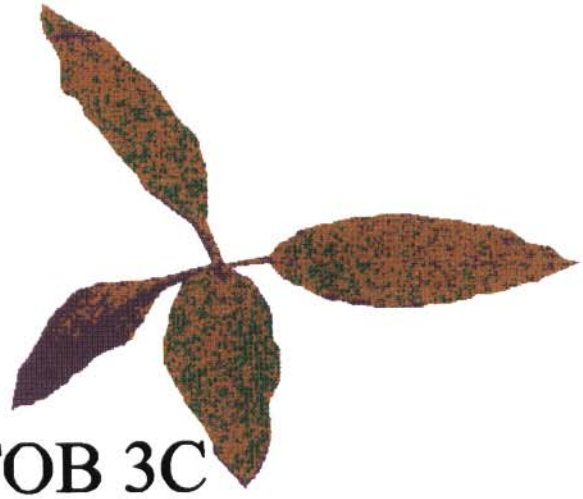

TOB 3C

TOB 3D

high stress
moderate stress
low stress

Plate 3

Tobacco (15/12/98) DCS NDVI featuremaps

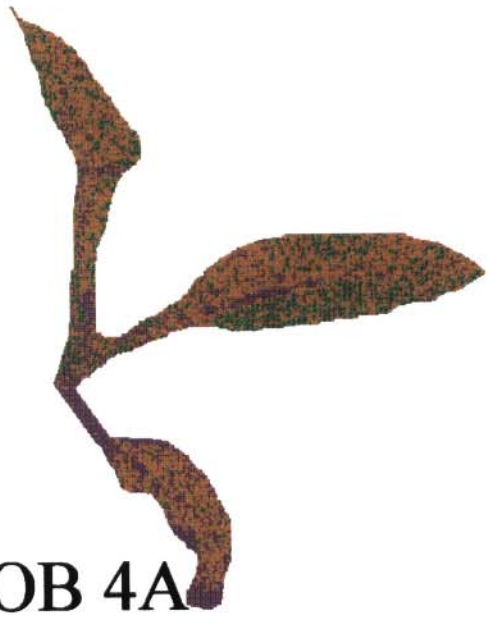

TOB 4A

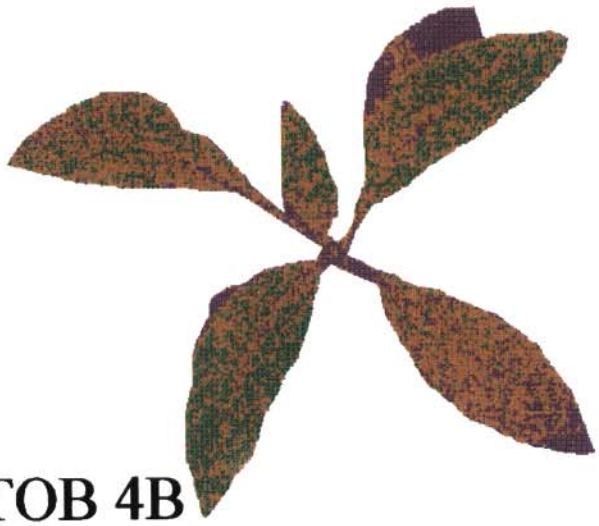

TOB 4B

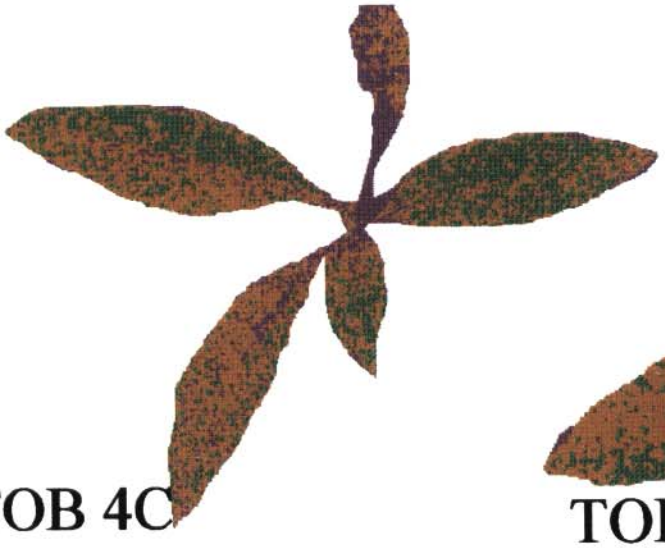

TOB 4C

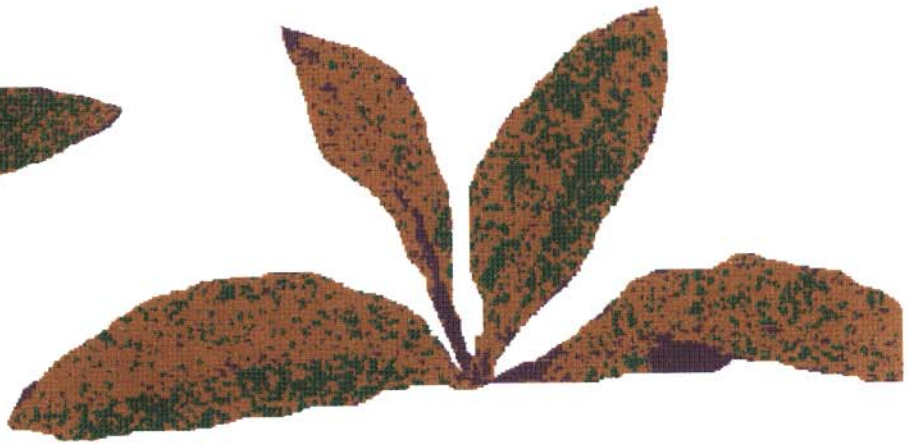

TOB 4D

high stress
moderate stress
low stress

Plate 4

Tobacco (09/02/99) DCS NDVI featuremaps

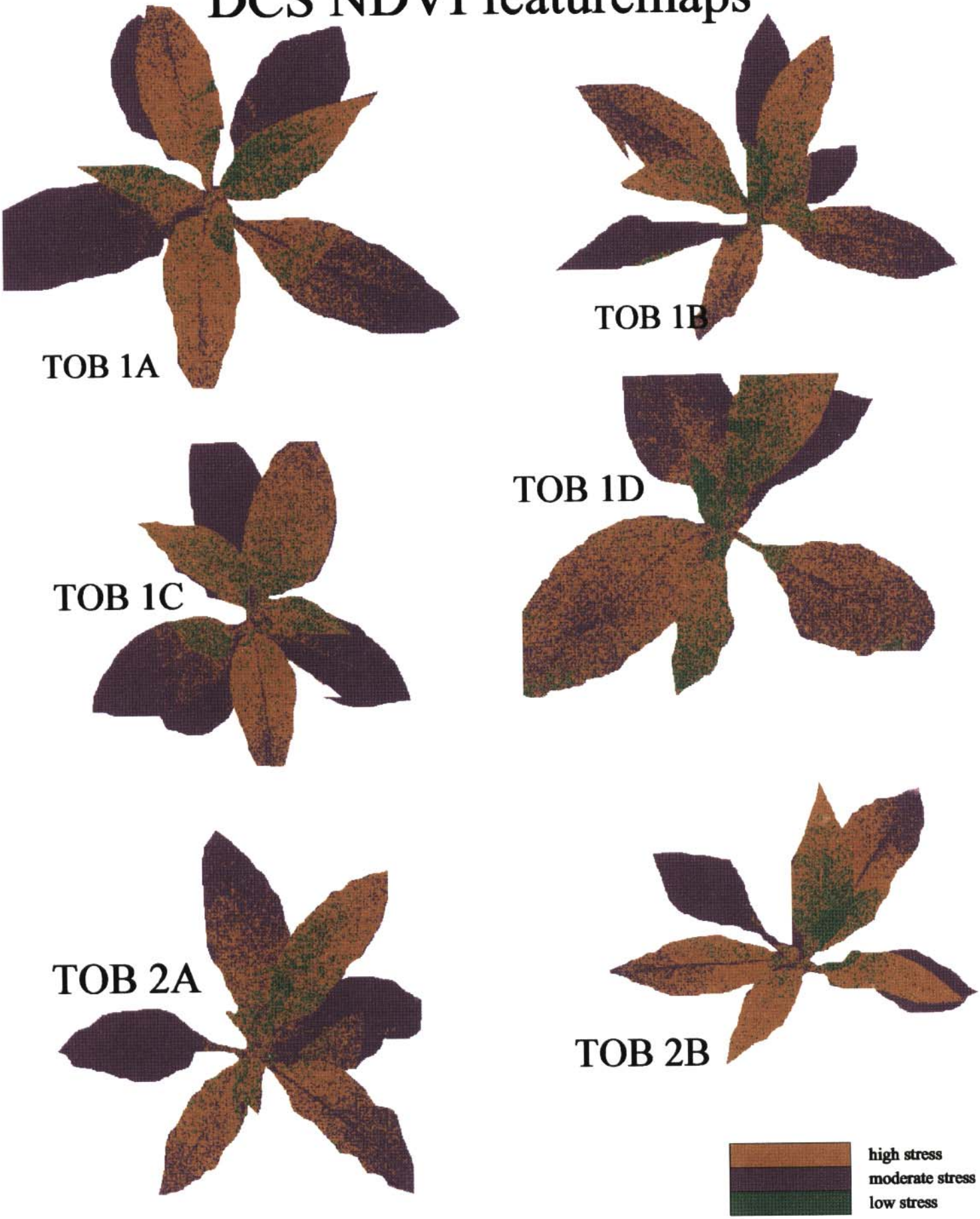

Plate 5

Tobacco (09/02/99) DCS NDVI featuremaps

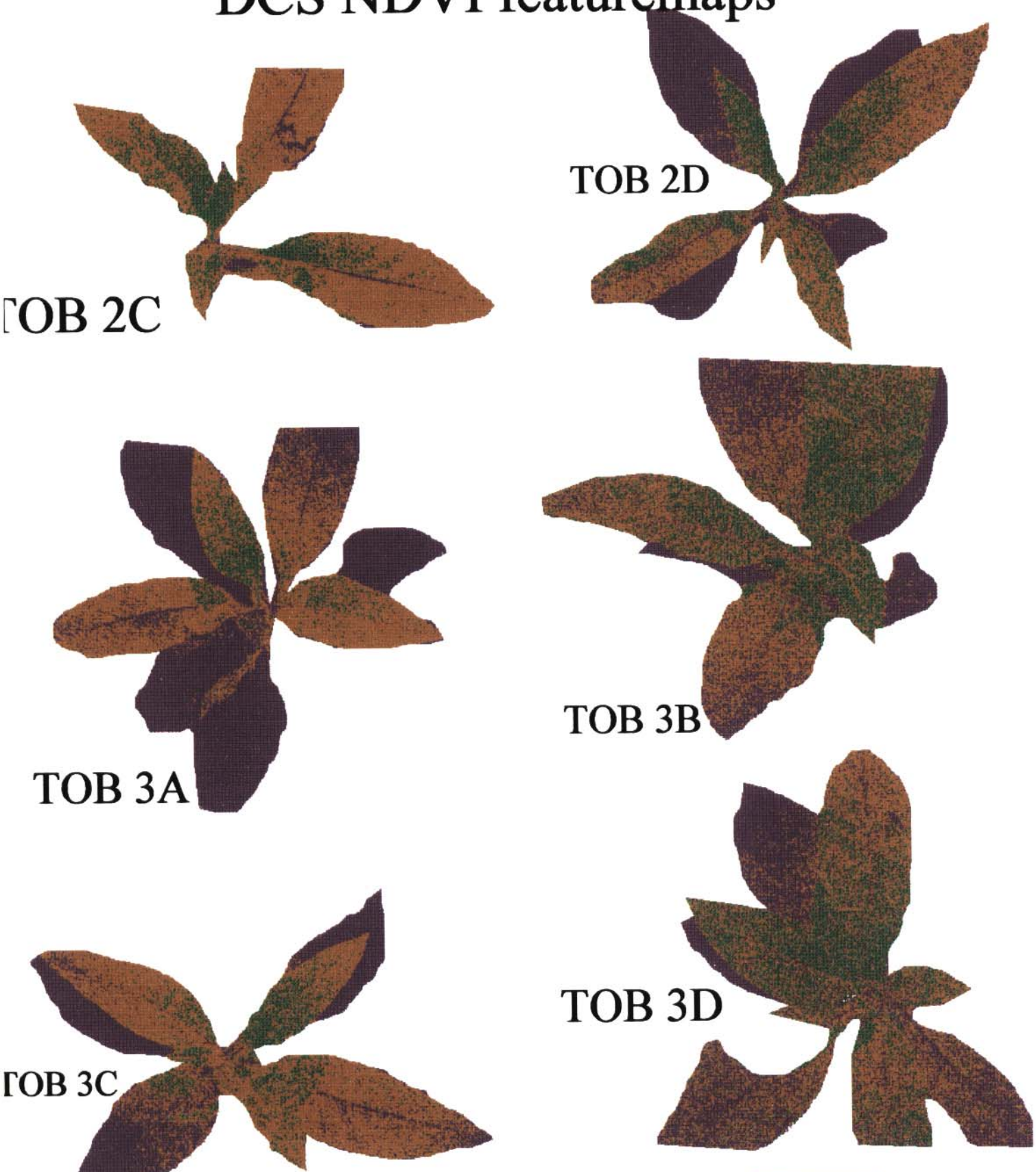

Plate 6

Tobacco (09/02/99) DCS NDVI featuremaps

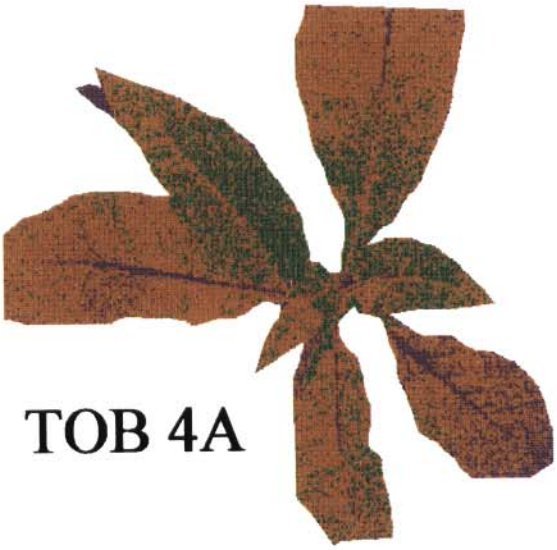

TOB 4A

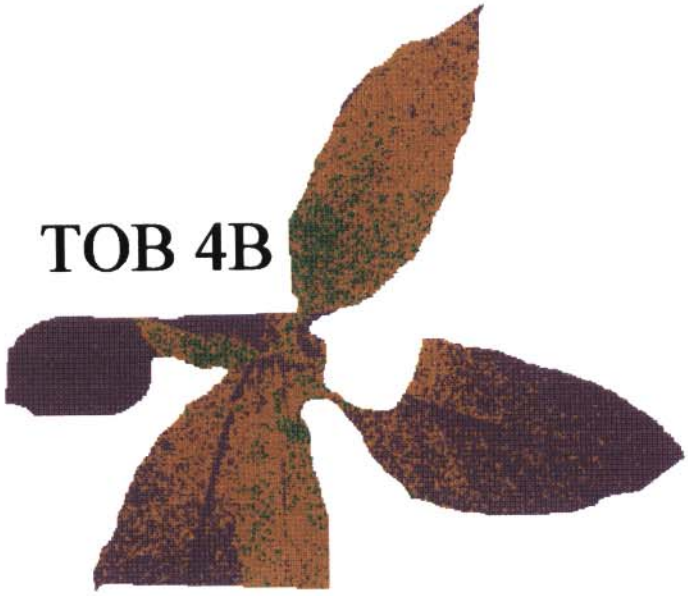

TOB 4B

TOB 4C

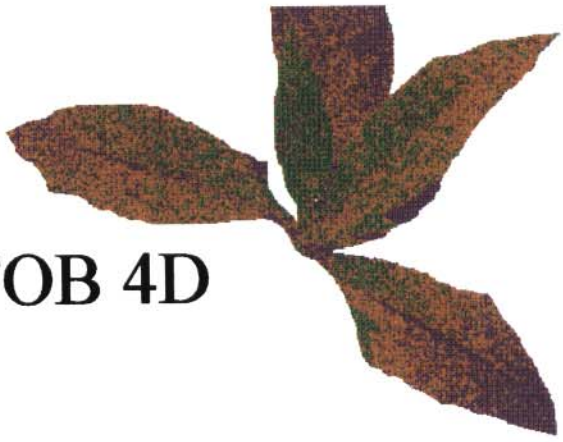

TOB 4D

high stress
moderate stress
low stress

Plate 7

Tobacco (15/12/98) video greenness featuremaps

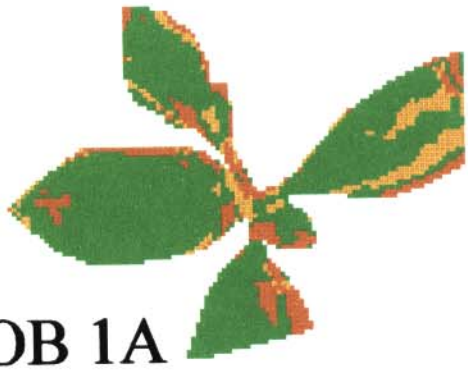

TOB 1A

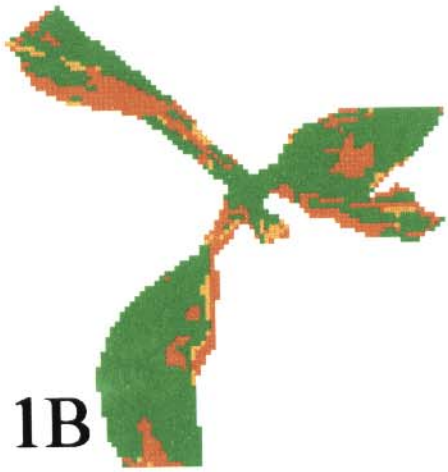

TOB 1B

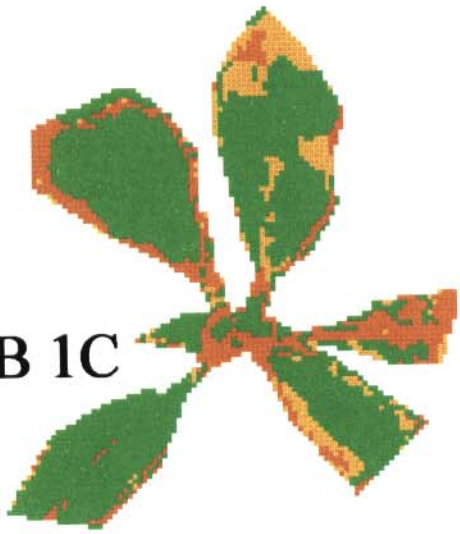

TOB 1C

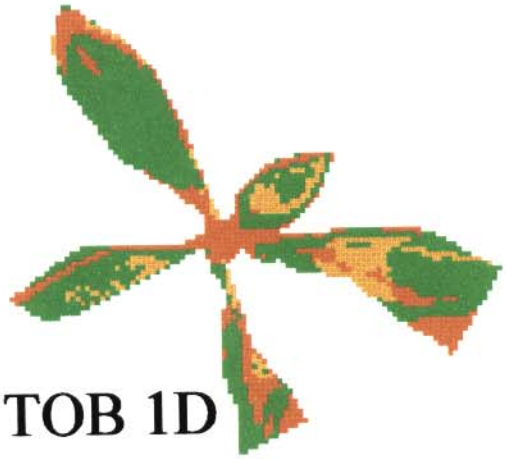

TOB 1D

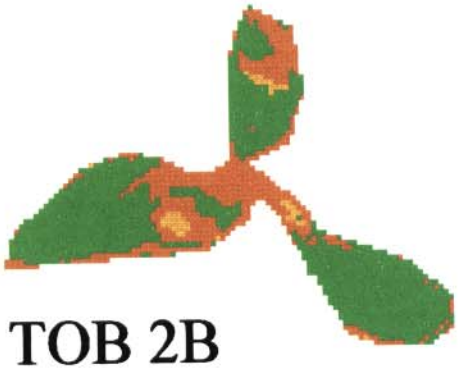

TOB 2B

TOB 2C

high stress
moderate stress
low stress

Plate 8

Tobacco (15/12/98) video greenness featuremaps

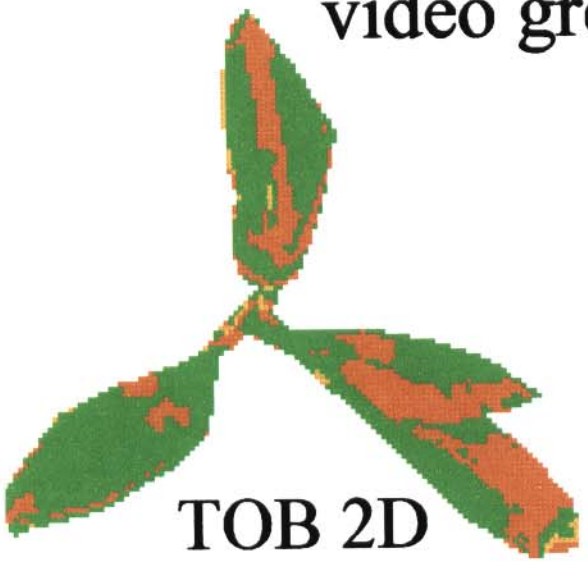

TOB 2D

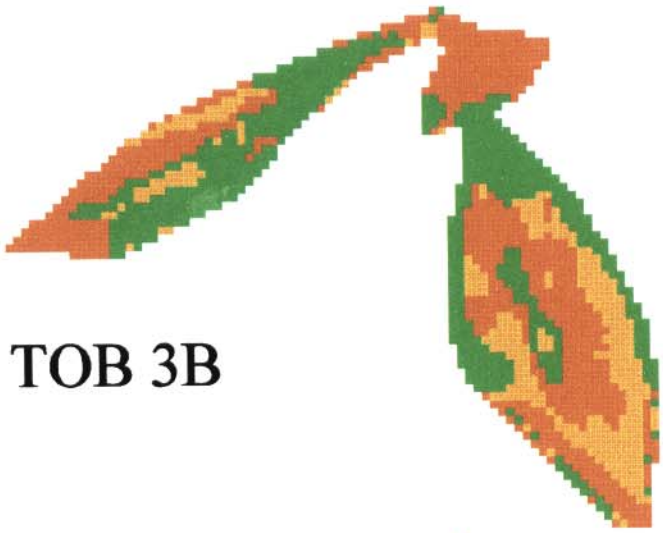

TOB 3B

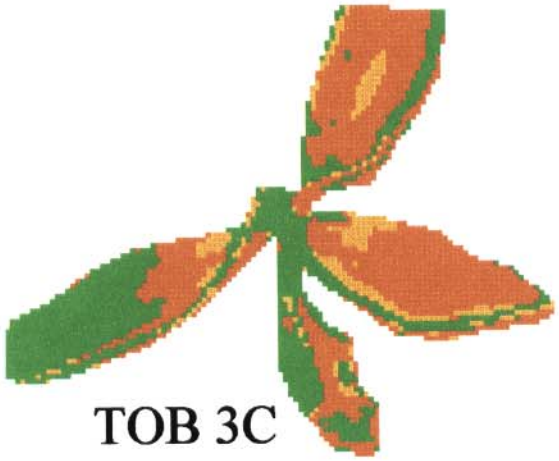

TOB 3C

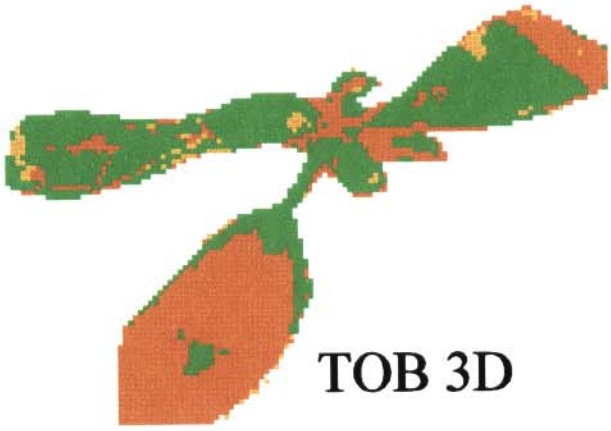

TOB 3D

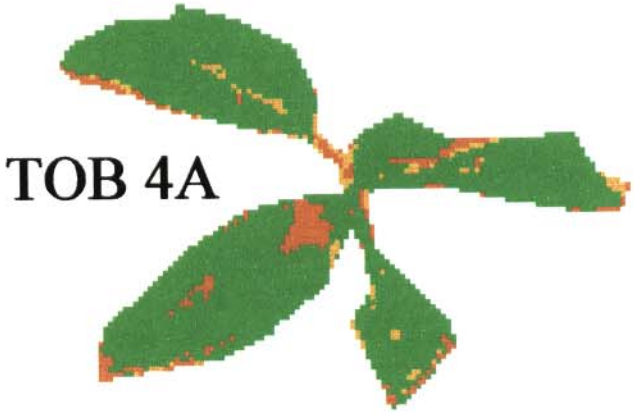

TOB 4A

TOB 4B

high stress
moderate stress
low stress

Plate 9

Tobacco (15/12/98) video greenness featuremaps

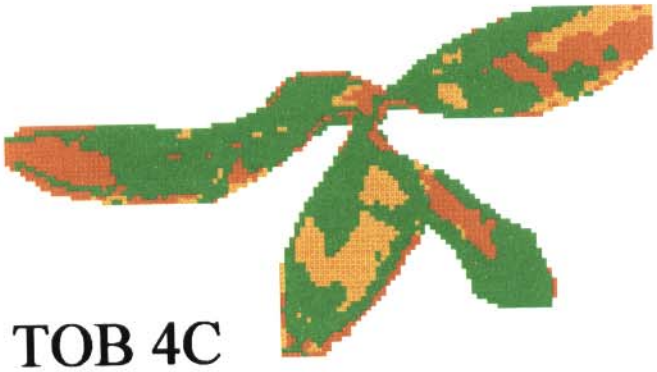

TOB 4C

Tobacco (15/12/98) video NDVI featuremaps

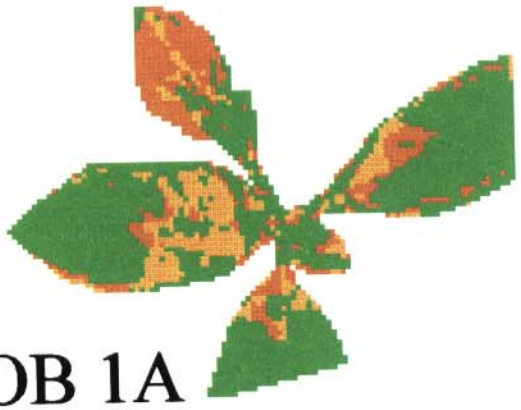

TOB 1A

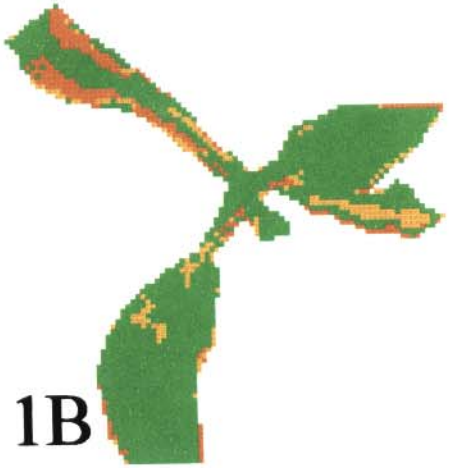

TOB 1B

high stress
moderate stress
low stress

Plate 10

Tobacco (15/12/98) video NDVI featuremaps

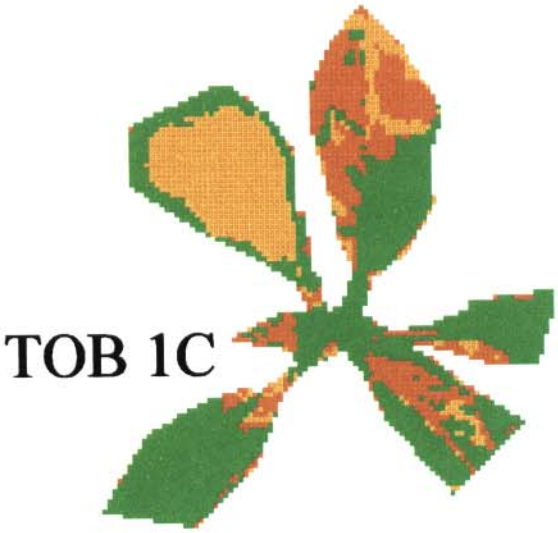

TOB 1C

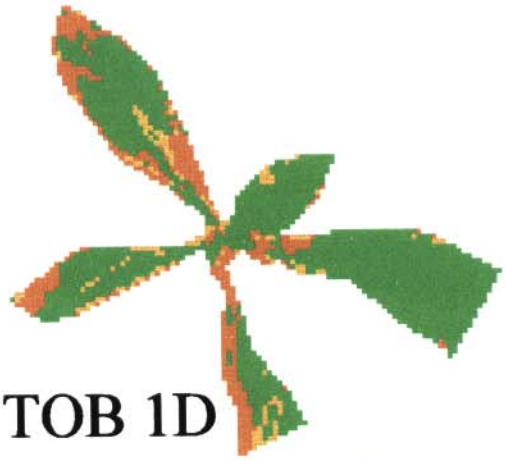

TOB 1D

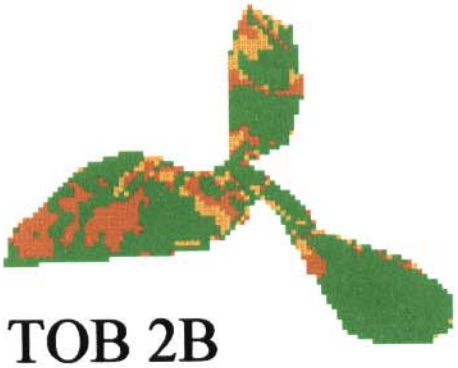

TOB 2B

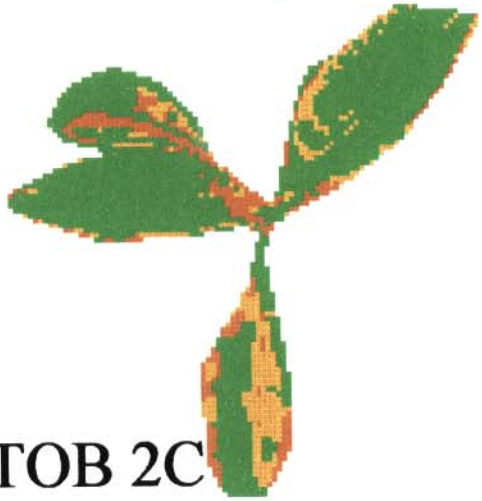

TOB 2C

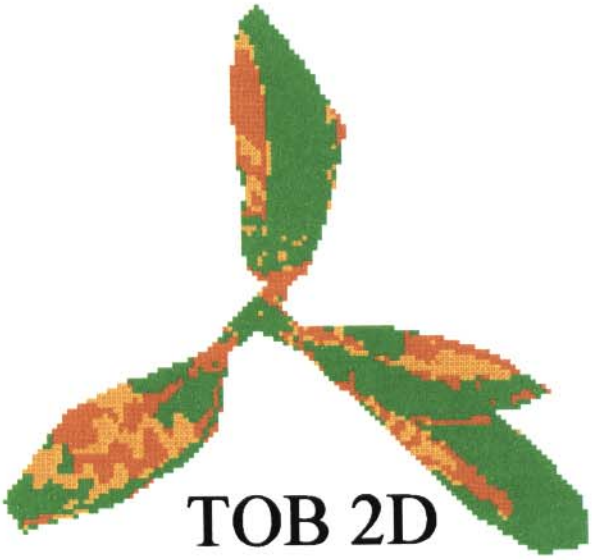

TOB 2D

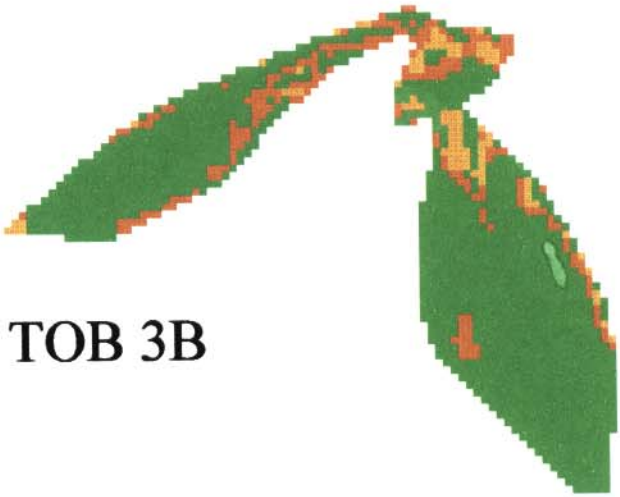

TOB 3B

high stress
moderate stress
low stress

Plate 11

Tobacco (15/12/98) video NDVI featuremaps

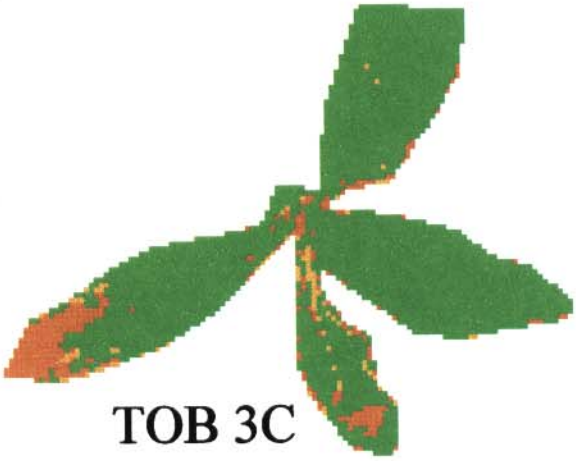

TOB 3C

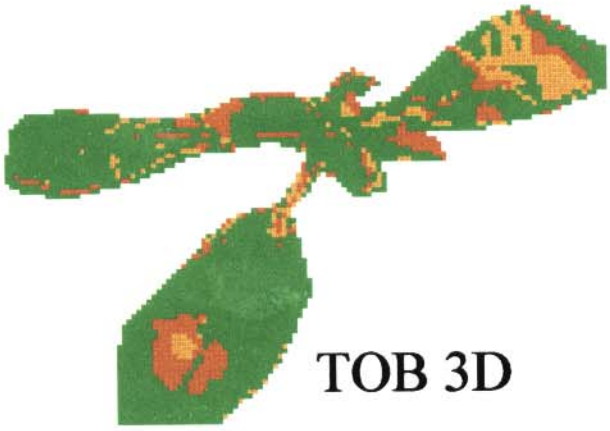

TOB 3D

TOB 4A

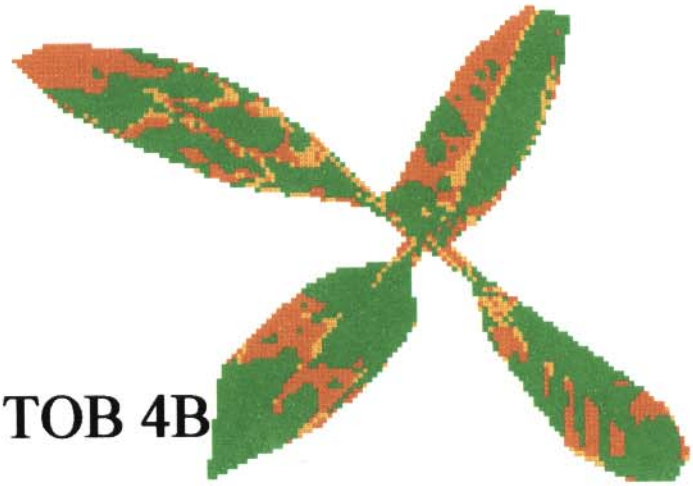

TOB 4B

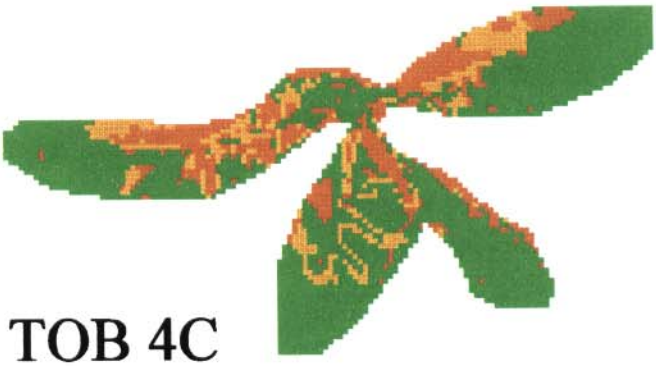

TOB 4C

high stress
moderate stress
low stress

Plate 12

Tobacco (09/02/99) video greenness featuremaps

TOB 1A

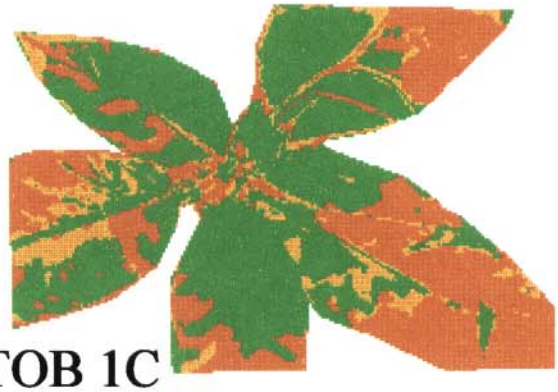

TOB 1C

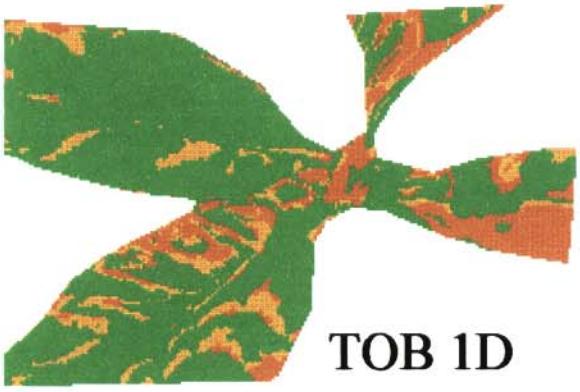

TOB 1D

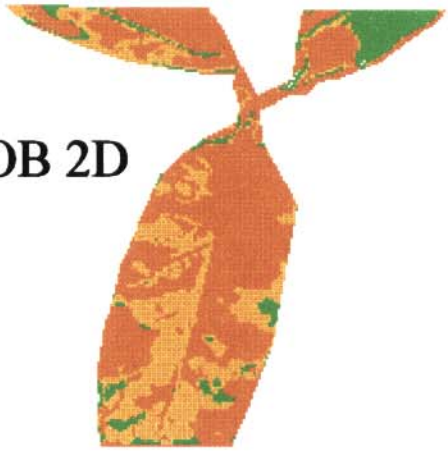

TOB 2D

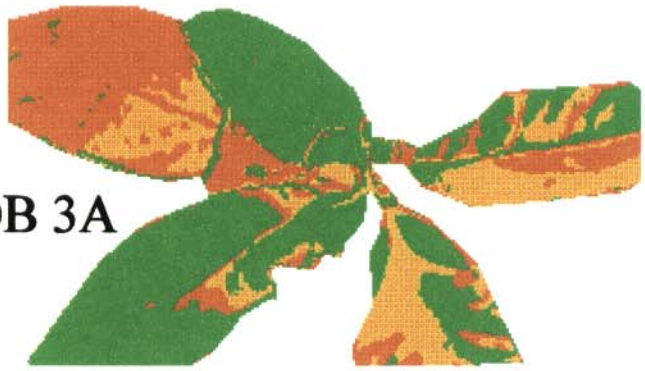

OB 3A

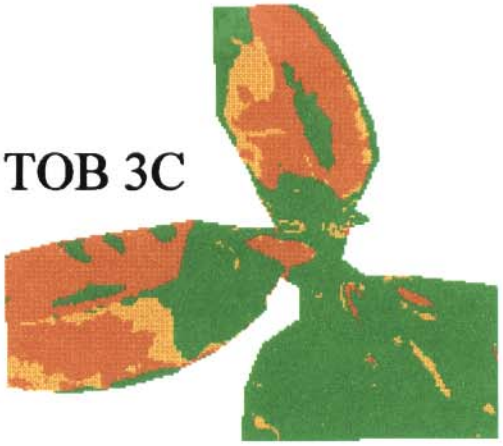

TOB 3C

high stress
moderate stress
low stress

Plate13

Tobacco (09/02/99) video greenness featuremaps

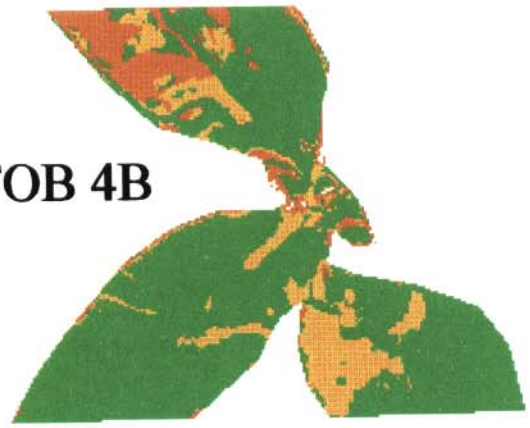

TOB 4B

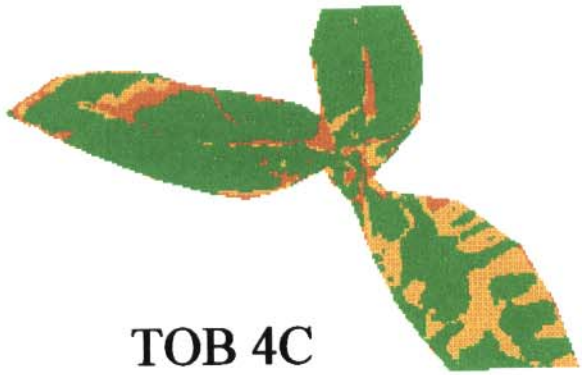

TOB 4C

TOB 4D

high stress
moderate stress
low stress

Plate 14

Tobacco (09/02/99) video NDVI featuremaps

TOB 1A

TOB 1C

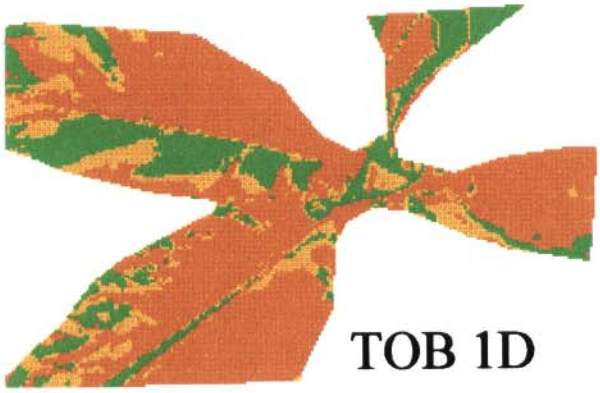

TOB 1D

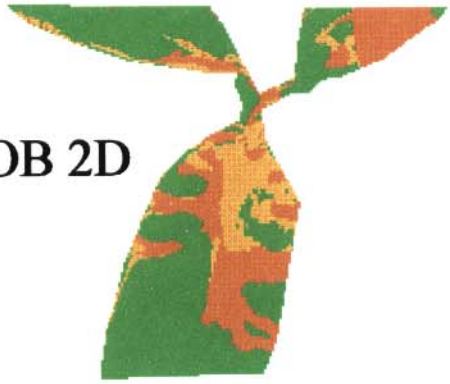

TOB 2D

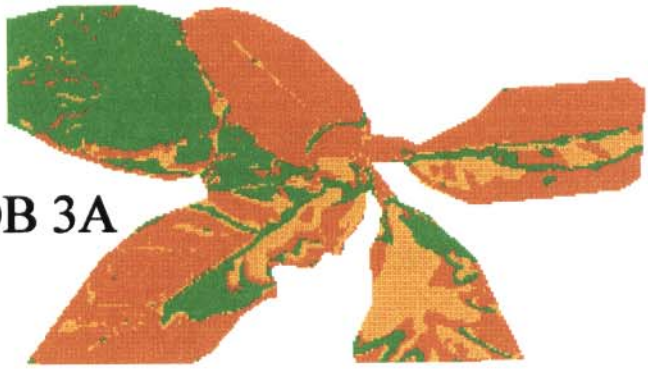

TOB 3A

TOB 3C

high stress
moderate stress
low stress

Plate 15

Tobacco (09/02/99) video NDVI featuremaps

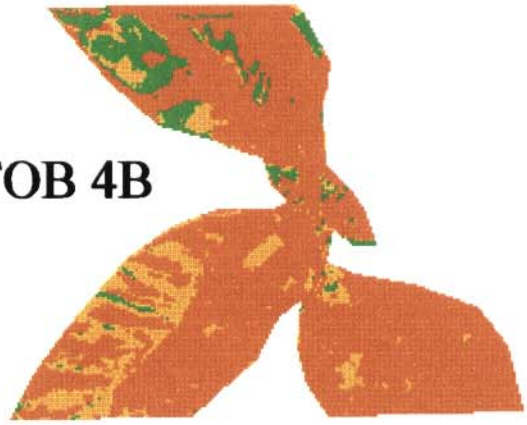

TOB 4B

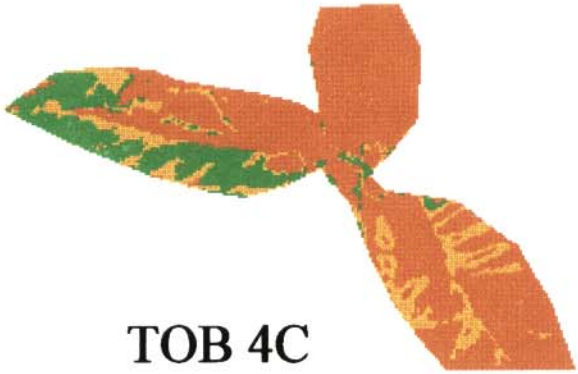

TOB 4C

TOB 4D

high stress
moderate stress
low stress

Plate 16

Sunflower (04/05/99) video NDVI featuremaps

S 1A

S 1B

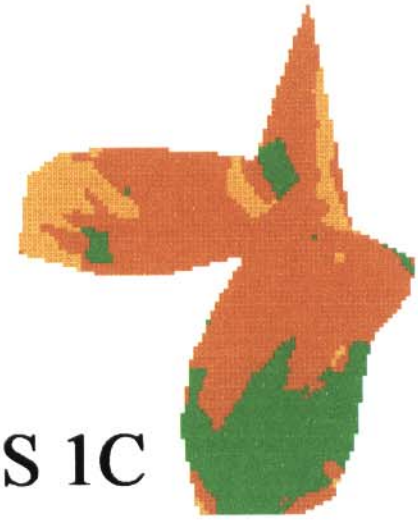

S 1C

S 1D

S 2A

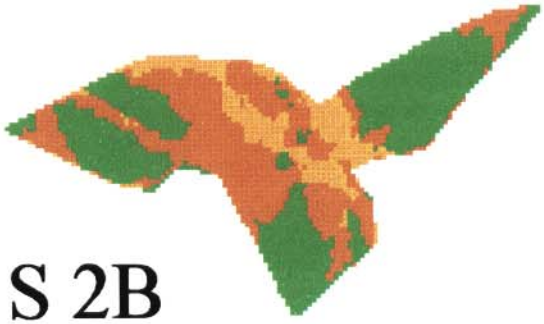

S 2B

class1 (low)
class2 (moderate)
class3 (high)

Plate 17

Sunflower (04/05/99) video NDVI featuremaps

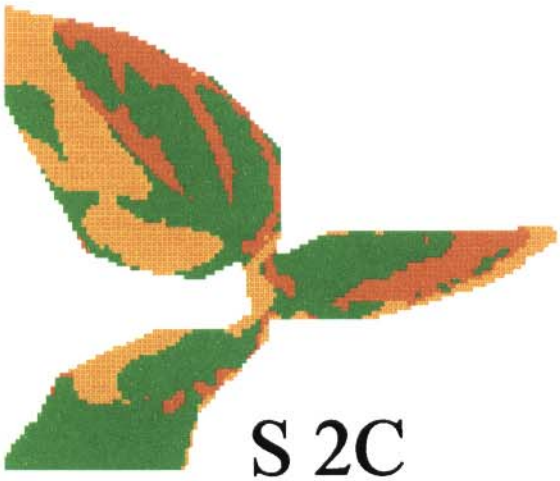

S 2C

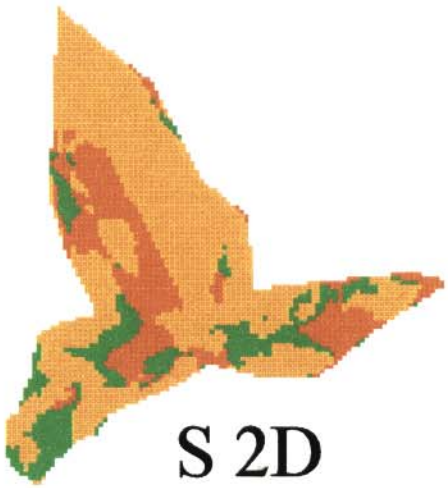

S 2D

S 3A

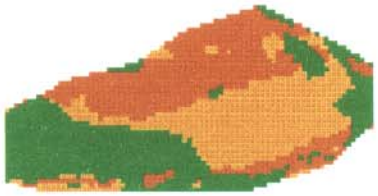

S 3b

S 3D

S 4A

class1 (low)
class2 (moderate)
class3 (high)

Sunflower (04/05/99) video NDVI featuremaps

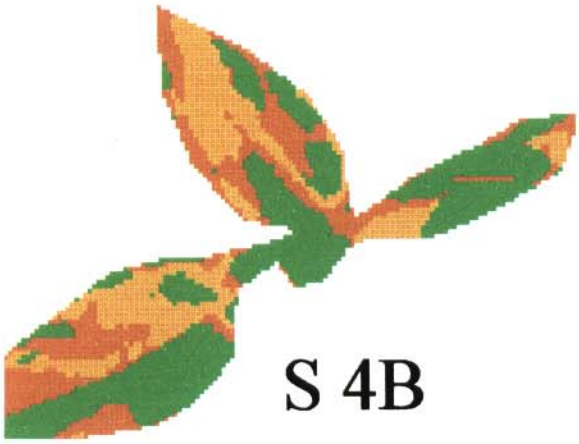

S 4B

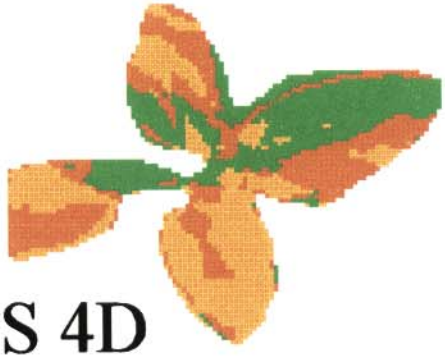

S 4D

Sunflower (04/05/99) video greenness index featuremaps

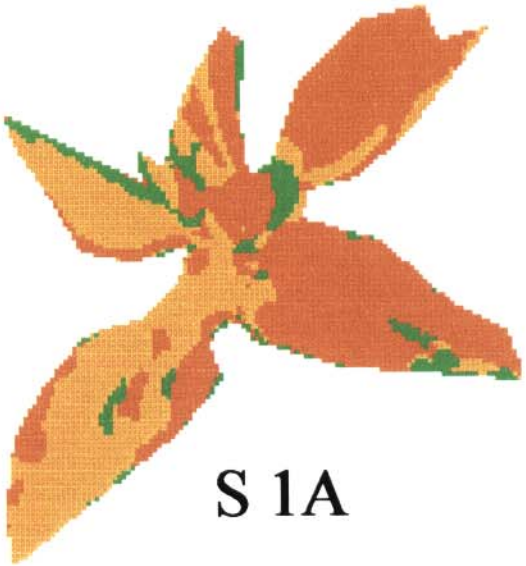

S 1A

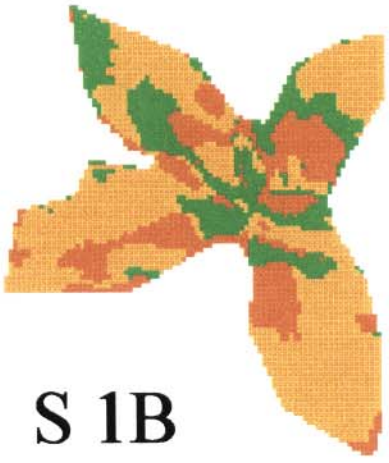

S 1B

class1 (low)
class2 (moderate)
class3 (high)

Plate19

Sunflower (04/05/99) video greenness index featuremaps

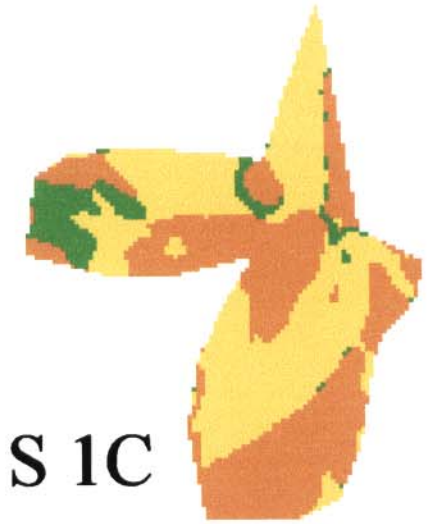

S 1C

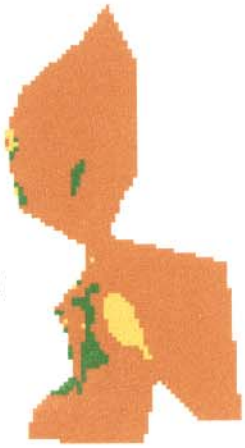

S 1D

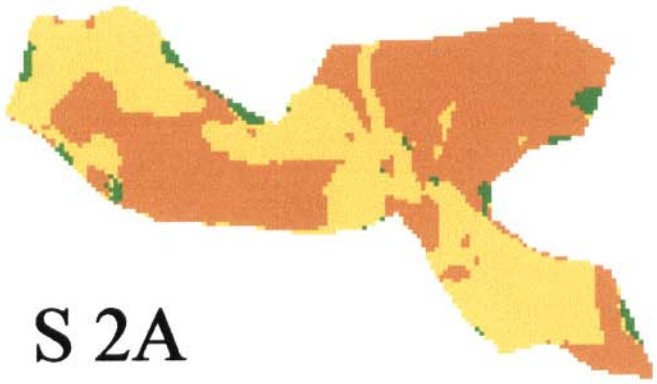

S 2A

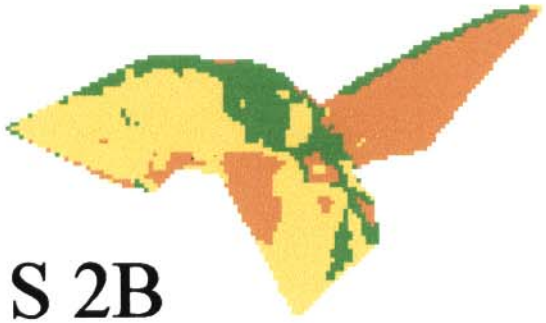

S 2B

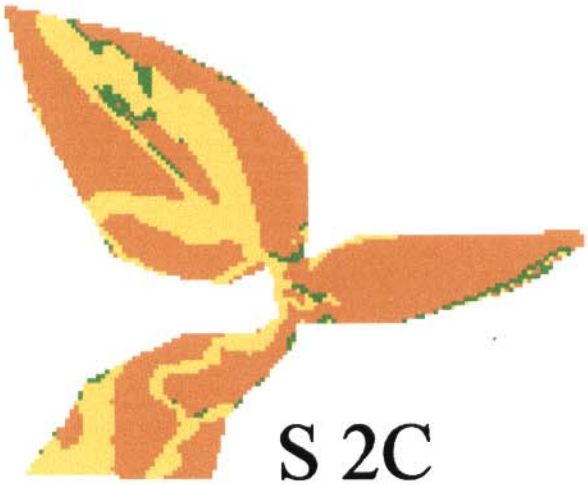

S 2C

S 2D

high stress
moderate stress
low stress

Plate 20

Sunflower (04/05/99) video greenness index featuremaps

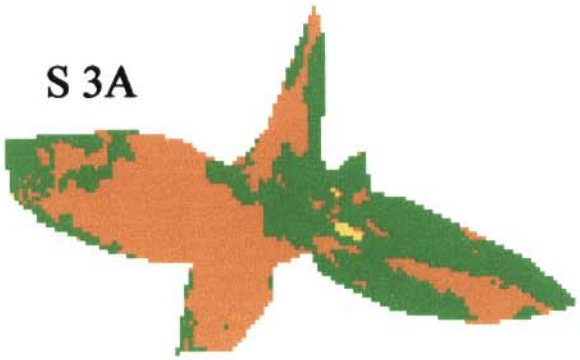

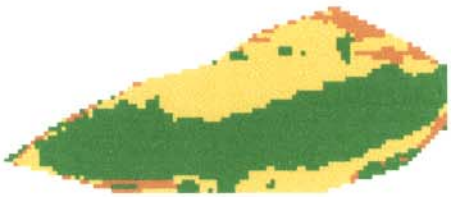

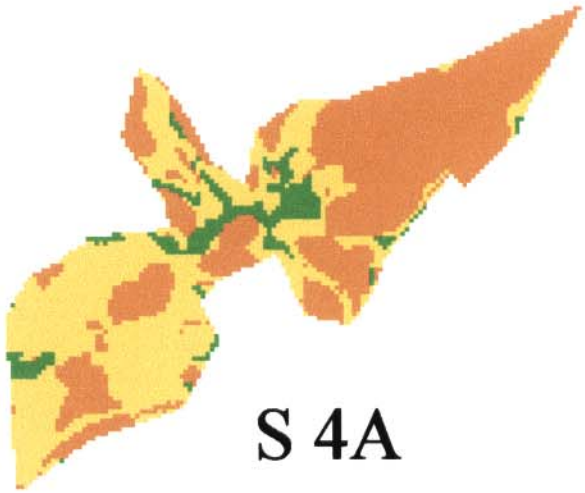

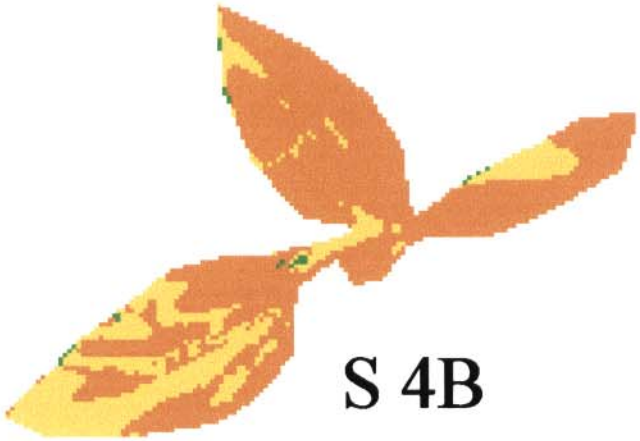

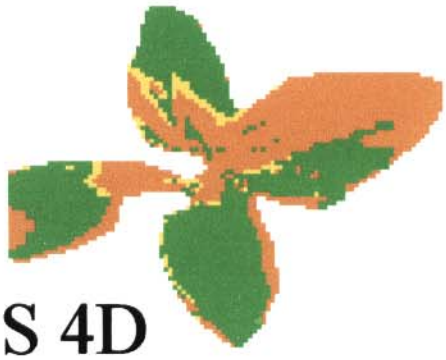

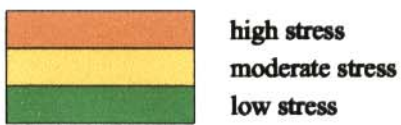

Plate 21

Sunflower (23/05/99) video NDVI featuremaps

S 1B

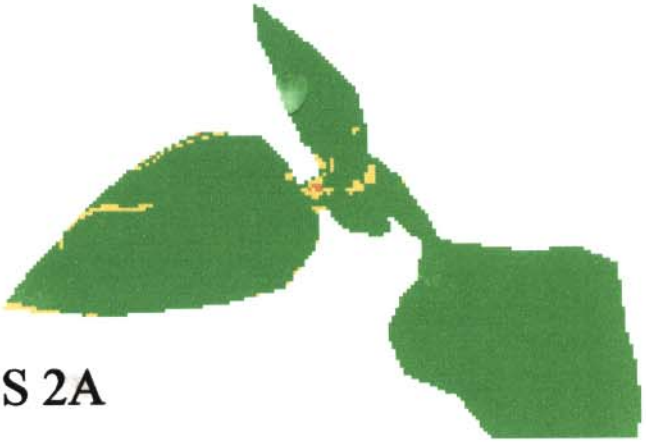

S 2A

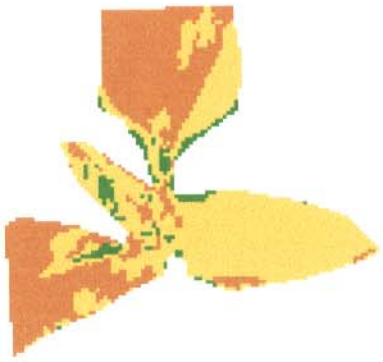

S2B

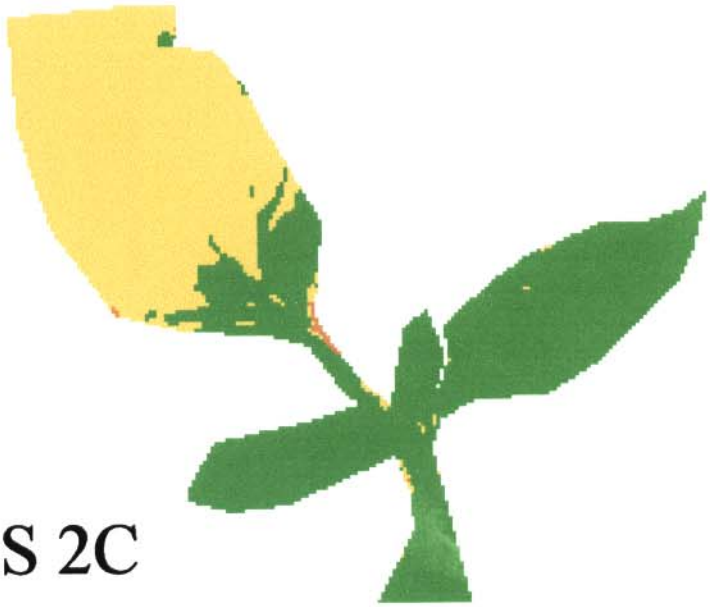

S 2C

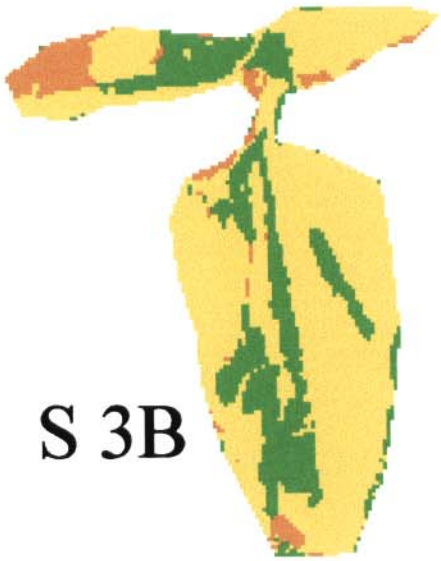

S 3B

S 3D

high stress
moderate stress
low stress

Plate 22

Sunflower (23/05/99) video NDVI featuremaps

S 4A

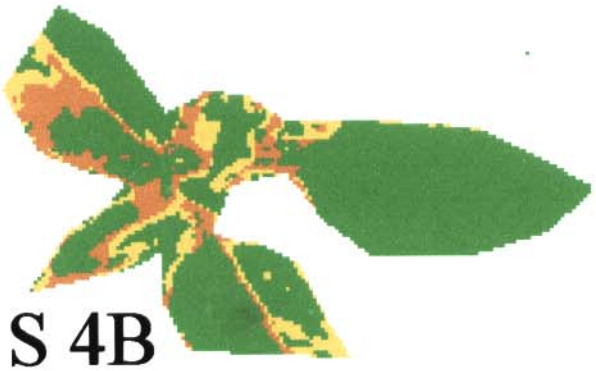

S 4B

S 4D

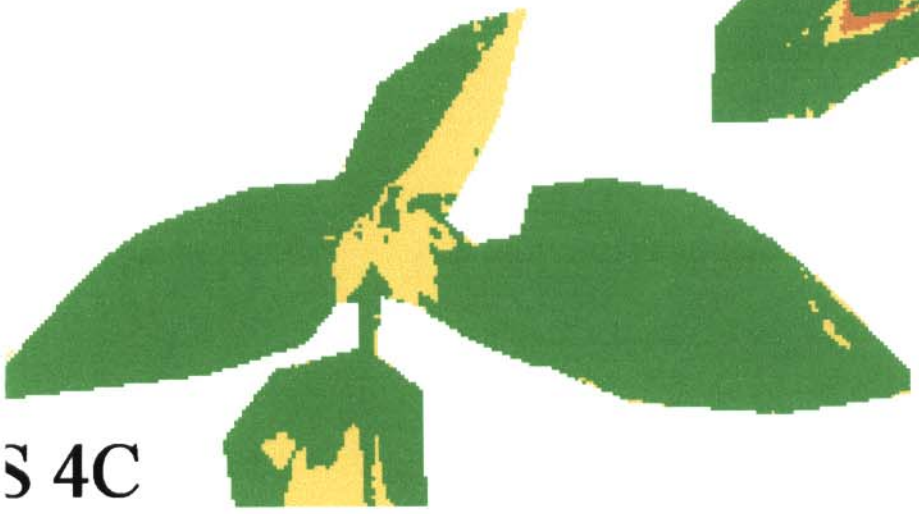

S 4C

high stress
moderate stress
low stress

Plate 23

Sunflower (23/05/99)
video greenness index featuremaps

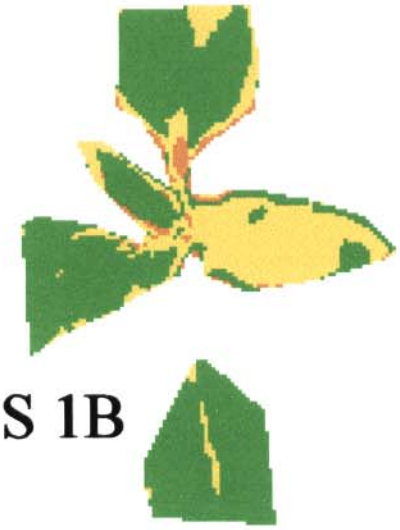

S 1B

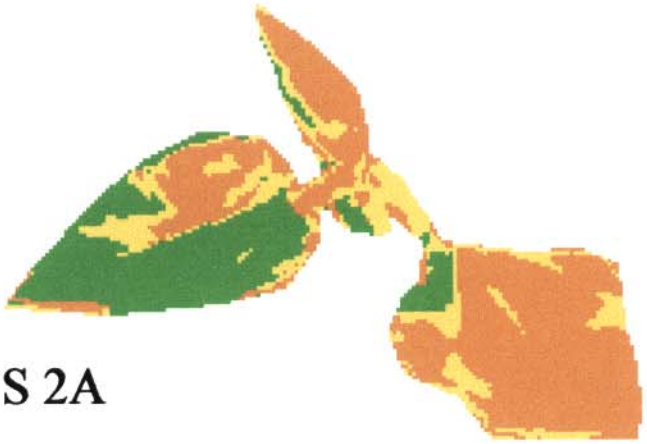

S 2A

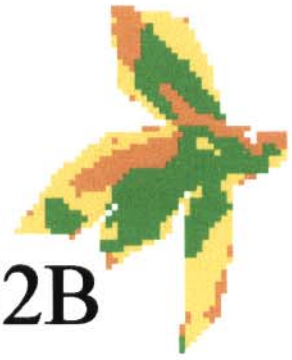

S2B

S 2C

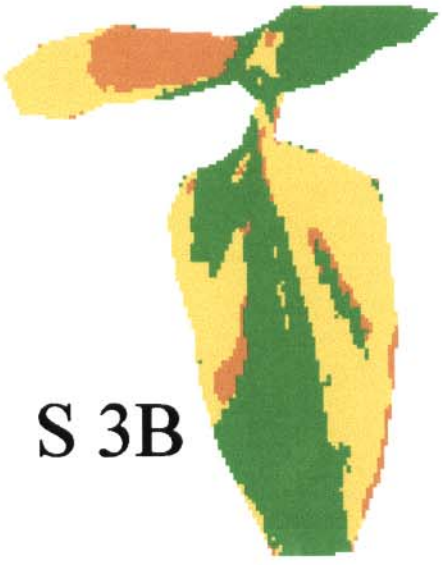

S 3B

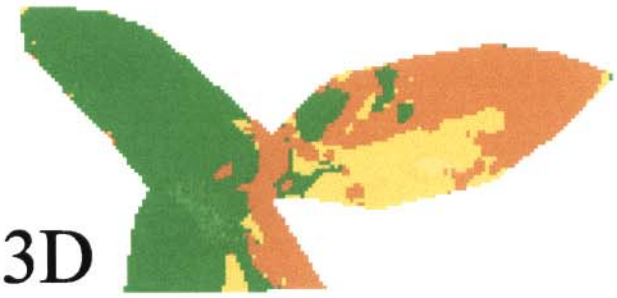

S 3D

high stress
moderate stress
low stress

Plate 24

Sunflower (23/05/99) video greenness index featuremaps

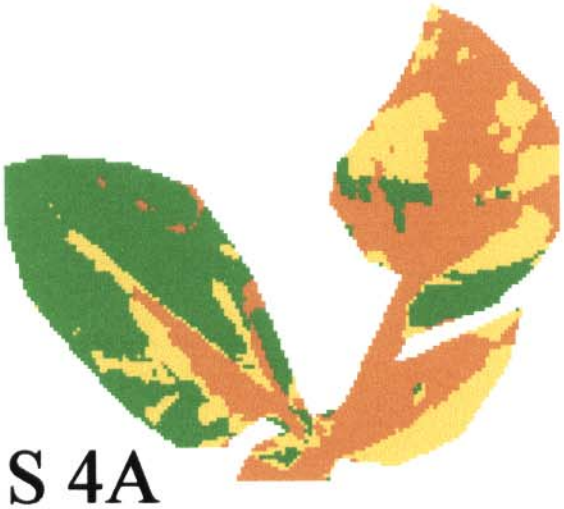

S 4A

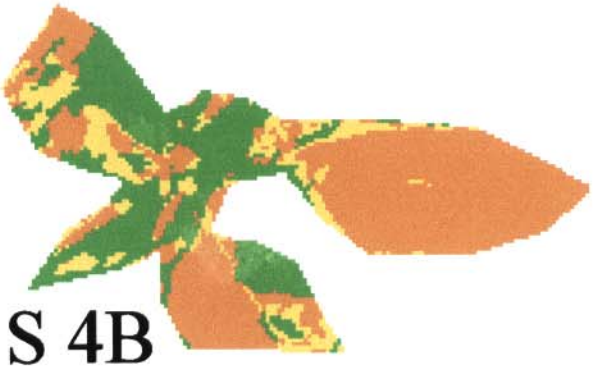

S 4B

S 4D

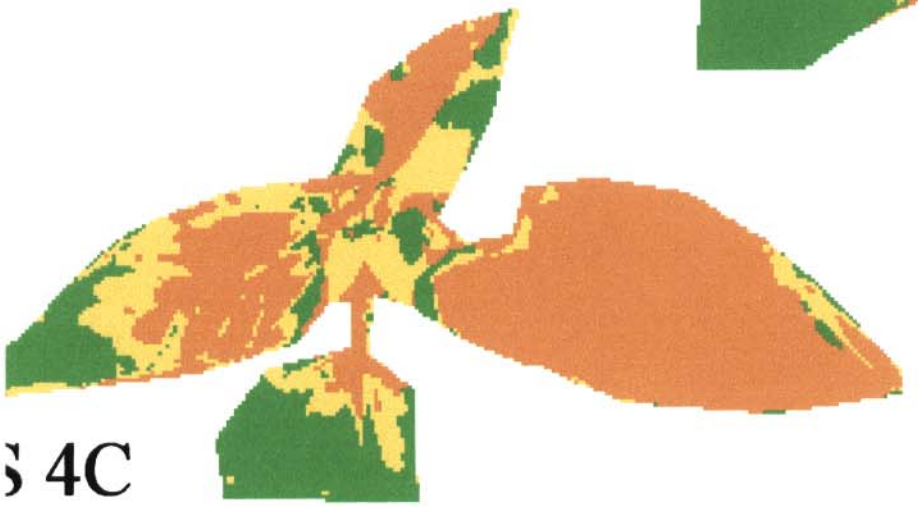

S 4C

high stress
moderate stress
low stress

Plate 25

Tomato (15/04/99) video NDVI featuremaps

T1A

T1B

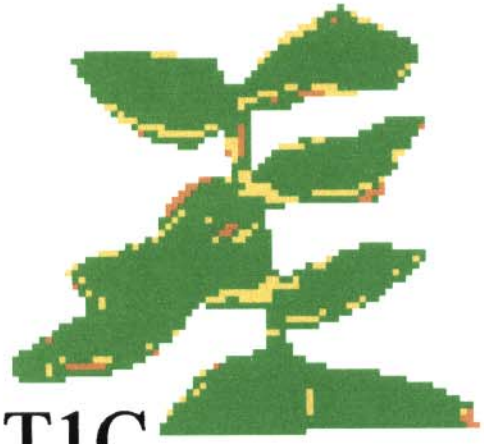

T1C

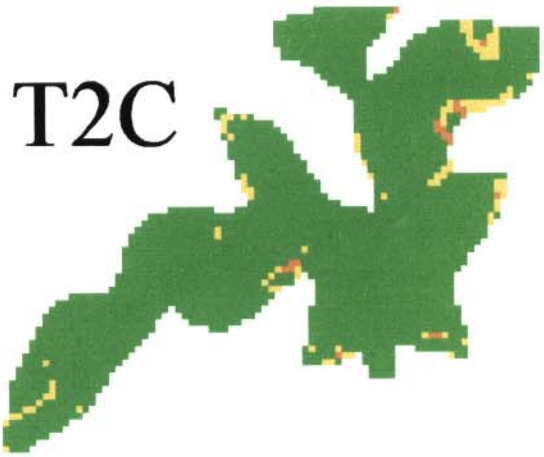

T2C

T2D

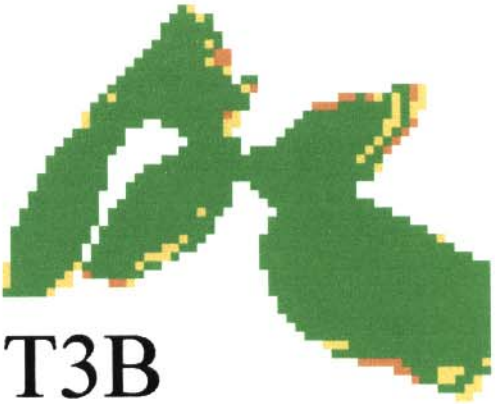

T3B

high stress
moderate stress
low stress

Plate 26

Tomato (15/04/99) video NDVI featuremaps

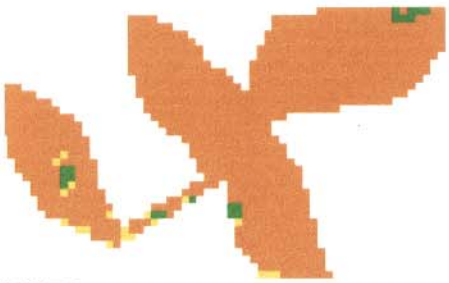

T3D

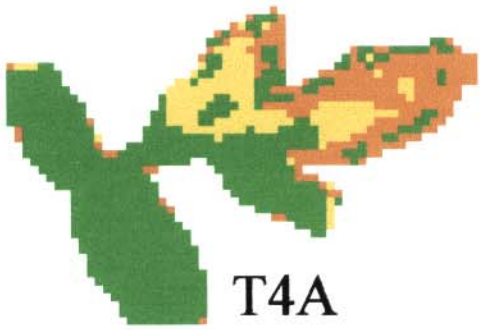

T4A

T4B

T4C

T4D

high stress
moderate stress
low stress

Plate 27

Tomato (15/04/99)
video greenness index featuremaps

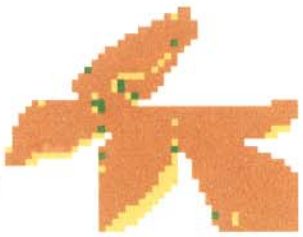

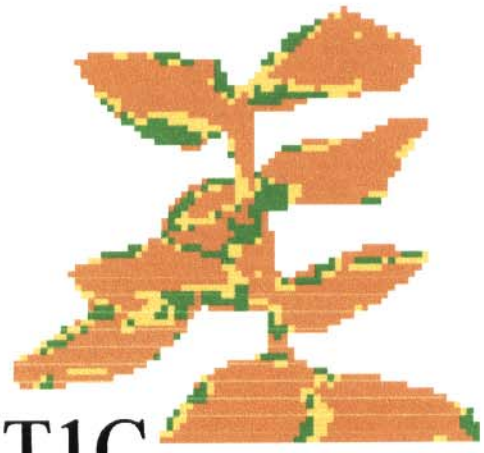

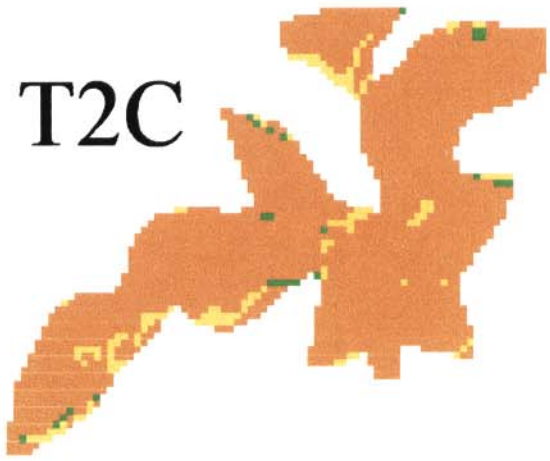

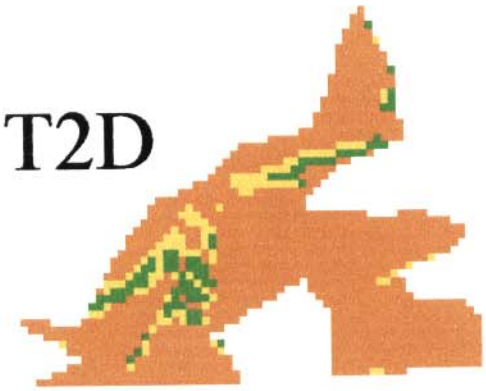

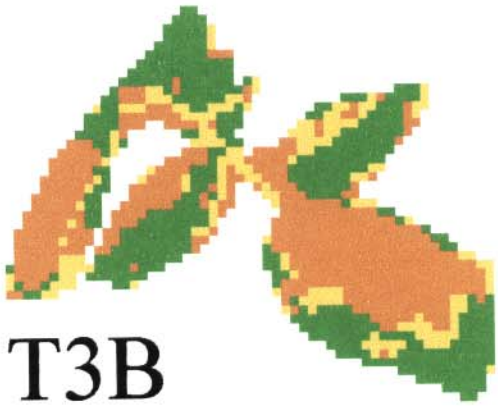

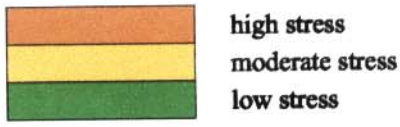

Plate 28

Tomato (15/04/99)
video greenness index featuremaps

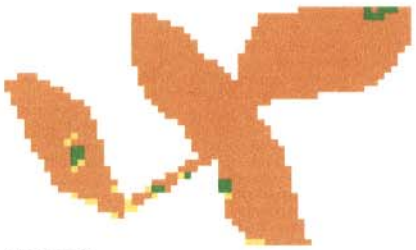

T3D

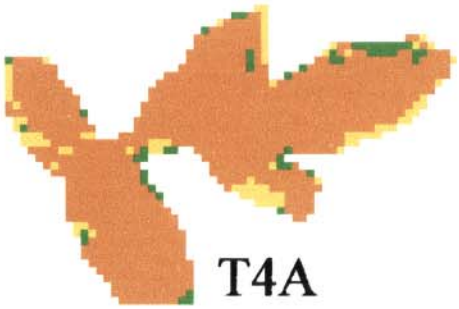

T4A

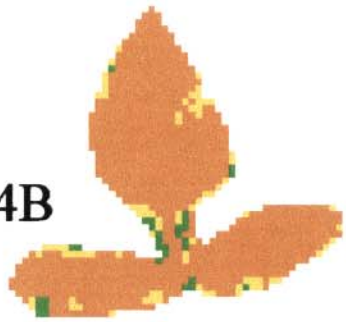

T4B

T4C

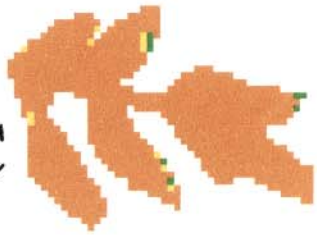

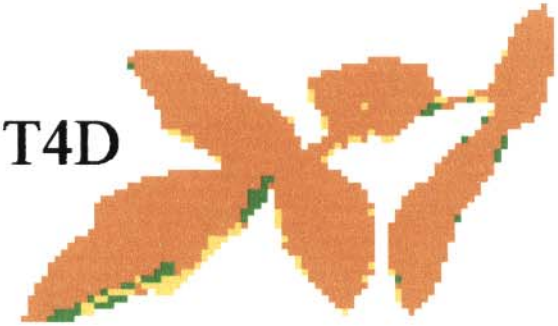

T4D

high stress
moderate stress
low stress

Plate 29

Tomato (03/05/99) video NDVI featuremaps

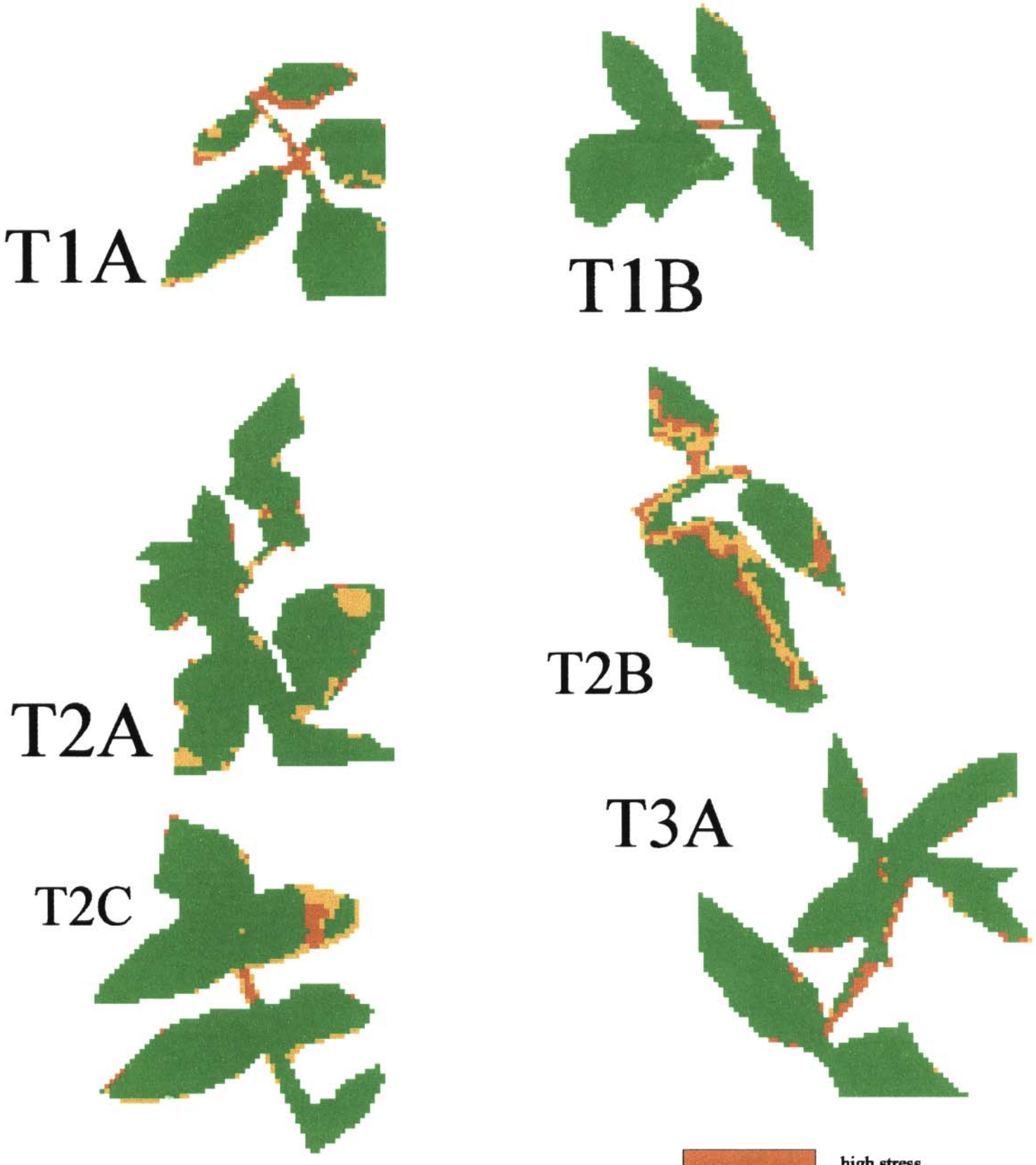

Plate 30

Tomato (03/05/99) video NDVI featuremaps

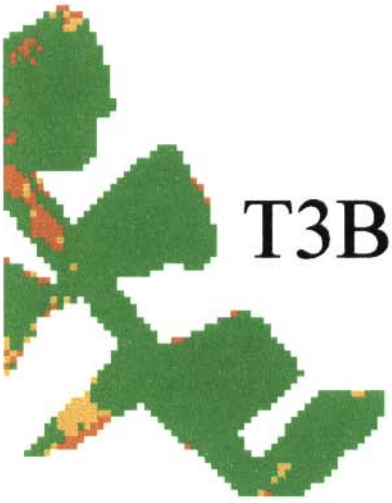

T3B

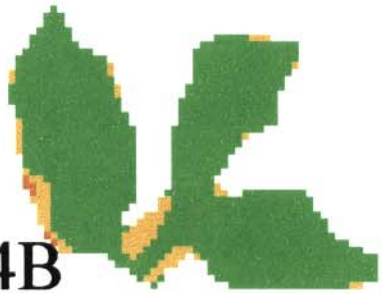

T4B

Tomato (03/05/99) video greenness index featuremaps

T1A

T1B

high stress
moderate stress
low stress

Plate 31 Tomato (03/05/99)
video greenness index featuremaps

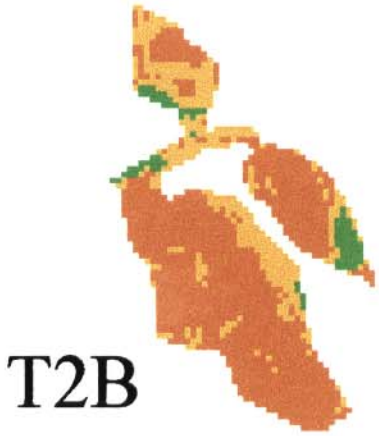

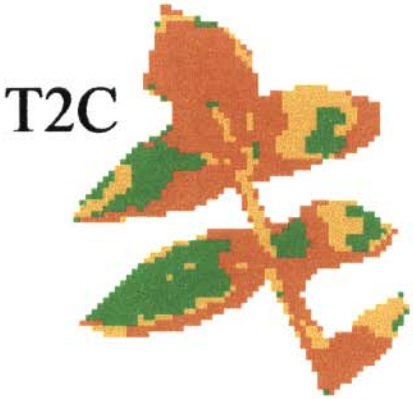

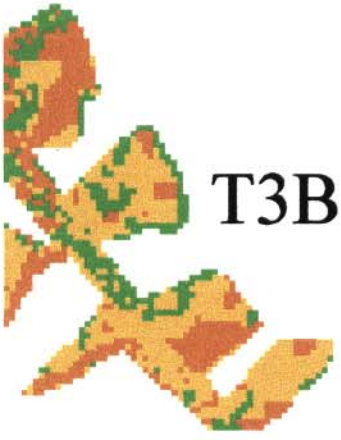

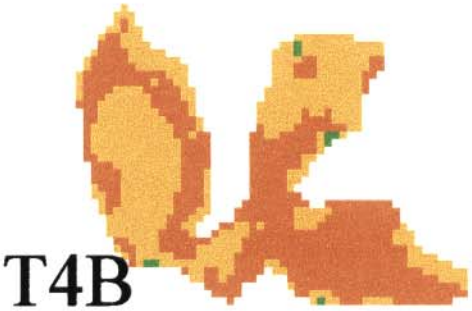

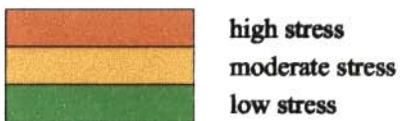

Plate 32

Tomato (14/05/99) video NDVI featuremaps

T1A

T1B

T1C

T1D

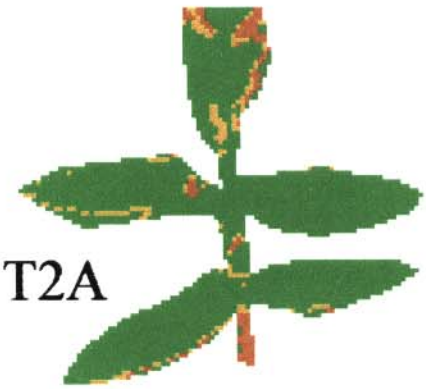

T2A

T2C

high stress
moderate stress
low stress

Plate 33

Tomato (14/05/99) video NDVI featuremaps

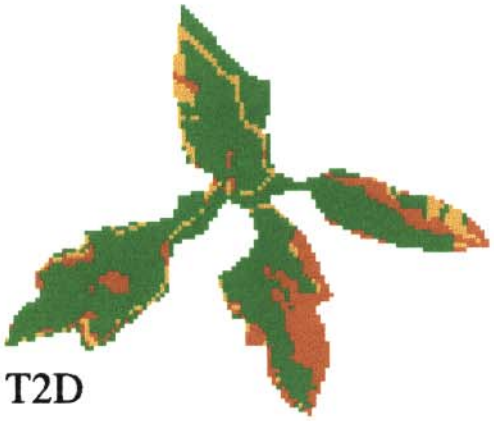

T2D

T3A

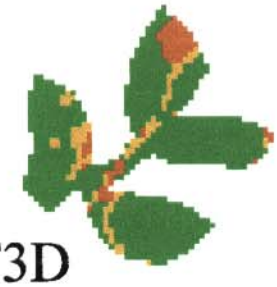

T3D

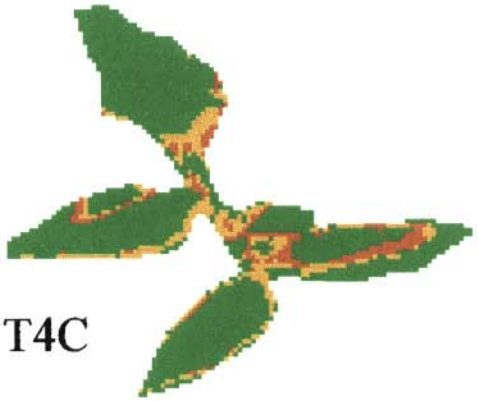

T4C

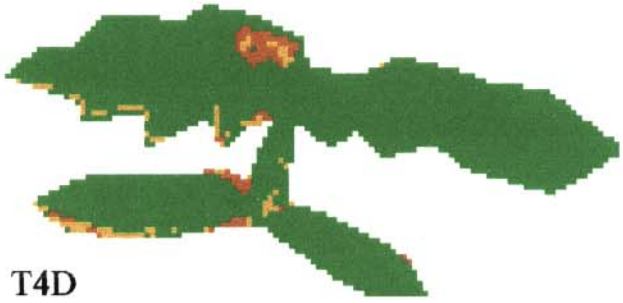

T4D

high stress
moderate stress
low stress

Plate 34

Tomato (14/05/99)
video greenness index featuremaps

T1A

T1B

T1C

T1D

T2A

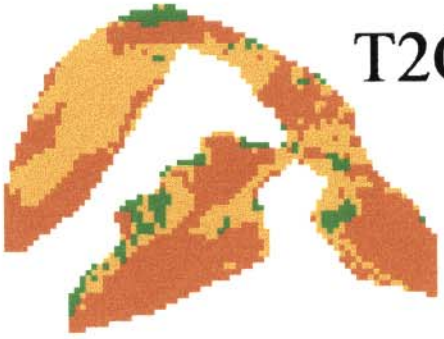

T2C

high stress
moderate stress
low stress

Plate 35

Tomato (14/05/99)
video greenness index featuremaps

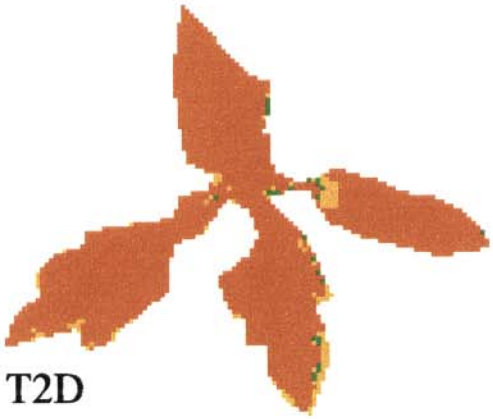

T2D

T3A

T3D

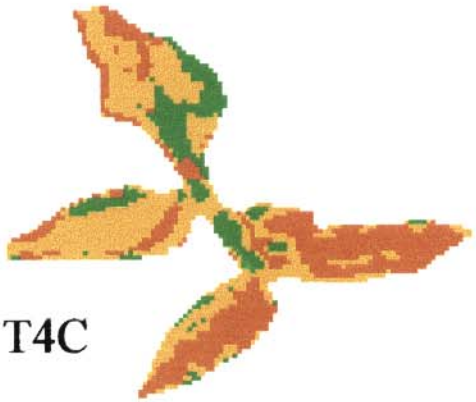

T4C

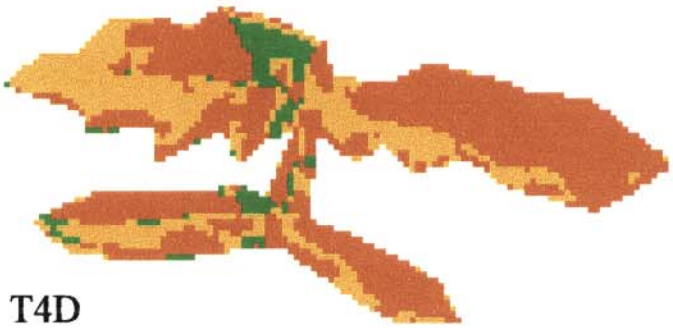

T4D

high stress
moderate stress
low stress